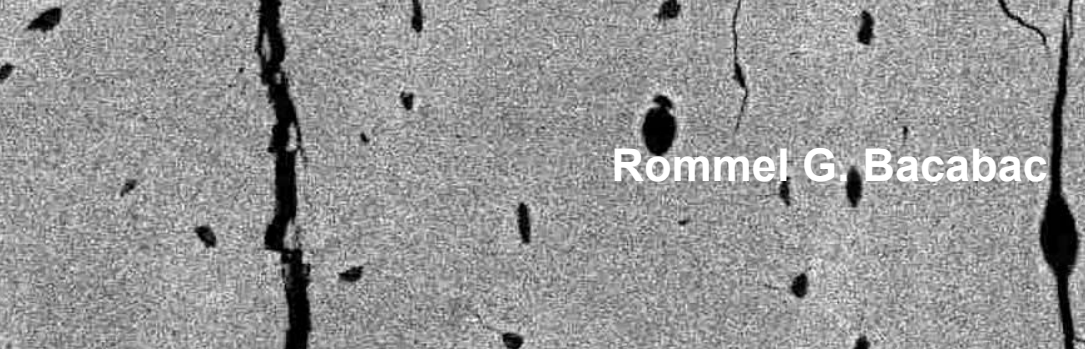
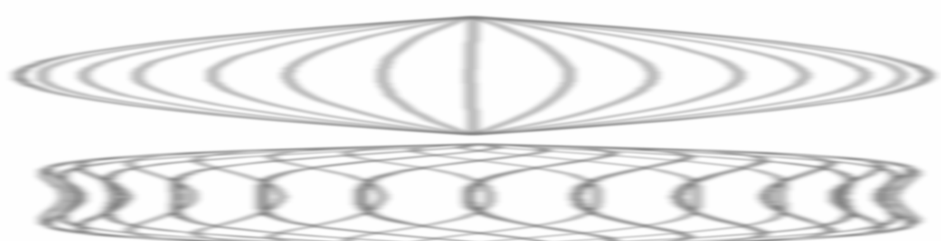


A high-magnification grayscale micrograph showing a dense network of bone tissue. Several large, dark, irregularly shaped structures, likely osteoclasts, are scattered throughout the field, some appearing to interact with the bone matrix.

BONE CELL
MECHANOSENSITIVITY
AND MICROGRAVITY



A high-magnification grayscale micrograph showing a dense network of bone tissue. Several large, dark, irregularly shaped structures, likely osteoclasts, are scattered throughout the field, some appearing to interact with the bone matrix.

Rommel G. Bacabac

BONE CELL MECHANOSENSITIVITY AND MICROGRAVITY

The studies described in this thesis were carried out at the Department of Oral Cell Biology of the Academic Centre for Dentistry Amsterdam (ACTA). Part of the studies were carried out at the Laboratory for Aero and Hydrodynamics, Delft University of Technology, and at the Department of Physics of Complex Systems, Vrije Universiteit Amsterdam.

Part of this thesis is a report of our experiment “FLOW”, one of the biological experiment entries to the DELTA mission (Dutch Expedition for Life Science, Technology and Atmospheric Research; Soyuz craft launched April 19, 2004: flight mission to the International Space Station). The studies were performed as part of the project “Microgravity and Bone Cell Mechanosensitivity”, financed by SRON Netherlands Institute for Space Research, project nr. MG-055.

Printing of this thesis has been supported by:

Interuniversitaire Onderzoekschool Tandheelkunde (IOT)
Dutch Society of Calcium and Bone Metabolism (NVCB)
Centre for Concepts in Mechatronics (CCM)
Netherlands Institute for Space Research (SRON)
Dutch Experiment Support Center (DESC)

Front cover illustration: scanning electron micrograph of a long bone section showing microcracks and canal openings, based on sample preparations and micrographs by Rommel G. Bacabac. Inset: oscillatory velocity profile between parallel plates below and above the critical frequency.

Back cover illustration: scanning electron micrograph of an osteocyte cell from round to flat morphology courtesy of Prof. Peter Nijweide.

ISBN-10: 9090202064

ISBN-13: 9789090202068

Copyright © Rommel G. Bacabac, Amsterdam, 2005.

Bone cell mechanosensitivity and microgravity.

Printed by PrintPartners Ipskamp B.V., Enschede.

All rights reserved. No part of this book may be reproduced, stored in a retrieval system, or transmitted in any form or by any means, mechanical, photocopying, recording, or otherwise, without prior written permission of the holder of the copyright.

VRIJE UNIVERSITEIT

BONE CELL MECHANOSENSITIVITY AND MICROGRAVITY

ACADEMISCH PROEFSCHRIFT

ter verkrijging van de graad van Doctor aan
de Vrije Universiteit Amsterdam,
op gezag van de rector magnificus
prof.dr. T. Sminia,
in het openbaar te verdedigen
ten overstaan van de promotiecommissie
van de faculteit der Tandheelkunde
op dinsdag 24 januari 2006 om 13.45 uur
in het auditorium van de universiteit,
De Boelelaan 1105

door

Rommel Gaud Bacabac

geboren te Manilla, Filippijnen

promotoren: prof.dr. J. Klein-Nulend
prof.dr. R.M. Heethaar

copromotoren: dr.ir. Th.H. Smit
dr. J.J.W.A. van Loon

For mom, dad, and my sisters

CONTENTS

Chapter 1. General Introduction	9
Chapter 2. Dynamic shear stress in parallel-plate flow chambers	19
Chapter 3. Nitric oxide production by bone cells is fluid shear stress rate dependent	37
Chapter 4. An initial stress-kick is required for the fluid shear stress-induced rate dependent activation of bone cells	59
Chapter 5. Stochastic resonance enhances the rapid response of bone cells to fluid shear stress	83
Chapter 6. Bone cell responses to high-frequency vibration stress: does the nucleus oscillate within the cytoplasm?	105
Chapter 7. Microrheology of mechanosensitive bone cells	127
Chapter 8. Microgravity and bone cell mechanosensitivity	155
Chapter 9. General Discussion	179
General Summary	195
Algemene Samenvatting	
A Word of Gratitude	
Curriculum Vitae	

CHAPTER 1

GENERAL INTRODUCTION

GENERAL INTRODUCTION

The capacity of bone tissue to alter its mass and structure in response to mechanical loading has long been recognized (1) but the cellular mechanisms involved remained poorly understood. Bone not only develops as a structure designed specifically for mechanical tasks, but it can adapt during life toward more efficient mechanical performance. The mechanical adaptation of bone is a cellular process and needs a biological system that senses the mechanical loading. The loading information must then be communicated to the effector cells that form new bone or destroy old bone (2, 3).

The *in vivo* operating cell stress derived from bone loading is likely the flow of interstitial fluid along the surface of osteocytes and lining cells (2, 4). The response of bone cells in culture to fluid flow includes prostaglandin (PG) synthesis and expression of prostaglandin G/H synthase inducible cyclooxygenase (COX-2) (5, 6). Cultured bone cells also rapidly produce nitric oxide (NO) in response to fluid flow as a result of activation of endothelial nitric oxide synthase (ecNOS), which enzyme also mediates the adaptive response of bone tissue to mechanical loading (7, 8). Earlier studies have shown that the disruption of the actin-cytoskeleton abolishes the response to stress, suggesting that the cytoskeleton is involved in cellular mechanotransduction (9). The cytoskeleton of the cell also determines its mechanical structure and as such, becomes crucial for the mechanical response of cells to environmental forces. Extracellular matrix receptors such as integrins and CD44 receptors, located in the cellular membrane, are attached to the extracellular matrix as well as to the cytoskeleton. They are prime candidates as mechanotransducers (10). Thus, the ability of cells to respond to mechanical loading is possibly closely related to its mechanical properties and the transfer of forces via intervening proteins linking the internal structure of the cell to its environment.

The influence of forces on cells has been recognized for a long time and the molecular processes involved are now being uncovered. Living bone is an

evident biological system where the interplay of force and metabolic response is exemplified both at the tissue and the cellular level. Forces are believed to be imparted on osteocytes and bone lining cells by the flow of fluid through the lacuno-canalicular system in mechanically loaded bone. Recently, it has been proposed theoretically, that fluid drag through the extra-cellular matrix concentric to the osteocytic processes is able to amplify strain upto two orders of magnitude (11). Theoretical modeling along with *in vitro* studies, exhibit that the range of stress capable of soliciting meaningful physiological response from bone cells are within the range 0.1- 20 Pa (12). The response of bone cells to mechanical stress has been studied using varying techniques for imparting mechanical loads *in vitro* (12, 13).

A number of studies emphasize the role of osteocytes as the professional mechanosensory cells of bone, and the lacuno-canalicular porosity as the structure that mediates mechanosensing (2, 4, 13). Strain-derived flow of interstitial fluid through this porosity seems to mechanically activate the osteocytes, as well as ensure transport of cell signaling molecules and nutrients and waste products. It has also been shown that the rapid production of NO in human bone cells in response to fluid flow results from activation of endothelial cells nitric oxide synthase (ecNOS) (8). These results suggest that the response of bone cells to mechanical stress resembles that of endothelial cells to blood flow (14-16). In the vascular system, changes in arterial diameter occur in response to changes in blood flow rate, in order to ensure a constant vessel tone, and endothelial cells are widely recognized as the mechanosensory cells of this response. The early response of endothelial cells to fluid flow *in vivo* includes the release of NO and prostaglandins (16). Surprisingly therefore, bone tissue seems to use a similar sensory mechanism to detect and amplify mechanical information as does the vascular system. This concept allows an explanation of the local bone gain and loss, as well as remodeling in response to fatigue damage, as processes supervised by mechanosensitive osteocytes.

Microgravity, as occurs under spaceflight, has negative effects on the skeleton, leading to bone loss. Several studies suggest that bone tissue is

directly sensitive to spaceflight conditions. Microgravity provides a unique mechanical environment that might directly affect the ability of cells to sense forces. Hence, the question remains as to how the lack of gravity is detected by bone cells. Could microgravity act directly on the bone cells? Or more precisely, could osteocytes and osteoblasts read the gravitational field change directly? To answer these questions, the fundamental properties of the way bone cells respond to stress in general, have to be addressed.

Therefore, in this thesis we addressed the following specific objectives:

1. To characterize parallel-plate flow chambers for high frequency flow regimes, and to determine how eventual limitations can be reduced for the use of this apparatus for different frequencies.
2. To investigate the response of bone cells to varying rates of fluid shear stress.
3. To investigate whether an initial stress-kick is required for the response of bone cells to varying rates of fluid shear stress.
4. To investigate whether the activation of bone cells by a small periodic loading stimulus is enhanced by broad-frequency, noisy fluid shear stress stimulation.
5. To test whether high frequency vibration stress applied with varying frequencies and amplitudes affects the nitric oxide (NO) and prostaglandin E₂ (PGE₂) production, and mRNA expression for COX-2 by MC3T3-E1 osteoblastic cells.
6. To investigate events occurring at the onset of mechanical stimulation of cells and characterize the chemical and mechanical activation of cells in response to stress by using a two-particle assay for measuring the viscoelastic properties of cells.
7. To test whether near weightlessness decreases the sensitivity of bone cells for mechanical stress through a decrease in early signaling molecules (NO, PGs) that are involved in the mechanical loading-induced osteogenic response.

The main goal of this thesis was to find characteristic properties of the response of bone cells to mechanical stress and to address the effects of microgravity on the mechanosensitivity of bone cells. To reach this goal, bone cells were subjected to stress using fluid flow stimulation at varying rates and regimes with a rich harmonic content in a parallel-plate fluid flow chamber *in vitro* system. Also, the effect of vibration stress on the activation of bone cells was investigated. Finally, mechanosensing at the single cell level was studied by probing the viscoelastic properties of bone cells.

In Chapter 2, the parallel-plate flow chamber was characterized for its use in dynamic flow regimes. This study re-visited a theoretical description of the parallel-plate chamber and derived parameters for designing the parallel-plate chamber for *in vitro* stimulation of cells at arbitrary frequencies, considering non-turbulent fluid flows.

To find specific properties on the way bone cells respond to dynamic stress, in Chapter 3, the response of bone cells to fluid shear stress at different rates was investigated. We compared the release of nitric oxide by bone cells in response to fluid shear stress regimes with frequencies mimicking the physiological condition. Nitric oxide was used as a parameter for bone cell activation, as it is an important signaling molecule for bone formation (17). The amplitude of the fluid shear stress was also varied to investigate the joint effect of frequency and amplitude of stress to the activation of bone cells.

In Chapter 4, we addressed the nature by which bone cells respond to fluid shear stress in a rate-dependent manner. This was done by introducing a pre-treatment phase to the fluid shear stress regimes used to stimulate bone cells, to either induce an initial stress-kick or remove it. By measuring the nitric oxide released by bone cells in response to the regimes with pre-treatment, the ability of bone cells to respond in a rate-dependent manner was put to the test. The response of bone cells to stress with or without an initial stress-kick, determined whether bone cells required overcoming a stress-threshold to respond in a rate-dependent manner.

The study of bone cell response to stress by fluid flow was then extended to regimes superposed with noisy fluid shear stress with a rich harmonic content. In Chapter 5, we addressed the question whether noise enhancement was possible for bone cells, considering the importance of the initial stress condition (i.e., the presence or absence of an initial stress-kick) for a rate dependent response. The possibility of a noise-enhanced response phenomenon was then used to derive other properties on the way bone cells respond to stress. In particular, differences in the response of MLO-Y4 and MC3T3-E1 cells, as models for osteocytes and osteoblasts, provided insights on the threshold mechanisms for specific signaling molecules (i.e., nitric oxide and prostaglandin E₂).

The properties by which bone cells respond to fluid shear stress as investigated in Chapters 3 and 4 in this thesis, provides possible general rules on bone cell mechanosensitivity. To further understand the effect of stress on bone cells in general, bone cells were also subjected to mechanical vibration by translational motion. In Chapter 6, the response of bone cells to vibration stress in terms of a rapid release of nitric oxide, prostaglandin E₂, and mRNA expression for COX-2, was studied.

However, a more complete understanding of the bone cellular response to stress requires a physical picture for finding characteristic properties at the single-cell level. Finally, the mechanical and physiological response of single bone cells was investigated in chapter 7, to find characteristic behaviors for the stress response of single bone cells. To perform this final study, a two-particle microrheology technique was adapted for investigating characteristic single-cell responses to minute forces.

In the course of this study, we had an opportunity for testing the mechanosensitivity of primary bone cells under the influence of microgravity during the Dutch Soyuz Mission, also called DELTA mission (Dutch Expedition for Life Science, Technology and Atmospheric Research; Soyuz craft launched April 19, 2004, flight mission to the International Space Station). The previous work on characterizing the parallel-plate chamber for

dynamic fluid shear stress was used in designing a downscaled version of an *in vitro* system for fluid flow stimulation of bone cells. A downscaled version was necessary considering strict requirements of a space flight experiment. In chapter 8, we describe the ground preparations and protocols for the experiment FLOW on board of the DELTA mission, where we investigated whether the mechanosensitivity of bone cells was decreased by microgravity.

REFERENCES

1. Wolff J 1892 Gesetz der transformation der knochen, Hirschwald, Berlin.
2. Burger EH, Klein-Nulend J 1999 Mechanotransduction in bone - Role of the lacuno-canalicular network. FASEB J 13(Supplement):S101-S112.
3. Smit TH, Burger EH, Huyghe JM 2002 A case for strain-induced fluid flow as a regulator of BMU-coupling and osteonal alignment. J Bone Min Res 17(11):2021-2029.
4. Cowin SC, Moss-Salentijn L, Moss ML 1991 Candidates for the mechanosensory system in bone. J Biomech Eng 113(2):191-197.
5. Ajubi NE, Klein-Nulend J, Alblas MJ, Burger EH, Nijweide PJ 1999 Signal transduction pathways involved in fluid flow-induced PGE2 production by cultured osteocytes. Endoc Metab 276(1):E171-E178.
6. Klein-Nulend J, Burger EH, Semeins CM, Raisz LG, Pilbeam CC 1997 Pulsating fluid flow stimulates prostaglandin release and inducible prostaglandin G/H synthase mRNA expression in primary mouse bone cells. J Bone Miner Res 12(1):45-51.

7. Johnson DL, McAllister TN, Frangos JA 1996 Fluid flow stimulates rapid and continuous release of nitric oxide in osteoblasts. *Am J Physiol* 271(1):E205-E208.
8. Klein-Nulend J, Helfrich MH, Sterck JG, MacPherson H, Joldersma M, Ralston SH, Semeins CM, Burger EH 1998 Nitric oxide response to shear stress by human bone cell cultures is endothelial nitric oxide synthase dependent. *Biochem Biophys Res Commun* 250(1):108-114.
9. Ajubi NE, Klein-Nulend J, Nijweide PJ, Vrijheid-Lammers T, Alblas MJ, Burger EH 1996 Pulsating fluid flow increases prostaglandin production by cultured chicken osteocytes- a cytoskeleton-dependent process. *Biochem Biophys Res Commun* 225(1):62-68.
10. Wang N, Butler JP, Ingber DE 1993 Mechanotransduction across the cell surface and through the cytoskeleton. *Science* 260(5111):1124-1127.
11. Han YF, Cowin SC, Schaffler MB, Weinbaum S 2004 Mechanotransduction and strain amplification in osteocyte cell processes. *Proc Natl Acad Sci USA* 101:16689-16694.
12. Brown TD 2000 Techniques for mechanical stimulation of cells in vitro: a review. *J Biomech* 33(1):3-14.
13. Klein-Nulend J, van der Plas A, Semeins CM, Ajubi NE, Frangos JA, Nijweide PJ, Burger EH 1995 Sensitivity of osteocytes to biomechanical stress in vitro. *FASEB J* 9(5):441-445.

14. Frangos JA, Eskin SG, McIntire LV, Ives CL 1985 Flow effects on prostacyclin production by cultured human endothelial cells. *Science* 227(4693):1477-1479.
15. Furchtgott RF, Vanhoutte PM 1989 Endothelium-derived relaxing and contracting factors. *FASEB J* 3(9):2007-2018.
16. Hecker M, Mulsch A, Bassenge E, Busse R 1993 Vasoconstriction and increased flow- 2 principal mechanisms of shear stress-dependent endothelial autacoid release. *Am J Physiol* 265(3):H828-H833.
17. Fox SW, Chambers TJ, Chow JWM 1996 Nitric oxide is an early mediator of the induction of bone formation by mechanical stimulation. *Bone* 19(6):687.

CHAPTER 2

DYNAMIC SHEAR STRESS IN PARALLEL-PLATE FLOW CHAMBERS

Rommel G. Bacabac¹, Theo H. Smit², Stephen C. Cowin³, Jack J.W.A. Van Loon^{1,5}, Frans T.M. Nieuwstadt⁴, Rob Heethaar², Jenneke Klein-Nulend¹

¹Department of Oral Cell Biology, Academic Centre for Dentistry Amsterdam-Universiteit van Amsterdam and Vrije Universiteit, Amsterdam, The Netherlands

²Department of Physics and Medical Technology, VU University Medical Center, Amsterdam, The Netherlands

³Departments of Biomedical and Mechanical Engineering, The City College of New York, New York, NY, USA

⁴J.M. Burgers Centre, Delft University of Technology, Delft, The Netherlands

⁵Dutch Experiment Support Center, Vrije Universiteit, Amsterdam, The Netherlands

Journal of Biomechanics 38:159-167, 2005

ABSTRACT

An *in vitro* model using a parallel-plate fluid flow chamber is supposed to simulate *in vivo* fluid shear stresses on various cell types exposed to dynamic fluid flow in their physiological environment. The metabolic response of cells *in vitro*, is associated with the wall shear stress. However, parallel-plate flow chambers have not been characterized for dynamic fluid flow experiments. We use a dimensionless ratio h/λ_v , in determining the exact magnitude of the dynamic wall shear stress, with its oscillating components scaled by a *shear factor* T . It is shown that, in order to expose cells to predictable levels of dynamic fluid shear stress, two conditions have to be met: 1) $h/\lambda_v < 2$, where h is the distance between the plates and λ_v is the *viscous penetration depth*; and 2) $f_o < f_c/m$, where the *critical frequency* f_c is the upper threshold for this flow regime, m is the highest harmonic mode of the flow, and f_o is the *fundamental frequency* of fluid flow.

INTRODUCTION

The parallel-plate flow chamber (PPFC) is used for flow stimulation of various cell types, *e.g.*, bone cells and endothelial cells (1). A cell monolayer attached to one of the internal plate surfaces is subjected to fluid flow by creating a pressure gradient along the chamber. To calculate the resulting shear stress on the cells, the mathematical model assumes a Newtonian fluid in which the shear tensor is proportional to the deformation tensor. For steady flow between infinitely wide parallel plates, wall shear stress τ_w is calculated as a function of the measured flow Q :

$$\tau_w = \frac{6\mu Q}{bh^2} \quad [1]$$

with μ = fluid viscosity, b = width of the chamber, h = distance between plates. For finite chamber dimensions (finite b/h), the fluid velocity profile remains parabolic between the plates, but vanishes at the boundaries of the rectangular channel (Figure 1A, B) (2, 3). The shear stress profile, calculated from the velocity gradient, has maximum magnitudes at the plate surfaces and vanishes at the corners of the channel (Figure 1C). Less than 1% difference from a full parabolic velocity profile occurs after an entry length $L_{entry} = 0.04hRe$ (Reynolds number $Re = Q\rho/(\mu b)$) (4). Practically, more than 85% of the surface is exposed to a homogenous wall shear stress for $b/h > 20$.

Equation [1] assumes steady flow, but is also used to estimate the average and maximum wall shear stress in dynamic flow regimes. Flow frequencies employed in stimulation of cells generally remain below 10 Hz (5-7), but physiological fluid flow might involve much higher frequencies. For example, small strains ($< 10 \mu\epsilon$) in bone show strain information extending to 40 Hz (8). Theoretical extrapolation predicts that strain induced flow in bone elicits shear stresses up to 3 Pa for 100-200 $\mu\epsilon$ at 20-30 Hz (9). Blood flow also involves dynamic regimes with non-negligible higher harmonics: the spectral content of flow in the abdominal aorta of dogs, for example, shows frequencies reaching 80 Hz (10). High frequency modes have been shown to be stimulative to cells

despite their small amplitudes; thus, fluid flow studies should be extended also to this range. It is questionable, though, if [1] is valid also for *dynamic* flows in PPFCs. Indeed, a dichotomy in oscillating flow regimes is reported for parallel-plate systems, characterized by the Womersley number W_o ($= \sqrt{(\omega/\nu)} L_c$, where $\omega = 2\pi f$, f = flow frequency, ν = kinematic viscosity, L_c = characteristic length; (11, 12)); this explicitly points at a limitation for the use of PPFCs under high frequency regimes.

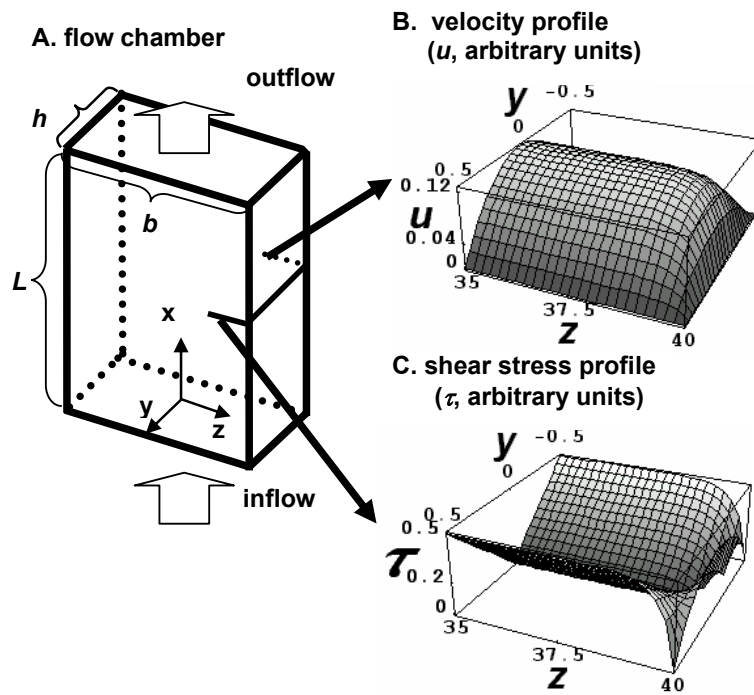


Figure 1. The flow chamber and its velocity and shear stress profile in arbitrary units. A. Diagram of a parallel-plate flow chamber of width b , height h , and length L , in its orientation in the x - y - z axes. The fluid is forced through the chamber by a steady pressure gradient along the x -axis. (b) and (c) show the calculated velocity profile u and the shear stress profile τ , respectively, for an aspect ratio $b/h = 80$. The arrows indicate that the profiles were taken very near the right edge of the flow chamber. The shear stress has its maximum value at the plate surfaces and vanishes at the chamber corners. Parabolic velocity profile and homogenous wall shear stress are characteristic for steady flow between parallel plates.

The aim of this paper is to characterize PPFCs for high frequency flow regimes, and to determine how eventual limitations can be reduced. We derived a relationship between the wall shear stress and flow, as well as between flow and pressure gradient under oscillating regimes, generalized to include higher harmonics.

MATHEMATICAL MODEL

Dynamic flow

The mathematical model assumes a laminar flow of a Newtonian fluid under isothermal conditions and imposes a no-slip boundary condition. The pressure gradient over the PPFC has a steady component γ and an oscillating component γ_o of frequency f . The Navier-Stokes equation is then:

$$\rho \frac{\partial u}{\partial t} - \mu \frac{\partial^2 u}{\partial y^2} = \gamma + \gamma_o \sin(\omega t) \quad [2]$$

where velocity field u is a function of y and time variable t . The principle of superposition implies a generalization to dynamic flow regimes with higher harmonics. The solution of the velocity field has the form (Appendix [A.1-4]; (13)):

$$u(y, t) = C_1(y) + C_2(y) \cos(\omega t) + C_3(y) \sin(\omega t) \quad [3]$$

In order to formulate the relations between the wall shear stress, the flow, and the pressure gradient, we introduce two dimensionless scaling factors: shear factor T and flow factor K , respectively.

Shear factor $T(h/\lambda_v)$

The oscillating wall shear stress component is related to flow amplitude q_o , chamber width b , height h , and viscous penetration depth λ_v ($= \sqrt{2\nu/\omega}$; ν = ratio of fluid viscosity to fluid mass density; $\omega = 2\pi f$) as:

$$\tau_{wo}(t) = q_o \frac{\mu}{bh^2} \left(\frac{h/\lambda_v}{cc_+(h/\lambda_v)} \right) \left(\sqrt{\frac{\sin^2(h/\lambda_v) + \sinh^2(h/\lambda_v)}{1 - 2(\lambda_v/h) \frac{ss_+(h/\lambda_v)}{cc_+(h/\lambda_v)} - 2(\lambda_v/h)^2 \frac{cc_-(h/\lambda_v)}{cc_+(h/\lambda_v)}}} \right) \sin(\omega t + \psi) \quad [4]$$

We simplify [4] by introducing shear factor $T(h/\lambda_v)$ including all functions with the argument h/λ_v , to scale the oscillating wall shear stress amplitude. The total wall shear stress τ_{wt} solution of [2] is then:

$$\tau_{wt}(t) = \frac{6\mu}{bh^2} Q_o \left(1 \pm \frac{q_o}{Q_o} T(h/\lambda_v) \sin(\omega t + \psi) \right) \quad [5]$$

where Q_o is the steady flow component and ψ is the phase difference between wall shear stress and flow. Figure 2 shows the velocity profile variations for various frequencies.

$T(h/\lambda_v)$ (Appendix [A.11]) is close to unity when the wall shear stress is proportional to flow, *i.e.*, when $h/\lambda_v < 2$ (Figure 3a). From [5] and [1], the oscillating wall shear stress amplitude becomes $6\mu QT/(bh^2)$. The critical frequency 11.2 Hz is calculated at $h/2 = \lambda_v$, using the fluid physical properties of the culture medium and $h = 0.3$ mm (Figure 2). Decreasing h increases the critical frequency (Figures 3b,c), increasing h demands increasing the fluid viscosity μ (Figure 3d). The physical properties of the fluid (μ, ρ), and the distance between the plates (h) determine the critical frequency f_c :

$$\left(\sqrt{\left(\frac{\rho\pi f_c}{\mu} \right)} \right) h = 2 \Rightarrow f_c = \frac{4\mu}{\rho\pi h^2} \quad [6]$$

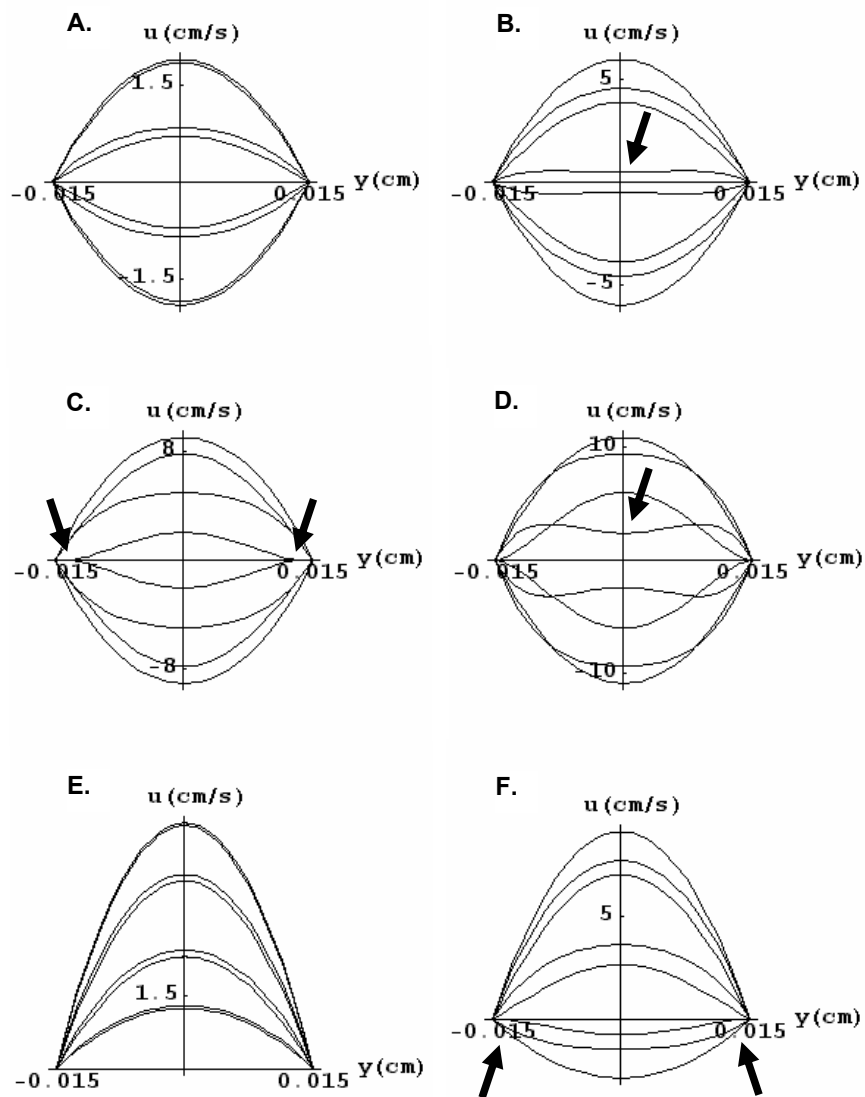


Figure 2. The velocity profiles in one cycle of oscillation. The graphs show the velocity profiles at time intervals an 8th part of the corresponding period. We simulated a typical cell culture medium (Dulbeccos' Modified Eagle Medium (DMEM) with supplements, viscosity = 0.0078 poise, density = 0.99 g/cm³, at 37°C), subjected to a flow amplitude of 0.15 ml/s between plates separated by 0.03 cm. A. The velocity profiles at 5 Hz, exhibit *quasi-parabolic form* throughout one flow cycle. B. At a frequency of 11.2 Hz, the quasi-parabolic velocity profile breaks down by an *arching* between the plates (arrow). At higher frequencies, *arching*, occurs near the plates (20 Hz, C), or between the plates (44.8 Hz, D). E and F show the velocity profiles at 5 Hz and 11.2 Hz respectively, imposed upon a steady flow component. Note that the symmetry about the y -axis is lost due to the steady flow component. However, the *quasi-parabolic form* of the velocity profile still breaks down at 11.2 Hz as indicated by the arrows in F. Quasi-parabolic velocity profile, indicative of quasi-steady flow breaks down when the flow frequency is above 11.2 Hz for the given fluid properties and chamber dimensions.

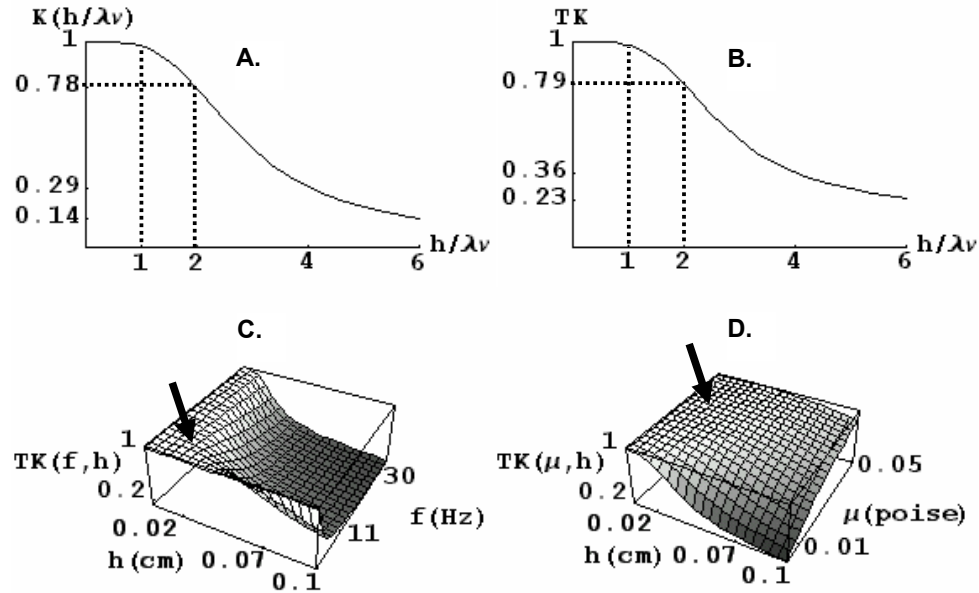


Figure 3. The shear factor. A. The shape of the shear factor (Appendix (A.11)) distinguishes a dichotomy in flow regimes separated by $h/\lambda_v = 2.0$. B. For a typical cell culture medium (DMEM, with supplements) the $T(h/\lambda_v)$ curve digresses from unity depending on the value of h . C. shows that the critical frequency can be raised by minimizing h while keeping $T(h/\lambda_v)$ close to unity for DMEM. D. Shows that the fluid viscosity μ can be increased (from 0.005 poise, assuming that ρ is not significantly changed) while keeping $T \sim 1.0$, even at higher h values up to about 1 mm. In both C and D, the arrow indicates the region where $T \sim 1.0$ i.e., where $h/\lambda_v < 2$ validating the adaptation of equation (1) for dynamic flow.

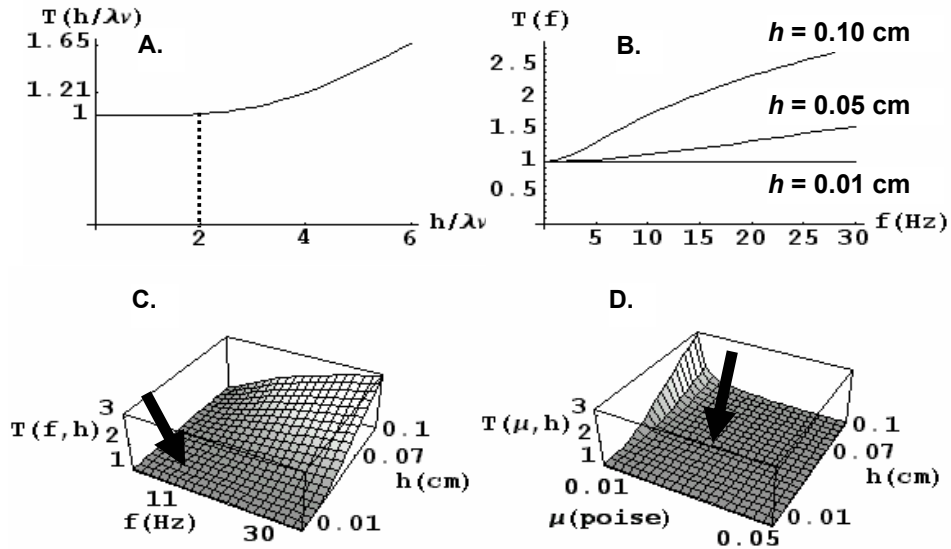


Figure 4. The flow factor. A. The flow factor $K(h/\lambda_v)$ (Appendix (A.12)) varies from unity by 2% at $h/\lambda_v = 1.0$ and drops to 0.78 at $h/\lambda_v = 2.0$. B. The product between the flow and shear factor is asymptotic to the horizontal axis. $T(h/\lambda_v)K(h/\lambda_v)$ scales the wall shear stress when the oscillating pressure gradient amplitude is kept constant as h/λ_v is varied ($TK = 0.79$ when $\alpha h = 2$). A and B illustrate that varying h/λ_v while keeping the pressure gradient amplitude constant leads to a lowering of the initial wall shear stress compared to its value if the flow were steady. C. TK drops faster at higher values of h and f . D. shows that TK drops faster for lower values of μ and higher h . In both C and D, the arrow indicates the region where $TK \sim 1.0$, i.e., $h/\lambda_v < 1$. Equation (1) is valid for $h/\lambda_v < 2$ provided that the flow measurement is simultaneous to the change in h/λ_v parameters.

Flow factor $K(h/\lambda_v)$

The oscillating flow amplitude q_o can be scaled by a flow factor $K(h/\lambda_v)$ in relation with the oscillating pressure gradient amplitude γ_o :

$$q_o = \frac{bh^3\gamma_o}{12\mu} K(h/\lambda_v) \quad [7]$$

K (Appendix [A.12]) is a decreasing function of h/λ_v (Figure 4). This shows that pressure gradient drops for $h/\lambda_v > 1$, which means that the wall shear stress is underestimated for $h/\lambda_v > 1$. For example, there is an overestimation of the magnitude of the wall shear stress by 21% at the critical frequency ($h/\lambda_v = 2$). In order to correct for that, the oscillating wall shear stress amplitude has to be scaled by the product TK when the oscillating pressure gradient amplitude is kept constant:

$$\frac{6\mu q_o}{bh^2} K(h/\lambda_v) T(h/\lambda_v) \quad [8]$$

So, [8] should be used in experimental set-ups in which the pressure gradient is controlled, because the resulting shear stress is underestimated. The wall shear stress is linear to flow when $h/\lambda_v < 2$ but the flow is linear with the pressure gradient when $h/\lambda_v < 1$.

Higher harmonic modes

The flow profile may show a more arbitrary shape depending on the type of pump mechanism used. When the flow is periodic, it can be expanded into a Fourier series (see [A.10]), and from [5] follows:

$$\tau(t) = \frac{6\mu}{bh^2} \left\{ Q_o + \sum_{n=1}^m T_n \left[q_n^c \cos((2\pi f_o n)t + \psi_n^c) + q_n^s \sin((2\pi f_o n)t + \psi_n^s) \right] \right\} \quad [9]$$

where ψ is the phase difference between the wall shear stress and the corresponding flow component at the given indices. Shear factor T is discretized due to the form of the angular frequency ($\omega_n = 2\pi f_o n$, for $n = 1, 2, 3, \dots$). The summation limit m imposes that for $n > m$, flow coefficients q_n^c or q_n^s become negligible compared to the average flow. To apply a flow regime

such that $h/\lambda_v < 2$ for all harmonics, the highest harmonic mode ($f_o m$) must be less than the critical frequency f_c .

DISCUSSION

For dynamic regimes in a PPFC, the relations between wall shear stress, flow, and pressure gradient, were derived using dimensionless scaling factors $T(h/\lambda_v)$ and $K(h/\lambda_v)$. The dimensionless parameter h/λ_v was the key for establishing quasi-steady flow in laminar regimes. The analysis was expanded to apply for arbitrary dynamic laminar flows, identifying the limits for the highest harmonic mode of the flow.

To establish laminar quasi-steady flow under dynamic regimes in PPFCs, the following conditions apply: 1) $h/\lambda_v < 2$ based on the consequent *quasi-parabolic* form of the velocity profile, and 2) $f_o < f_c / m$, where the *critical frequency* f_c is the upper threshold for this flow regime and m is the highest harmonic of flow. Quasi-steady flow means that the dynamic wall shear stress follows the changing flow linearly. When the flow is beyond the quasi-steady regime, there will be less oscillation due to backflow (figure 2 b-d), but shearing might increase at the plate walls since the shear factor $T(h/\lambda_v) > 1$ (Figure 3, [5]).

Attached cells occupy $< 4.1\%$ of the chamber height, based on unsheared endothelial monolayers ($3.4 \pm 0.7 \mu\text{m}$, see (14); for $h = 100\text{-}300 \mu\text{m}$). Since the wall shear stress is estimated by average parameters (flow or pressure gradient), assumption of smooth rigid walls is reasonable. The Reynolds and the Womersley numbers empirically predict the transition from laminar to turbulent oscillating flow. Measurement on a dog's blood vessel relates the maximum Re to 150-250 times W_o (11). The transition to turbulent flow is reached at $Re < 2640$ (15), however, values as low as $Re \sim 1000$ have been found experimentally. Assuming that the transition to turbulent flow for flow between parallel-plates is $Re = 2000$, this transition occurs at a supplementary

condition: $h/\lambda_v = 8/\sqrt{2} \approx 5.7$. The flow regime where $h/\lambda_v < 2$, is far from turbulence provided the fluid properties remain stable.

Our findings provide guidelines in adapting the PPFC in terms of parameters in h/λ_v for investigating cell mechanosensitivity *in vitro*. Using the PPFC, the effect of physiological flow regimes on cells can be studied involving a wide range of frequencies, types of viscous fluids, and values for h that approximate actual shearing flow in various anatomical sites, such as blood vessels or the lacuno-canicular network in bone.

ACKNOWLEDGEMENTS

This work was supported by funds from the Space Research Organization of The Netherlands (SRON), project number: MG-055. We thank Dr. Mathieu Pourquie (Delft University of Technology, Delft, The Netherlands) for his contribution in numerically testing some of our analytical results.

REFERENCES

1. Brown TD 2000 Techniques for mechanical stimulation of cells in vitro: a review. *J Biomech* 33(1):3-14.
2. Belansky R, Wanser K 1993 Laser Doppler velocimetry using a bulk optic Michelson interferometer: A student laboratory experiment. *Am J Phys* 61(11):1014-1019.
3. Booij W, de Jongh A, de Mul F 1995 Flow profile study using miniature laser-doppler velocimetry. *Am J Phys* 63(11):1028-1033.
4. Schlichting H 1968 Boundary layer theory, McGraw-Hill, New York.

5. Frangos JA, Eskin SG, McIntire LV, Ives CL 1985 Flow effects on prostacyclin production by cultured human endothelial cells. *Science* 227(4693):1477-1479.
6. Jacobs CR, Yellowley CE, Davis BR, Zhou Z, Cimbala JM, Donahue HJ 1998 Differential effect of steady versus oscillating flow on bone cells. *J Biomech* 31(11):969-976.
7. Klein-Nulend J, Semeins CM, Ajubi NE, Nijweide PJ, Burger EH 1995 Pulsating fluid flow increases nitric oxide (NO) synthesis by osteocytes but not periosteal fibroblasts--correlation with prostaglandin upregulation. *Biochem Biophys Res Commun* 217(2):640-648.
8. Fritton SP, McLeod J, Rubin CT 2000 Quantifying the strain history of bone: spatial uniformity and self-similarity of low-magnitude strains. *J Biomech* 33(3):317-325.
9. Weinbaum S, Cowin SC, Zeng Y 1994 A model for the excitation of osteocytes by mechanical loading-induced bone fluid shear stresses. *J Biomech* 27(3):339-360.
10. Newman DL, Sipkema P, Greenwald SE, Westerhof N 1986 High frequency characteristics of the arterial system. *J Biomech* 19(10):817-824.
11. Loudon C, Tordesillas A 1998 The use of the dimensionless Womersley number to characterize the unsteady nature of internal flow. *J Theoret Biol* 191(1):63-78.

12. Yakhot A, Arad M, Ben Dor G 1999 Numerical investigation of a laminar pulsating flow in a rectangular duct. *Internat J Numer Meth Fluids* 29(8):935-950.
13. Landau LD, Lifshitz EM 1959 Fluid Mechanics, Permagon Press, Reading, MA.
14. Barbee KA, Davies PF, Lal R 1994 Shear stress-induced reorganization of the surface topography of living endothelial cells imaged by atomic force microscopy. *Circ Res* 74(1):163-171.
15. Orszag SA, Patera AT 1983 Secondary Instability of Wall-bounded Shear Flows. *J Fluid Mech* 128:347-385.

APPENDIX

The velocity profile for dynamic flow between parallel plates takes the form of equation [3] with:

$$C_1(y) = -\frac{\gamma}{2\mu} \left(y^2 - \frac{h^2}{4} \right) \quad [\text{A.1}]$$

$$C_2(y) = \frac{\gamma_o}{\rho\omega} \left[\frac{CC[\frac{1}{\lambda_v}(-y+h/2), \frac{1}{\lambda_v}(y+h/2)] + CC[\frac{1}{\lambda_v}(y+h/2), \frac{1}{\lambda_v}(-y+h/2)]}{cc_+(\frac{h}{\lambda_v})} - 1 \right] \quad [\text{A.2}]$$

$$C_3(y) = \frac{\gamma_o}{\rho\omega} \left[\frac{SS[\frac{1}{\lambda_v}(-y+h/2), \frac{1}{\lambda_v}(y+h/2)] + SS[\frac{1}{\lambda_v}(-y+h/2), \frac{1}{\lambda_v}(y+h/2)]}{cc_+(\frac{h}{\lambda_v})} \right] \quad [\text{A.3}]$$

where the following functions were defined:

$$\begin{aligned} SS(x_1, x_2) &= \sin(x_1)\sinh(x_2) \\ CC(x_1, x_2) &= \cos(x_1)\cosh(x_2) \\ ss_{\pm}(x) &= \sin(x) \pm \sinh(x) \\ cc_{\pm}(x) &= \cos(x) \pm \cosh(x) \end{aligned} \quad [\text{A.4}]$$

The phase difference between the velocity of a fluid layer and the pressure gradient is:

$$\sigma = \tan^{-1} \left(\frac{C_2(y)}{C_3(y)} \right) \quad [\text{A.5}]$$

when the velocity profile takes the form:

$$u(y, t) = C_1(y) + \sqrt{C_2(y)^2 + C_3(y)^2} \sin(\omega t + \sigma) \quad [\text{A.6}]$$

The oscillating wall shear stress calculated from the gradient of the velocity is then:

$$\tau_{wo} = \gamma_o \frac{\mu\alpha}{\rho\omega} \frac{\sqrt{ss_-^2(h/\lambda_v) + ss_+^2(h/\lambda_v)}}{cc_+(h/\lambda_v)} \sin(\omega t + \vartheta) \quad [\text{A.7}]$$

where the phase difference is:

$$\vartheta = \tan^{-1} \left(\frac{\frac{d}{dy} C_2(y)}{\frac{d}{dy} C_3(y)} \right)_{y=\pm\frac{h}{2}} = \tan^{-1} \left(\frac{ss_-(h/\lambda_v)}{ss_+(h/\lambda_v)} \right) \quad [\text{A.8}]$$

For an expression when the oscillating wall shear stress is related with the flow (see equation (4)), the phase difference is:

$$\psi = \tan^{-1} \left(\frac{\int_{-h/2}^{h/2} C_2(y) dy}{\int_{-h/2}^{h/2} C_3(y) dy} \right) = \tan^{-1} \left(\frac{\alpha h (cc_+(h/\lambda_v)) - ss_+(h/\lambda_v)}{ss_-(h/\lambda_v)} \right) \quad [A.9]$$

A smooth periodic continuous flow can be expanded into its Fourier series with an upper index indicating a “hard” limit giving a series termination at m , or a “soft” limit giving negligible terms after m :

$$Q(t) = Q_o + \sum_{n=1}^m [q_n^c \cos(2\pi f_o n t) + q_n^s \sin(2\pi f_o n t)] \quad [A.10]$$

The shear factor $T(h/\lambda_v)$ and the flow factor $K(h/\lambda_v)$, are derived from (A.7):

$$T(h/\lambda_v) = \frac{1}{6} \left(\frac{h/\lambda_v}{cc_+(h/\lambda_v)} \right) \left(\sqrt{\frac{\sin^2(h/\lambda_v) + \sinh^2(h/\lambda_v)}{1 - 2(\lambda_v/h) \frac{ss_+(h/\lambda_v)}{cc_+(h/\lambda_v)} - 2(\lambda_v/h)^2 \frac{cc_-(h/\lambda_v)}{cc_+(h/\lambda_v)}}} \right) \quad [A.11]$$

$$K(h/\lambda_v) = \frac{6}{(h/\lambda_v)^2} \left(1 - \frac{2}{(h/\lambda_v)} \right) \left(\frac{ss_+(h/\lambda_v)}{cc_+(h/\lambda_v)} \right) \quad [A.12]$$

LIST OF SYMBOLS

γ = constant pressure gradient component for dynamic fluid flow

γ_o = amplitude of the oscillating pressure gradient component for dynamic flow

ϑ = phase difference between the oscillating wall shear stress and the oscillating pressure gradient

h/λ_v = viscous penetration depth

μ = fluid viscosity

$\mu\epsilon$ = microstrain

ν = kinematic viscosity

ρ = fluid density

σ = phase difference between the velocity and the oscillating pressure gradient

τ_w = wall shear stress for steady flow

τ_{wo} = oscillating wall shear stress

τ_{wt} = total wall shear stress for dynamic flow

τ = fluid shear stress

ψ = phase difference between the wall shear stress and the oscillating flow

$\omega = 2\pi f$ = angular frequency

∇ = del operator

∇^2 = Laplacian operator

A_n = velocity field amplitudes in the summation term of the steady flow solution

b = PPFC width

c_n = velocity field function arguments in the summation term of the steady flow solution

f = flow frequency

f_c = critical frequency

F = external force density term

h = distance between the plates

K = flow factor

L = wetted length of the flow chamber

m = highest frequency mode

Pa = Pascal

p = pressure

q_o = amplitude of the oscillating flow component

Q or Q_o = flow

Re = Reynolds number

T = shear factor

u = velocity field

W_o = Wormesley number

x = length axis

y = height axis

z = width axis

CHAPTER 3

NITRIC OXIDE PRODUCTION BY BONE CELLS IS FLUID SHEAR STRESS RATE DEPENDENT

Rommel G. Bacabac¹, Theo H. Smit², Margriet G. Mullender¹, Saskia J. Dijcks¹, Jack J.W.A. Van Loon^{1,3}, Jenneke Klein-Nulend¹

¹Department of Oral Cell Biology, Academic Centre for Dentistry Amsterdam-Universiteit van Amsterdam and Vrije Universiteit, Amsterdam;

²Department of Physics and Medical Technology, VU University Medical Center, Amsterdam;

³Dutch Experiment Support Center, Vrije Universiteit, Amsterdam, The Netherlands

Biochemical Biophysical Research Communications 315:823-829, 2004

ABSTRACT

Shear stress due to mechanical loading-induced flow of interstitial fluid through the lacuno-canicular network is a likely signal for bone cell adaptive responses. Moreover, the rate (determined by frequency and magnitude) of mechanical loading determines the amount of bone formation. Whether the bone cells' response to fluid shear stress is rate dependent is unknown. Here we investigated whether bone cell activation by fluid shear stress is rate dependent. MC3T3-E1 osteoblastic cells were subjected for 15 min to fluid shear stress of varying frequencies and amplitudes, resulting in peak fluid shear stress rates ranging from 0 to 39.6 Pa-Hz. Nitric oxide production, a parameter for bone cell activation, was found to be linearly dependent to the fluid shear stress rate; the slope was steepest at 5 min (0.11 Pa-Hz^{-1}), and decreased to 0.03 Pa-Hz^{-1} at 15 min. We conclude that the fluid shear stress rate is an important parameter for bone cell activation.

INTRODUCTION

Bone as a living tissue has long been recognized to be capable of adapting its mass and structure in response to the demands of mechanical loading (Wolff's Law) (1, 2). However, the underlying cellular processes remain poorly understood. It has been postulated that due to loading and unloading, extracellular fluid flows through the lacuno-canalicular network to the bone surface and back (3). Streaming potentials measured on loaded bone confirmed the transfer of ions due to fluid movement in bone (4). The loading-induced movement of labeled molecules of varying sizes directly demonstrated fluid flow in the mineralized matrix of bone, both *in vivo* and *ex vivo* (5, 6). The flow of interstitial fluid through the lacuno-canalicular network induces shear stress on the membrane of bone cells. This shear stress is a likely candidate signal for bone cell adaptive responses (7-10). Bone cells respond to fluid flow stimulation *in vitro* (11-18). They are sensitive to fluid shear stress (16, 18), rather than to streaming potentials mediated by the transport of ions with the flow (18). Bone cells are also more responsive (in terms of nitric oxide (NO) and prostaglandin E₂ production) to shear stress by fluid flow stimulation than to direct mechanical strain by substrate stretching (19, 20). However, how fluid shear stress activates bone cells is not well understood.

The fluid shear stress amplitudes and frequencies in bone can be determined theoretically from known physiological loading parameters. By applying Biot's theory of poroelasticity to bone, the predicted range of *in vivo* fluid shear stress ranges from 0.8 – 3 Pa due to loading-induced strains ranging between 1000 – 3000 $\mu\epsilon$ (21, 22). That this range of fluid shear stress magnitudes is enough to stimulate bone cells, was confirmed by *in vitro* studies (11-17).

Several studies have suggested that the rate (determined by the frequency and amplitude) rather than the magnitude alone of the applied loading stimulus correlates to bone formation (23, 24). This implies that bone formation is essentially enhanced by dynamic loading. Thus, both the magnitude (or

amplitude) and the frequency of loading are important parameters for bone formation. Indeed, it has been shown that low magnitude ($< 10 \mu\epsilon$), high frequency (10 – 100 Hz) loading is capable of stimulating bone growth and inhibiting disuse osteoporosis (25). Furthermore, it has been shown that high-amplitude, low-frequency stimuli are rare in the activities of daily life, whereas high-frequency, low-amplitude stimuli are common (26). High rates of loading, as in high impact physical activity including jumps in unusual directions, have a great osteogenic potential in humans (27) and in osteopenic ovariectomized rats (28). High stress rate, as in step-wise increased fluid shear stress, was also shown to stimulate neonatal rat calvarial bone cells (29). Therefore, the osteogenic response to high impact activity might be related to the response of bone cells to a sudden increase (i.e., high rate) in fluid shear stress. The rate of loading seems to be a decisive factor in bone formation and maintenance. However, how bone cells respond to the rate of loading is not well understood.

In this study, we investigated the response of bone cells to varying rates of fluid shear stress. We used NO production as a parameter for bone cell activation since it is an early mediator of mechanical loading-induced bone formation (30). Furthermore, NO has been shown to be essential to adaptive bone formation *in vivo* (31). To our knowledge this is the first study that aimed at a quantitative relationship between bone cell activation and the rate of fluid shear stress.

MATERIALS AND METHODS

Bone cell cultures

MC3T3-E1 cells were cultured up to near-confluence in 75 cm² cell culture flasks (Nunc, Roskilde, Denmark), using α -Modified Eagle's Medium (α -MEM; Gibco, Paisley, UK) supplemented with 10% fetal bovine serum (FBS; Gibco), ascorbate (50 µg/ml; Merck, Darmstadt, Germany), β -

glycerophosphate disodium salt hydrate (10 mM; Sigma, St. Louis, MO, USA), l-glutamine (300 µg/ml; Merck), gentamycine (50 µg/ml; Gibco), fungizone (1.25 µg/ml; Gibco). Cells were then harvested and seeded at 2×10^5 cells per polylysine-coated (50 µg/ml; poly-L-lysine hydrobromide; Sigma) glass slide (5 cm²), and incubated overnight in α-MEM with 10% FBS to promote cell attachment, at 37°C with 5% CO₂ in air, prior to fluid shear stress experimental treatment as described below.

Calculation of frequency spectra after loading

To determine the precise flow regimes to stimulate bone cells (as described under Fluid shear stress), we first calculated the frequency spectra after loading of bone (Fig. 1). We used the results from the studies of Bergmann et al. (32), in which forces on a human hip were measured using strain sensors. The frequency spectra of the resultant forces on the hip showed a rich harmonic content ranging between 1-3 Hz for walking cycles, and reaching 8-9 Hz for running cycles (Fig. 1).

NO response by bone cells is fluid shear stress rate dependent

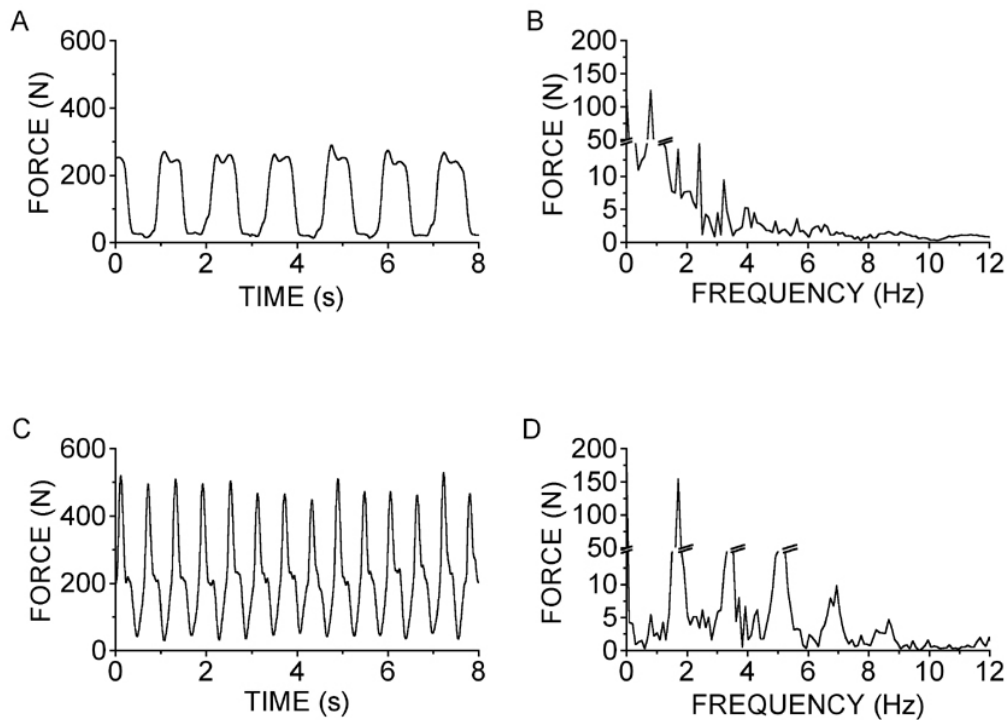


Figure 1. Hip joint forces. A. Resultant force on the left hip joint of a male human subject (62 kg.) as a function of time, measured by implanted sensors inside a femur at normal walking on a treadmill (2 km/h). B. The frequency spectrum of the resultant hip joint force due to normal walking. C. Resultant force on the hip as a function of time at jogging pace on a treadmill (8 km/h). D. The frequency spectrum of the resultant force due to jogging pace. Data taken with permission from Bergmann and co-workers (25).

Fluid shear stress

Pulsating fluid shear stress was generated using a flow apparatus containing a parallel plate flow chamber (PPFC) as described earlier (14, 33, 34). Fluid shear stress was induced on the monolayer of cells attached to the polylysine-coated glass slide serving as the bottom of the parallel plate flow chamber, by circulating 9 ml of α -MEM containing 2% FBS plus supplements as described above using a computer-controlled micro annular gear pump (developed by HNP Mikrosysteme GmbH, Parchim, Germany). Precise flow regimes (see Table 1 and Fig. 2) were implemented by controlling the pump using

computer-mediated instrumentation by LabViewTM (National Instruments Corp., Austin, Texas, USA). The flow through the PPFC was monitored online using a small animal blood flowmeter (T206, Transonic Systems Inc., Ithaca, New York, USA).

Table 1. Data of applied pulsating fluid shear stress (PFSS) regimes

Regime	5 Hz lo	5 Hz hi	9Hz lo	9Hz hi	steady
mean shear stress (Pa)	0.70	0.70	0.70	0.70	0.70
pulse amplitude (Pa)	0.31	0.70	0.31	0.70	0
*peak fluid shear stress rate (Pa-Hz)	9.70	22.0	17.5	39.6	0
average flow (ml/min)	8.30	8.30	8.30	8.30	8.30

lo, low amplitude; hi, high amplitude; steady, steady flow.

*peak fluid shear stress rate = pulse amplitude x frequency x (2π) .

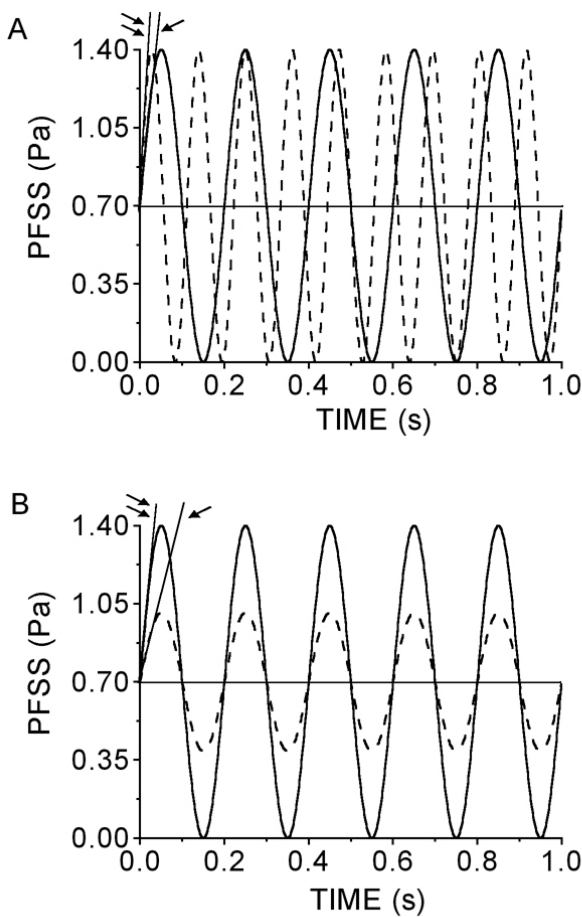


Figure 2. Fluid shear stress regimes applied to bone cells for 15 min. Only 1 s duration of the regimes are shown. A. The slope of the lines equals the peak fluid shear stress rate. The rate increases with higher flow regime frequency (double arrows, 9 Hz high amplitude; single arrow, 5 Hz high amplitude; solid line, 5 Hz; dashed line, 9 Hz). The steady flow regime is constant at 0.7 Pa, hence having zero rate. B. The peak fluid shear stress rate is also varied by changing the amplitude from a 0.31 Pa to 0.70 Pa (double arrows, 5 Hz high amplitude; single arrow, 5 Hz low amplitude; solid line, high amplitude; dashed line, low amplitude).

During the shear stress experiment the flow apparatus was placed in a 37°C incubator, and connected to a gassing system that maintained a pH of 7.4 in the medium using 5% CO₂ in air. For the PFFS experiments, the culture medium was changed to α-MEM with 2% FBS plus supplements as described above (fluid viscosity = 0.69×10^{-4} Pa·s). Cells were incubated for 15 min in the

presence of: 1) steady fluid shear stress (0.70 Pa), 2) low amplitude pulsating fluid shear stress (PFSS, 0.70 ± 0.31 Pa) at two different frequencies (5 Hz or 9 Hz), and 3) high amplitude pulsating fluid shear stress (0.70 ± 0.70 Pa, 5 Hz or 9 Hz), 4) no shear stress (static controls) (Table 1). Medium samples were taken at 5, 10 and 15 min for measuring the response to fluid flow parameterized as production of NO in the medium.

The PPFC was designed such that it is capable of inducing high frequency fluid shear stress on the cells (33). The PPFC geometry and the flow frequencies that were utilized allowed for the use of the formula: $\tau = 6\mu Q/(bh^2)$ under dynamic flow. This formula is used to calculate the peak fluid shear stress τ (acting on the cells), due to a flow Q , in a chamber of width b and plate separation h , with a fluid of viscosity μ .

Nitric Oxide determination

The conditioned medium was assayed for NO, which was measured as nitrite (NO_2^-) accumulation in the conditioned medium, using Griess reagent (1% sulfanilamide, 0.1% naphtylethylene-diamine-dihydrochloride, and 2.5 M H_3PO_4). The absorbance was measured at 540 nm. NO concentrations were determined using a standard curve derived from known concentrations of NaNO_2 in non-conditioned culture medium. Data from separate experiments were collected and normalized with respect to static controls, and expressed as treatment-over-control (T/C) ratios, or as absolute values where indicated.

Statistics

Data were pooled from the results of at least five experiments for each fluid shear stress regime tested (Table 1). The effects of treatment with fluid shear stress were analyzed with the non-parametric Wilcoxon rank sum test of the S-Plus 2000 package (release 1). Differences were considered significant at a p value <0.05 . The relation between NO production and the peak rate of fluid shear stress was analyzed by linear regression.

RESULTS

Application of fluid flow for 15 min to the MC3T3-E1 cells did not result in visible changes in cell shape or alignment of the cells in the direction of the fluid flow (data not shown). No cells were removed by any of the fluid shear stress regimes, as assessed by visually inspecting the cultures before and after fluid shear stress treatment, and by measuring the total amount of DNA (control, 261 ± 19 ng; PFSS, 279 ± 27 ng; mean \pm SEM of 6 experiments).

The NO response of MC3T3-E1 cells to a fluid shear stress with zero rate was first studied separately, by culturing cells under steady flow conditions (Table 1, Fig. 3). MC3T3-E1 cells treated with a steady fluid shear stress of 0.70 Pa showed a significantly increased NO release as compared to static control cultures within the first five minutes of treatment (Fig. 3A), but not thereafter. The 2-fold increase in NO production in response to steady shear stress remained significant during the 15 minute treatment period (Fig. 3B).

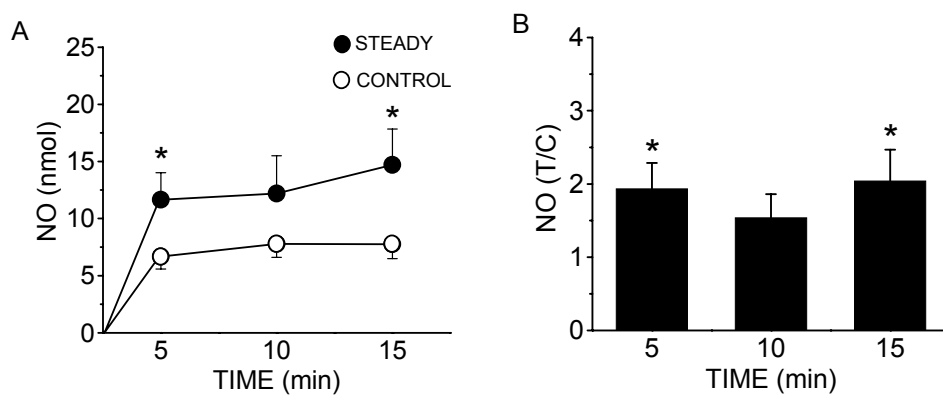


Figure 3. Effect of steady fluid shear stress on the NO production by MC3T3-E1 bone cells. A. The absolute amount of NO production by bone cells subjected to steady fluid shear stress, increased after 5 min and continued thereafter as compared to control cultures not subjected to flow. B. Treatment-over-control ratios showed that the response to steady shear stress increases 2-fold throughout 15 min. $*p < 0.05$.

To study the effect of the fluid shear stress amplitude and frequency on the NO response of the bone cells, they were subjected to varying pulsating fluid shear stress (PFSS) regimes (see Table 1). The NO response to PFSS became higher with increasing shear stress amplitude after 5, 10 and 15 min of treatment (Fig. 4). In addition, the NO response was more pronounced at higher frequencies (Fig. 4). Treatment with 5 Hz lo (low amplitude; see Table 1) elicited a comparable 2-fold increase in NO response by the cells as steady fluid shear stress within the first 5 min (Fig. 4). Treatment with 9 Hz lo caused a rapid 3-fold increase of NO after 5 min, as did treatment with 5 Hz hi (high amplitude; see Table 1). Treatment with 9 Hz hi elicited the highest, 5-fold, increase in NO production after 5 min (Fig. 4). So, high amplitude PFSS (5 Hz or 9 Hz hi) elicited a higher level of NO production than low amplitude PFSS (Fig. 4). Similarly, high frequency PFSS (9 Hz) treatment elicited a higher NO response by bone cells than low frequency PFSS (5 Hz), despite having the same fluid shear stress average. Thus, both the applied frequency and amplitude of PFSS affected the response of MC3T3-E1 bone cells.

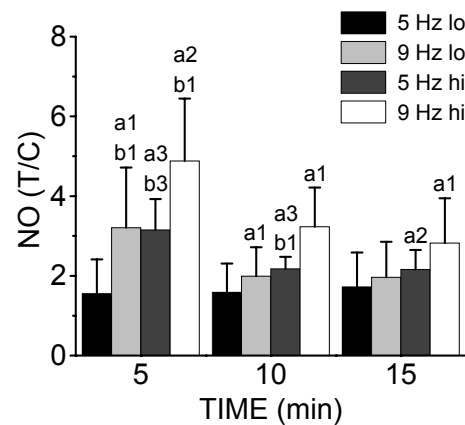


Figure 4. Effect of PFSS frequency and amplitude on the NO production by MC3T3-E1 bone cells during 15 min. NO production was between 0.31 to 0.90 μM per 2×10^5 cells for all cell cultures without fluid shear stress treatment. The effect of fluid shear stress on NO production is maximal within 5 min of treatment for all PFSS regimes. Treatment with high amplitude (or frequencies) elicited higher NO production than low amplitude (or frequencies). Values are mean treatment-over-control ratios (T/C) \pm SEM. lo, low amplitude (0.31 Pa); hi, high amplitude (0.70 Pa). ^aSignificantly different from 1.0: a1, $p < 0.05$; a2, $p < 0.01$; a3, $p < 0.006$. ^bSignificantly different from 5 Hz low amplitude: b1, $p < 0.05$; b2, $p < 0.01$; b3, $p < 0.006$.

NO response by bone cells is fluid shear stress rate dependent

Next we tested whether there was a correlation between the fluid shear stress rate and the NO response of the bone cells (Fig. 5). At 5 min MC3T3-E1 bone cells reacted to the application of a fluid shear stress rate of 21.99 Pa-Hz (5 Hz hi) with a 3-fold enhanced NO production ($p<0.02$), similar to the bone cell's response to a comparable shear rate of 17.53 Pa-Hz (9 Hz lo) (Fig. 5A). At 5 and 10 min the NO production was linearly related with the peak rate of the PFSS (Fig. 5A,B). At 15 min there was still a trend of a linear relationship (Fig. 5C). This means that a higher PFSS rate induced a higher NO production.

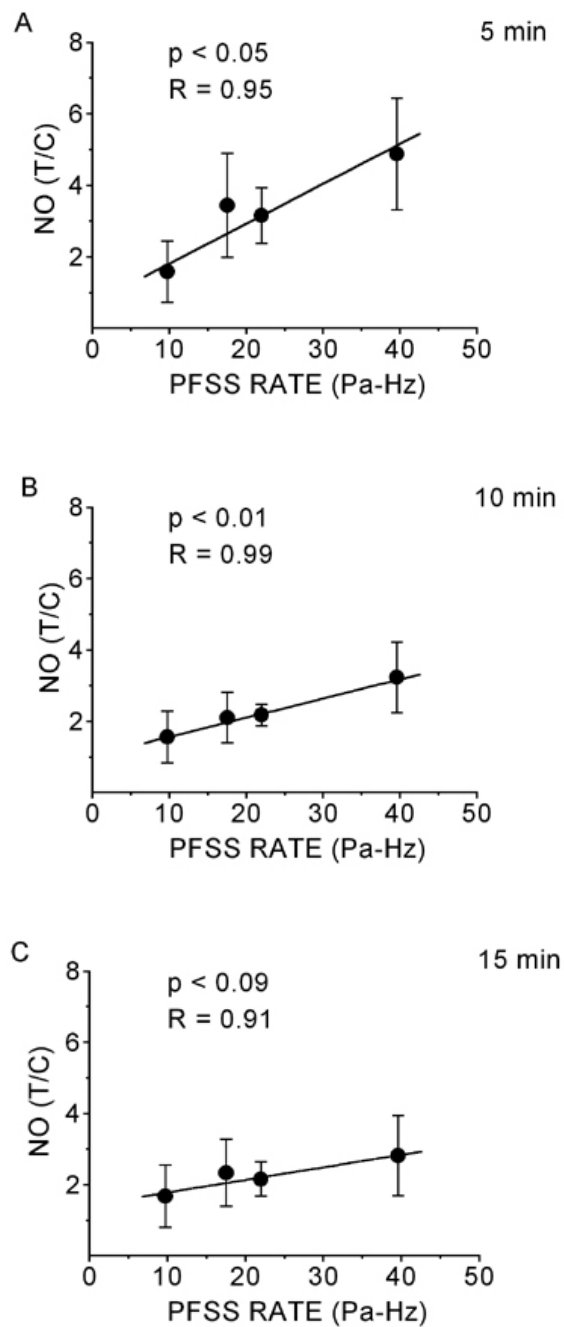


Figure 5. Nitric oxide production by bone cells is linearly proportional to the rate of fluid shear stress. The steepest slope was found at 5 min ($0.11 \text{ Pa}\cdot\text{Hz}^{-1}$), indicating that the highest bone cell response to fluid shear stress rate occurs rapidly. At 10 and 15 min, NO levels were lower than those found at 5 min. Values are mean treatment-over-control ratios (T/C) \pm SEM.

The slope of the linear curve relating the NO production to the PFSS rate indicates the magnitude of the bone cell response (Fig. 5A-C). The slope was 0.11 Pa-Hz^{-1} (or 2-fold per 20 Pa-Hz) at the 5-min time point (Fig. 5A), and decreased to 0.05 Pa-Hz^{-1} and 0.03 Pa-Hz^{-1} at the 10-min and 15-min time points respectively (Fig. 5B,C). Therefore, the NO production response to PFSS by bone cells was highest immediately after 5 min after the onset of flow (Fig. 5).

DISCUSSION

The present study suggests that the bone cell response to fluid shear stress is rate- dependent. Increasing either shear stress amplitude or frequency, without increasing the average stress, enhanced NO production by bone cells *in vitro*. Bone cells responded similarly to similar rates of fluid shear stress, despite different frequencies (5 Hz, 21.99 Pa-Hz or 9 Hz, 17.53 Pa-Hz). Hence, a useful parameter for predicting a proportional increase of NO production of bone cells by fluid flow is the peak rate of fluid shear stress, which is proportional to the product of the fluid shear stress amplitude and frequency.

Our results support the notion that bone formation is stimulated by dynamic rather than static loads (34), and that low magnitude, high frequency mechanical stimuli may be as stimulatory as high-amplitude, low frequency stimuli. Low amplitude, high frequency loading in bone has been shown to occur more often in normal daily activities *in vivo* (26). Since we showed that bone cells are responsive to the rate of loading, high frequency, low amplitude strain-derived fluid shear stresses might be enough to stimulate the cells. This could then result in adaptive bone formation. Hence, the finding that the bone cell's response to fluid shear stress is rate dependent provides an explanation why adaptive bone formation can occur despite the sporadic occurrence of high amplitude strains in daily life (26). The application of vibration on bone *in vivo*

and bone cells *in vitro* has been shown to elicit adaptive responses (35, 36). Vibration, or low amplitude, broad frequency spectrum stimulation, was shown to enhance the osteogenic response of bone *in vivo* (35). In addition, osteoblasts cultured on collagen gels, were shown to be more sensitive to low amplitude, broad frequency vibration than sinusoidal strain alone (36). In these studies vibratory stimulation on bulk specimen did not account for the direct forces acting on bone cells (35, 36), while in our current investigation we directly applied a homogenous fluid shear stress on a monolayer of bone cells. Therefore our study provides a cellular basis for explaining the role of the rate of loading on bone formation as observed *in vivo* (23, 24, 37).

Steady, non-dynamic shear stress provides a zero shear rate, but in the present study it elicited, like dynamic fluid shear stress regimes, also a significant NO response by bone cells. However, when the steady shear stress was applied, the cells experienced a sudden increase of fluid shear stress from 0 to 0.70 Pa by switching on the pump. This sudden increase in stress gave a very high rate of stress, which probably was sufficient to elicit a strong response by the bone cells. This also confirms our finding that the cellular response to shear stress is rate-dependent.

The NO production by bone cells in response to fluid shear stress was rapid (i.e., within 5 min). The slope relating bone cell activation and fluid shear stress rate was highest after 5 min of stimulation, and decreased afterwards. The slope of NO production against the peak PFSS rate indicates how much NO is produced per unit of peak PFSS rate. Since this slope was highest within the first 5 min of stimulation (2-fold increase of NO production per 20 Pa-Hz), bone cells were responsive to PFSS quite rapidly and the response declined thereafter. This suggests that a continuous bone cell stimulation might not be necessary to maintain bone mass and structure. Hence, the rare occurrence of high strains *in vivo* is not necessarily predictive of bone loss. The rapid NO response by bone cells to fluid shear stress indicates a possible mechanism by

NO response by bone cells is fluid shear stress rate dependent

which bone can make use of rarely occurring high amplitude strains to maintain proper metabolism.

Based on both the rapid and rate dependent response of bone cells to fluid shear stress, bone loss after prolonged bed rest (37) or microgravity (38) might depend on other factors aside from the lack of loading itself. Our results might suggest that if that bone cells do not require continuous loading to maintain bone mass and structure, then sporadic bouts of exercise should fully counteract bone loss under conditions of prolonged unloading. However, full recovery from bone loss does not always occur (39, 40). Thus, the observation of bone loss after prolonged bed rest or under microgravity suggests another cellular mechanism that might be impaired under such conditions (41).

Our finding that the bone cell response to fluid shear stress, in terms of NO production, is rapid and rate-dependent, might further the description and prediction of bone loss by existing theoretical models (42, 43). Although these models considered cellular activity, a truly dynamic simulation of adaptive bone formation, incorporating how fast bone cells produce signaling molecules, and build or resorb bone has yet to be attempted. Our results might provide a basis for a dynamic simulation of adaptive bone formation for predicting bone loss under environments of unloading as in prolonged bed rest or microgravity.

The transfer of forces from the effects of loading on the whole bone tissue, down to the cellular level might be complex, however our results clearly indicate that dynamic loading plays an essential role for the activation of bone cells. We conclude that NO production by bone cells subjected to fluid flow is linearly dependent on the rate of fluid shear stress. Both the amplitude and frequency of stress contribute to the flow-induced activation of bone cells.

ACKNOWLEDGEMENTS

The authors would like to thank C.M. Semeins for his technical assistance. The Space Research Organization of the Netherlands supported the work of R.G. Bacabac (SRON grant MG-055) who also received financial assistance from the Netherlands Organization For International Cooperation In Higher Education (Physics Development Project PHL-146). The European Community supported the work of J. Klein-Nulend (fifth framework grant QLK3-1999-00559).

REFERENCES

1. Wolff J 1892 Gesetz der transformation der knochen, Hirschwald, Berlin.
2. Wolff J 1986 The law of bone remodelling, Springer, Berlin.
3. Piekarski K, Munro M 1977 Transport mechanism operating between blood supply and osteocytes in long bones. *Nature* 269(5623):80-82.
4. Starkebaum W, Pollack SR, Korostoff E 1979 Microelectrode studies of stress-generated potentials in four-point bending of bone. *J Biomed Mater Res* 13(5):729-751.
5. Knothe Tate ML, Niederer P, Knothe U 1998 In Vivo Tracer Transport Through the Lacunocanicular System of Rat Bone in an Environment Devoid of Mechanical Loading. *Bone* 22(2):107-117.
6. Knothe Tate ML, Knothe U 2000 An ex vivo model to study transport processes and fluid flow in loaded bone. *J Biomech* 33(2):247-254.

NO response by bone cells is fluid shear stress rate dependent

7. Cowin SC, Moss-Salentijn L, Moss ML 1991 Candidates for the mechanosensory system in bone. *J Biomech Eng* 113(2):191-197.
8. Burger EH, Klein-Nulend J, Cowin SC 1998 Mechanotrasduction in bone. *Adv Org Biol* 5A:123-136.
9. Burger EH, Klein-Nulend J 1999 Mechanotransduction in bone - Role of the lacuno-canalicular network. *FASEB J* 13(Supplement):S101-S112.
10. Smit TH, Burger EH, Huyghe JM 2002 A case for strain-induced fluid flow as a regulator of BMU-coupling and osteonal alignment. *J Bone Min Res* 17(11):2021-2029.
11. Frangos JA, Johnson D 1995 Fluid flow in bone: stimulated release at remodeling mediators. *Biorheology* 32(2-3):187.
12. Klein-Nulend J, Semeins CM, Ajubi NE, Nijweide PJ, Burger EH 1995 Pulsating fluid flow increases nitric oxide (NO) synthesis by osteocytes but not periosteal fibroblasts--correlation with prostaglandin upregulation. *Biochem Biophys Res Commun* 217(2):640-648.
13. Klein-Nulend J, Roelofsen J, Sterck JGH, Semeins CM, Burger EH 1995 Mechanical loading stimulates the release of transforming growth factor-beta activity by cultured mouse calvariae and periosteal cells. *J Cell Physiol* 163(1):115-119.
14. Klein-Nulend J, van der Plas A, Semeins CM, Ajubi NE, Frangos JA, Nijweide PJ, Burger EH 1995 Sensitivity of osteocytes to biomechanical stress in vitro. *FASEB J* 9(5):441-445.

15. Johnson DL, McAllister TN, Frangos JA 1996 Fluid flow stimulates rapid and continuous release of nitric oxide in osteoblasts. *Am J Physiol* 271(1):E205-E208.
16. Jacobs CR, Yellowley CE, Davis BR, Zhou Z, Cimbala JM, Donahue HJ 1998 Differential effect of steady versus oscillating flow on bone cells. *J Biomech* 31(11):969-976.
17. Chen NX, Ryder KD, Pavalko FM, Turner CH, Burr DB, Qiu J, Duncan RL 2000 Ca(2+) regulates fluid shear-induced cytoskeletal reorganization and gene expression in osteoblasts. *Am J Physiol Cell Physiol* 278(5):C989-C997.
18. Bakker AD, Soejima K, Klein-Nulend J, Burger EH 2001 The production of nitric oxide and prostaglandin E2 by primary bone cells is shear stress dependent. *J Biomech* 34(5):671-677.
19. Owan I, Burr DB, Turner CH, Qiu J, Tu Y, Onyia JE, Duncan RL 1997 Mechanotransduction in bone: osteoblasts are more responsive to fluid forces than mechanical strain. *Am J Physiol* 273(3 Pt 1):C810-C815.
20. Smalt R, Mitchell FT, Howard RL, Chambers TJ 1997 Induction of NO and prostaglandin E2 in osteoblasts by wall-shear stress but not mechanical strain. *Am J Physiol* 273(4 Pt 1):E751-E758.
21. Weinbaum S, Cowin SC, Zeng Y 1994 A model for the excitation of osteocytes by mechanical loading-induced bone fluid shear stresses. *J Biomech* 27(3):339-360.
22. Cowin SC 1999 Bone poroelasticity. *J Biomech* 32(3):217-238.

23. Turner CH, Owan I, Takano Y 1995 Mechanotransduction in bone: role of strain rate. *Am J Physiol* 269(3 Pt 1):E438-E442.
24. Mosley JR, Lanyon LE 1998 Strain rate as a controlling influence on adaptive modeling in response to dynamic loading of the ulna in growing male rats. *Bone* 23(4):313-318.
25. Rubin CT, Sommerfeldt DW, Judex S, Qin YX 2001 Inhibition of osteopenia by low magnitude, high-frequency mechanical stimuli. *Drug Discov Tod* 6(16):848-858.
26. Fritton SP, McLeod J, Rubin CT 2000 Quantifying the strain history of bone: spatial uniformity and self-similarity of low-magnitude strains. *J Biomech* 33(3):317-325.
27. Nordstrom P, Pettersson U, Lorentzon R 1998 Type of physical activity, muscle strength, and pubertal stage as determinants of bone mineral density and bone area in adolescent boys. *J Bone Miner Res* 13(7):1141-1148.
28. Tanaka M, Ejiri S, Nakajima M, Kohno S, Ozawa H 1999 Changes of cancellous bone mass in rat mandibular condyle following ovariectomy. *Bone* 25(3):339-347.
29. Williams JL, Iannotti JP, Ham A, Bleuit J, Chen JH 1994 Effects of fluid shear stress on bone cells. *Biorheology* 31(2):163-170.
30. Fox SW, Chambers TJ, Chow JWM 1996 Nitric oxide is an early mediator of the increase in bone formation by mechanical stimulation. *Am J Physiol* 33(6):E955-E960.

31. Turner CH, Takano Y, Owan I, Murrell GA 1996 Nitric oxide inhibitor L-NAME suppresses mechanically induced bone formation in rats. Am J Physiol 270(4 Pt 1):E634-E639.
32. Bergmann G, Graichen F, and Rohlmann A. Hip joint force measurements. <http://www.medizin.fu-berlin.de/biomechanik/Homeframe.htm> . 3-6-2003.
33. Bacabac RG, Smit TH, Heethaar RM, Van Loon JJWA, Pourquie MJMB, Nieuwstadt FTM, Klein-Nulend J 2004 Characteristics of the parallel-plate flow chamber for mechanical stimulation of bone cells under microgravity. J Gravit Physiol 9:P181-P182.
34. Rubin CT, Lanyon LE 1984 Regulation of bone formation by applied dynamic loads. J Bone Joint Surg Am 66(3):397-402.
35. Tanaka SM, Alam I, Turner CH 2002 Stochastic resonance in osteogenic response to mechanical loading. FASEB J :02-0561fje.
36. Tanaka SM, Li J, Duncan RL, Yokota H, Burr DB, Turner CH 2003 Effects of broad frequency vibration on cultured osteoblasts. J Biomech 36(1):73-80.
37. Schneider VS, McDonald J 1984 Skeletal calcium homeostasis and countermeasures to prevent disuse osteoporosis. Calcif Tiss Int 36(Suppl 1):S144-S151.
38. Van Loon JJWA, Veldhuijzen JP, Burger EH 1996 Bone and space flight: an overview, in Biological and medical research in space. In: Moore D, Bie P, Oser H (eds) Springer, Berlin, Germany, pp. 259-299.

NO response by bone cells is fluid shear stress rate dependent

39. Zerath E, Novikov V, LeBlanc A, Bakulin A, Oganov V, Grynpas M 1996 Effects of spaceflight on bone mineralization in the rhesus monkey. *J Appl Physiol* 81:194-200.
40. Vico L, Lafage-Proust MH, Alexandre C 1998 Effects of gravitational changes on the bone system in vitro and in vivo. *Bone* 22(Suppl 5):95S-100S.
41. Burger EH, Klein-Nulend J 1998 Microgravity and bone cell mechanosensitivity. *Bone* 22(5 Suppl):127S-130S.
42. Huiskes R, Ruimerman R, van Lenthe GH, Janssen JD 2000 Effects of mechanical forces on maintenance and adaptation of form in trabecular bone. *Nature* 405:704-706.
43. Ruimerman R, Van Rietbergen B, Huiskes R 2003 A 3-dimensional computer model to simulate trabecular bone metabolism. *Biorheol* 40:315-320.

CHAPTER 4

INITIAL STRESS-KICK IS REQUIRED FOR FLUID SHEAR STRESS-INDUCED RATE DEPENDENT ACTIVATION OF BONE CELLS

Rommel G. Bacabac¹, Theo H. Smit², Margriet G. Mullender¹, Jack J.W.A. Van Loon^{1,3}, Jenneke Klein-Nulend¹

¹Department of Oral Cell Biology, Academic Centre for Dentistry Amsterdam - Universiteit van Amsterdam and Vrije Universiteit, Amsterdam, The Netherlands

²Department of Clinical Physics and Informatics, VU University Medical Center, Amsterdam, The Netherlands

³Dutch Experiment Support Center, Vrije Universiteit, Amsterdam, The Netherlands

Annals of Biomedical Engineering 33:104-110, 2005

ABSTRACT

The shear stress induced by the loading-mediated flow of interstitial fluid through the lacuno-canalicular network is a likely stimulus for bone cell adaptive responses. Furthermore, the magnitude of the cellular response is related to the rate of mechanical loading rather than its magnitude. Thus, bone cells might be very sensitive to sudden stress-kicks, as occurring e.g., during impact loading. There is evidence that cells change stiffness under stress, which might make them more sensitive to subsequent loading. We studied the influence of a stress-kick on the mechanosensitivity of MC3T3-E1 osteoblast-like cells under different peak shear rate conditions, as measured by nitric oxide production. MC3T3-E1 bone cells were treated with steady or pulsating fluid shear stress (PFSS) for 5 min with different peak rates (9.70 Pa-Hz, 17.5 Pa-Hz, and 22.0 Pa-Hz) using varying frequencies (5 Hz, 9 Hz), and amplitudes (0.70 Pa, 0.31 Pa). PFSS treatment was done with or without fluid flow pre-treatment phase, which removed the initial stress-kick by first applying a slow fluid flow increase. Nitric oxide production in response to fluid shear stress was rate dependent, but necessitated an initial stress-kick to occur. This suggests that high-rate stimuli condition bone cells to be more sensitive for high-frequency, low-amplitude loads.

INTRODUCTION

During life, bones adapt their mass and structure to the prevailing mechanical loads, in order to resist mechanical failure with minimum material expense. It is currently believed that this process of adaptation is governed by osteocytes, which respond to the loading-induced flow of interstitial fluid through the lacuno-canalicular network (1). When bones are loaded, the resulting deformation will drive the thin layer of interstitial fluid surrounding the network of osteocytes within the calcified bone matrix to flow from regions under high pressure to regions under low pressure (2, 3). The loading-induced movement of labeled molecules directly demonstrated fluid flow in the mineralized matrix of bone both *in vivo* (4) and *ex vivo* (5). Osteocytes have been proven to be sensitive to this type of fluid shear stress (6). Subsequently, the osteocytes may signal the osteoblasts and osteoclasts to change their bone remodeling activities (1, 7).

Bone cells (osteocytes, and to a lesser extent also osteoblasts) respond to fluid flow stimulation *in vitro* (6, 8-15). They are sensitive to fluid shear stress (9, 16), rather than to streaming potentials mediated by the transport of ions with the flow (17, 18). Bone cells are also more responsive to shear stress by fluid flow stimulation than to direct mechanical strain by substrate stretching (19-21). Bone cells respond to fluid flow with increased nitric oxide (NO) and prostaglandin E₂ production, which are essential for the induction of new bone formation in reaction to mechanical loading *in vivo* (22, 23). In particular, we have recently found that MC3T3-E1 osteoblastic cells produce NO in response to fluid shear stress in a rate dependent manner (8). Since osteoblasts respond to fluid shear stress as osteocytes, although to a lesser extent, osteoblasts could provide a practical model for osteocyte response to fluid shear stress. However, how bone cell sensitivity is modulated by the various flow parameters (amplitude, frequency, duration, etc.) is not well understood.

The fluid shear stress amplitudes and frequencies in bone can be determined theoretically from known physiological loading parameters. By applying Biot's theory of poroelasticity to bone, the predicted range of *in vivo* fluid shear stress ranges from 0.8 – 3 Pa due to loading-induced strains ranging between 1000 – 3000 $\mu\epsilon$ (3, 24). Several *in vitro* studies (6, 8-15) have confirmed that this range of fluid shear stress magnitudes is able to stimulate bone cells.

It has been suggested that the rate (determined by the frequency and amplitude) rather than the magnitude alone of the applied loading stimulus correlates to bone formation (8, 25, 26). This implies that bone formation is enhanced by dynamic loading. Thus, both the magnitude (or amplitude) and the frequency of loading seem to be important parameters for bone formation. Indeed, it has been shown that low magnitude ($< 10 \mu\epsilon$), high-frequency (10 – 100 Hz) loading is capable of stimulating bone growth and inhibiting disuse osteoporosis (27). Furthermore, it has been shown that high-amplitude, low-frequency stimuli are rare in the activities of daily life, whereas high-frequency, low-amplitude stimuli are common (28). The rate of loading seems to be a decisive factor in bone formation and maintenance. However, how bone cells respond to the rate of loading is not well understood.

High impact physical activity, including jumps in unusual directions, has a great osteogenic potential in humans (29) and in osteopenic ovariectomized rats (30). High impact drop jumps were shown to significantly increase bone formation rates compared to that of baseline walking (31). Furthermore, an initial high stress rate, as in step-wise increased fluid shear stress, was shown to stimulate neonatal rat calvarial bone cells (32). Therefore, the osteogenic response to high impact activity might be related to the response of bone cells to a sudden increase (i.e., stress-kick) in fluid shear stress. The osteogenic benefits of high impact activity might imply that the bone cell response to fluid shear stress is non-linear.

Tanaka and colleagues (33) showed that stochastic resonance enhances bone formation. Stochastic resonance is a phenomenon by which non-linear systems

are able to amplify a response to small periodic stimuli with the aid of noise (34). Stochastic resonance has been used to explain various phenomena in biological systems (34, 35) including the activity of cells under microgravity (36). During exercise, as in active sports, bone is subjected to quick variations in loading, which is equivalent to a noisy loading environment. Therefore, the possibility arises that bone cells are more responsive to fluid shear stress mediated by high impact activity compared to low impact activity. If so, the bone cell response to fluid shear stress might be non-linear, that is, requiring an initial stress-kick.

In this study, we investigated whether an initial stress-kick is required for the response of bone cells to varying rates of fluid shear stress. The initial stress-kick occurs during the quick transition from 0 to a non-zero stress initiating a fluid shear stress stimulation of cells. We used NO production as a parameter for bone cell activation since it is an early mediator of mechanical loading-induced bone formation (37), and it has been shown to be essential to adaptive bone formation *in vivo* (23).

MATERIALS AND METHODS

Bone cell cultures

MC3T3-E1 cells (Kodama, et al, 1981; kindly provided by Dr. Kumegawa, Mekai University School of Dentistry, Sakado, Saitama, Japan) were cultured up to near-confluence in 75 cm² cell culture flasks (Nunc, Roskilde, Denmark), using α -Modified Eagle's Medium (α -MEM; Gibco, Paisley, UK) supplemented with 10% fetal bovine serum (FBS; Gibco), ascorbate (50 µg/ml; Merck, Darmstadt, Germany), β -glycerophosphate disodium salt hydrate (10 mM; Sigma, St. Louis, MO, USA), L-glutamine (300 µg/ml; Merck), gentamycin (50 µg/ml; Gibco), fungizone (1.25 µg/ml; Gibco), at 37°C with 5% CO₂ in air. Cells were then harvested using 0.25% trypsin (Difco

Laboratories, Detroit, MI, USA) and 0.1% EDTA (Sigma) in PBS, and seeded at 2×10^5 cells per polylysine-coated (50 $\mu\text{g}/\text{ml}$; poly-L-lysine hydrobromide; Sigma) glass slide (5 cm^2), then incubated overnight in α -MEM with 10% FBS to promote cell attachment prior to fluid shear stress experimental treatment as described below.

Parallel-plate flow chamber (PPFC) design for dynamic fluid shear stress

The PPFC was designed such that it is capable of inducing high-frequency fluid shear stress on the cells. This chamber was designed for dynamic flow regimes utilizing flow frequencies up to 11.2 Hz (the critical frequency, as discussed below). A dimensionless parameter αh ($\alpha = \sqrt{\pi f \rho / \mu}$, where f = flow frequency, ρ = fluid density, μ = fluid viscosity; h = distance between the plates, 300 μm ; a more detailed derivation of this parameter has been done elsewhere, see (38, 39)) determines the magnitude of the dynamic wall shear stress, with its oscillating component scaled by a dimensionless “shear factor” $T(\alpha h)$:

$$\tau_w(t) = \frac{6\mu}{bh^2} QT(\alpha h) \sin(\omega t + \psi)$$

where Q is the flow amplitude, $\omega = 2\pi f$, and ψ is the phase difference between the flow and the wall shear stress τ_w . When $T(\alpha h) = 1.0$, ψ vanishes and the flow and wall shear stress are always in phase giving a quasi-parabolic velocity profile throughout one flow period. A critical frequency f_c exists (when $\alpha h = 2$, f in α is the critical frequency), above which, the parabolic velocity profile does not occur (i.e., when $\alpha h > 2$). The quasi-steady flow regime for exposing cells to predictable levels of dynamic wall shear stress requires $\alpha h < 2$ based on the velocity profile and the magnitude of $T(\alpha h)$ (Fig. 1).

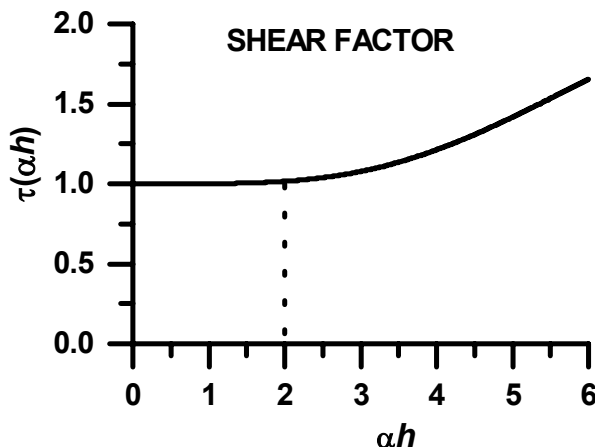


Figure 1. The shear factor predicts homogenous wall shear stress in the parallel-plate flow chamber. The shear factor $T(\alpha h)$ is equal to 1.0 when $\alpha h < 2$. Under this condition, the fluid flow regime is quasi-steady, which induces a homogenous wall shear stress.

Fluid shear stress

Pulsating fluid shear stress was generated using a flow apparatus containing a parallel- plate flow chamber (PPFC) as described earlier (6, 8). Briefly, fluid shear stress was induced on the monolayer of cells attached to the polylysine-coated glass slide serving as the bottom of the parallel-plate flow chamber, by circulating 9 ml of α -MEM containing 2% FBS plus supplements as described above using a computer-controlled micro-annular gear pump (developed by HNP Mikrosysteme GmbH, Parchim, Germany). Precise flow regimes were implemented by controlling the pump using computer-mediated instrumentation by LabView™ (National Instruments Corp., Austin, Texas, USA). The flow through the PPFC was monitored online using a small animal blood flowmeter (T206, Transonic Systems Inc., Ithaca, NY, USA).

During the shear stress experiment the flow apparatus was placed in a 37°C incubator, and connected to a gassing system that maintained a pH of 7.4 in the medium using 5% CO₂ in air. For the fluid shear stress experiments, the culture medium was changed to α -MEM with 2% FBS plus supplements as described above (fluid viscosity = 0.69×10^{-4} Pa-s). Cells were incubated for 5 min in the

presence of: 1) steady fluid shear stress (0.70 Pa; 0 rate), 2) low-amplitude pulsating fluid shear stress (PFSS, 0.70 ± 0.31 Pa) at two different frequencies (5 Hz, with PFSS rate 9.70 Pa-Hz or 9 Hz, with PFSS rate 17.5 Pa-Hz), and 3) high-amplitude pulsating fluid shear stress (0.70 ± 0.70 Pa) at 5 Hz, with PFSS rate 22.0 Pa-Hz, 4) no shear stress (static controls). Pa-Hz was the unit introduced for the fluid shear stress rate, which has a maximum value of $2\pi \times$ fluid shear stress amplitude \times frequency. Medium samples were taken after 5 min for measuring the response to fluid flow parameterized as production of NO in the medium.

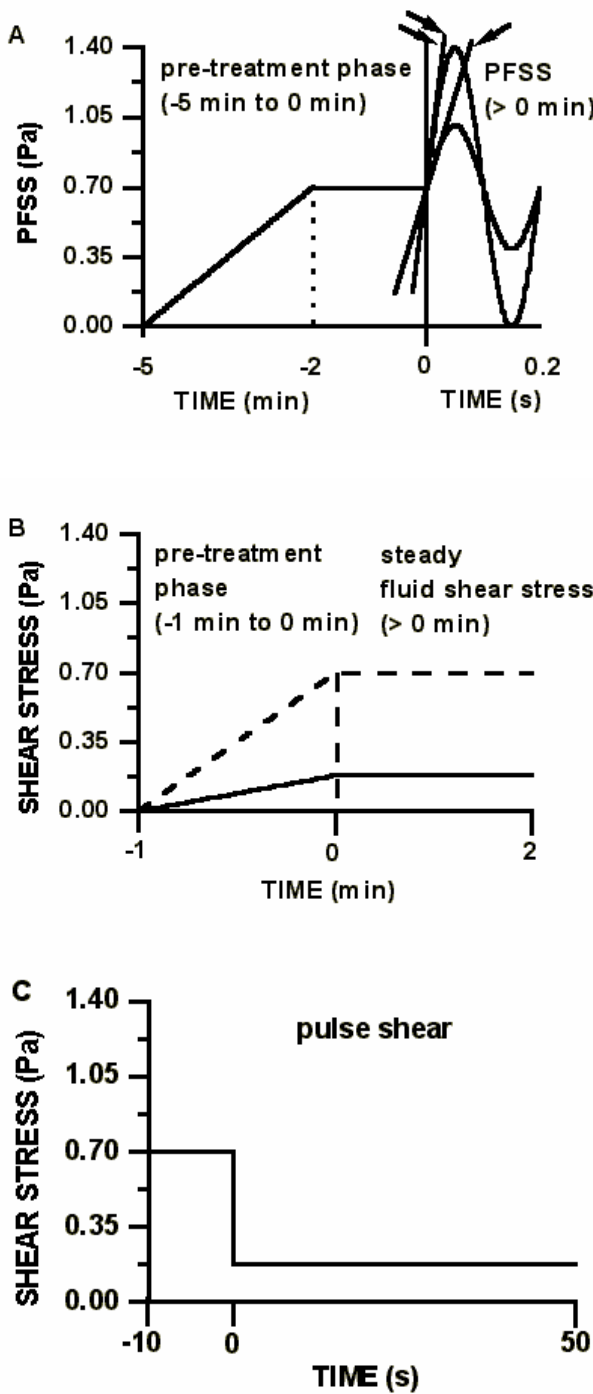


Figure 2. Fluid shear stress regimes applied to MC3T3-E1 bone cells for 5 min. A. The stress-kick was removed in the fluid shear stress regime by inducing a slowly rising shear stress from 0 to 0.70 Pa within 3 min, then a steady shear stress at 0.70 Pa for 2 min (5 min pre-treatment phase), followed by a pulsating fluid shear stress with an average of 0.70 Pa for 5 min (only 0.2 sec is shown). The slope of the lines shown equaled the peak fluid shear stress rate of the flow regime. The rate was increased by raising the flow regime amplitude from 0.31 Pa to 0.70 Pa (double arrows, 5 Hz high-amplitude; single arrow, 5 Hz low-amplitude). The peak fluid shear stress rate was also varied by changing the frequency. The steady flow regime was constant at 0.7 Pa, hence having zero rate. B. The initial stress kick at an earlier time point was removed by introducing a slow rise from 0 to 0.18 Pa (solid line) or 0.7 Pa (dashed line) (the 1 min pre-treatment phase) before applying a subsequent steady shear stress (0.18 or 0.7 Pa, respectively). C. A single pulse shear stress (i.e. a short duration stress-kick) was applied with an amplitude of 0.7 Pa for 10 sec followed by a constant 0.18 Pa for 5 min (only 50s is shown).

Removal of the initial stress-kick and application of a single pulse stress

The PFSS regimes applied give an initial stress-kick by the immediate rise of fluid flow to induce a 0.7 Pa fluid shear stress average. To remove the initial stress-kick, a pre-treatment phase for 5 min was introduced to the regimes. The same set of experiments was performed with a pre-treatment phase (Fig. 2A), composed of a linearly increasing flow from 0 to 8.3 ml/min to induce fluid shear stress from 0 to 0.7 Pa, within 3 min followed by a 2-min steady flow of 8.3 ml/min inducing a steady fluid shear stress at 0.7 Pa. Immediately after the 5 min pre-treatment phase, the cell monolayers were independently subjected to the same flow regimes described above. The shear rates ($2\pi \times \text{amplitude} \times \text{frequency}$) we used in our experiments were chosen due to their physiological relevance. We used 5 and 9 Hz as in a previous paper (8), where we calculated the frequency content of forces acting on a hip, and found that for jogging pace, the frequencies reach up to 9 Hz. Note that with the 5 min pre-treatment phase, the flow regime does not induce an initial stress kick as in the PFSS regimes.

To investigate the effect of the initial-stress kick at an earlier time point, cells were incubated with a 1 min pre-treatment phase before inducing a steady fluid shear stress. In these experiments, the initial stress-kick was removed by increasing the flow to induce a fluid shear stress from 0 to 0.18 Pa or from 0 to 0.7 Pa within 1 min. Immediately after the 1 min pre-treatment phase, a steady fluid shear stress followed to induce 0.18 Pa or 0.7 Pa, for 5 min (Fig 2B).

To investigate the effect of a single pulse shear stress, cells were incubated in the presence of a 10 sec pulse with an amplitude of 0.7 Pa followed by a steady fluid shear stress of 0.18 Pa for 5 min (Table1, Fig 2B).

Nitric Oxide determination

The conditioned medium was assayed for NO, which was measured as nitrite (NO_2^-) accumulation in the conditioned medium, using Griess reagent (1% sulfanilamide, 0.1% naphtylethelene-diamine-dihydrochloride, and 2.5 M H_3PO_4). The absorbance was measured at 540 nm. NO concentrations were

determined using a standard curve derived from known concentrations of NaNO₂ in non-conditioned culture medium. Data from separate experiments were collected and normalized with respect to static controls, and expressed as treatment-over-control (T/C) ratios, or as absolute values where indicated.

Statistics

Data were pooled from the results of at least five experiments for each fluid shear stress regime tested. The effects of treatment with fluid shear stress were analyzed with the non-parametric Wilcoxon rank sum test of the S-Plus 2000 package (release 1). Differences were considered significant at a p value <0.05.

RESULTS

Application of fluid flow for 5 min to the MC3T3-E1 cells did not result in visible changes in cell shape or alignment of the cells in the direction of the fluid flow (data not shown). No cells were removed by any of the fluid shear stress regimes, as assessed by visually inspecting the cultures before and after fluid shear stress treatment, and by measuring the total amount of DNA (control, 261 ± 19 ng; PFSS, 279 ± 27 ng; mean \pm SEM of 6 experiments). We have measured the response to 10 and 15 min of steady and PFSS regimes (data not shown). We found that after 10 min of pulsating fluid shear stress, the NO response is still rate dependent, but only to a lesser extent; and that the response to a steady fluid shear stress, remains the same even after 10 min (8).

The NO response of MC3T3-E1 cells to a fluid shear stress with zero rate was first studied separately, by culturing cells under steady flow conditions for 5 min. Cells produced 6.67 ± 1.07 nmol after 5 min without flow treatment but with steady fluid shear stress, cells produced 11.65 ± 2.36 nmol NO after 5 min (values are mean \pm SEM) (Fig. 3). Cells treated with the steady fluid shear

stress of 0.70 Pa gave a significant ($p<0.05$), almost two-fold NO release as compared to static control levels (Fig. 3).

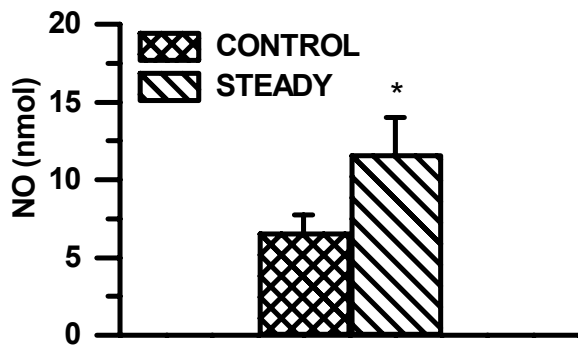


Figure 3. Effect of steady fluid shear stress on the NO production by MC3T3-E1 bone cells after 5 min. The absolute amount of NO produced by bone cells subjected to steady fluid shear stress (0.7 Pa), increased after 5 min as compared to static control cultures, which were not subjected to flow. Under steady fluid shear stress, cells produced 11.65 ± 2.36 nmol NO after 5 min. Cells produced 6.67 ± 1.07 nmol after 5 min without flow treatment (values are mean \pm SEM). The response to steady shear stress increased 2-fold after 5 min. *significant effect of steady fluid shear stress, $p<0.05$.

To study the effect of the fluid shear stress frequency and amplitude on the NO response, cells were subjected to varying pulsating fluid shear stress (PFSS) regimes. NO production was between 3.63 ± 1.19 to 5.14 ± 1.26 nmol (mean \pm SEM) per 2×10^5 cells for cell cultures without fluid shear stress treatment. Treatment with 5 Hz low-amplitude PFSS (0.70 ± 0.31 Pa) did not affect NO production after 5 min (Fig. 4). Treatment with 9 Hz low-amplitude PFSS (0.70 ± 0.31 Pa) caused a rapid 3-fold increase of NO production after 5 min ($p<0.05$), as did treatment with 5 Hz high-amplitude PFSS (0.70 ± 0.70 Pa) after 5 min ($p<0.006$) (Fig. 4). Thus, bone cells showed increased NO production in response to PFSS with increased frequency or amplitude.

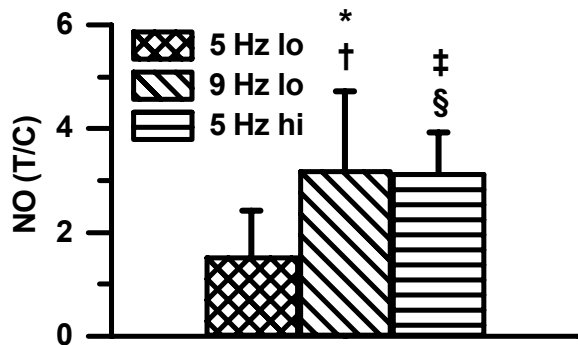


Figure 4. Effect of PFSS frequency and amplitude on the NO production by MC3T3-E1 bone cells after 5 min. NO production was between 3.63 ± 1.19 to 5.14 ± 1.26 nmol (mean \pm SEM) per 2×10^5 cells for all cell cultures without fluid shear stress treatment (static controls). Treatment with high- amplitude or frequency elicited higher NO response than low amplitude or frequency. Values are mean treatment-over-control ratios (T/C) \pm SEM. lo, low-amplitude (0.31 Pa); hi, high-amplitude (0.70 Pa). *, Significantly different from 1.0, $p < 0.05$; †, significantly different from 5 Hz low-amplitude, $p < 0.05$; ‡, significantly different from 1.0, $p < 0.006$; §, significantly different from 5 Hz low-amplitude, $p < 0.006$.

The effect of flow regimes on the NO response of bone cells, without an initial stress-kick was then studied by subjecting bone cells to PFSS with a 5 min pre-treatment phase (Fig. 2A, Fig. 5A). The initial stress-kick was avoided by slowly rising the fluid shear stress from 0 to 0.7 Pa for 3 min, and then inducing steady fluid shear stress for 2 min (the 5 min pre-treatment phase, Fig. 2A) before the application of the PFSS regimes for 5 min (Fig. 5A). Application of the 5 min pre-treatment phase as well as the subsequent application of PFSS did not affect the NO production of the cells (Fig. 5A). The effect of a steady fluid shear stress without an initial stress-kick at a shorter time point was studied by subjecting bone cells to a slow rise of shear stress from 0 to 0.18 Pa or 0.7 Pa for 1 min (the 1 min pre-treatment phase, Fig. 2B) before inducing a steady shear stress of 0.18 Pa or 0.7 Pa for 5 min,

respectively (Fig. 2A, Fig. 5B). NO production was between 2.54 ± 0.54 to 3.30 ± 1.01 nmol (mean \pm SEM) per 2×10^5 cells for cell cultures without fluid shear stress treatment (static controls for both pre-treatment and subsequent PFSS treatment). Application of the 1 min pre-treatment phase as well as the subsequent steady fluid shear stress also did not affect the NO production (Fig. 5B). To investigate the effect of a short duration stress-kick, the cells were subjected to a single pulse shear (10 sec) with an amplitude of 0.7 Pa followed by a 5 min steady shear stress at 0.18 Pa (Fig. 2C, Fig. 5B). Application of the single pulse shear stress as well as the subsequent steady shear stress at 0.18 Pa did not affect the NO production.

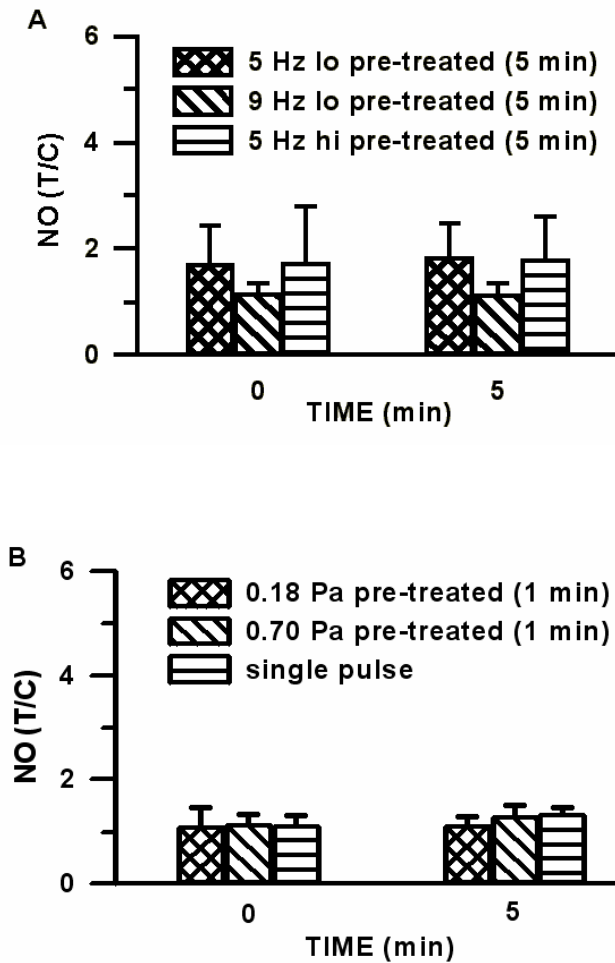


Figure 5. A. Nitric oxide production by bone cells in response to PFSS regimes without an initial stress-kick after 5 min. NO production was between 2.54 ± 0.54 to 3.30 ± 1.01 nmol (mean \pm SEM) per 2×10^5 cells for all cell cultures without fluid shear stress treatment (static controls for both pre-treatment and subsequent PFSS treatment). The pre-treatment phase is composed of a slowly rising flow from 0 to 8.30 ml/min to induce 0 to 0.7 Pa fluid shear stress for 3 min, followed by a steady flow at 8.30 ml/min to induce 0.7 Pa steady fluid shear stress for 2 min. The graph shows that application of the pre-treatment phase as well as the subsequent application of PFSS did not affect the NO production by bone cells. B. Nitric oxide production by bone cells in response to a single pulse shear stress. NO production without fluid shear stress treatment was similar as in A (static controls for both pre-treatment or pulse shear and the subsequent application of shear stress). The single pulse shear stress was applied with a 10s steady shear of 0.7 Pa, followed by a 5 min steady shear stress of 0.18 Pa. Application of the single pulse shear stress as well as the subsequent 0.18 Pa did not affect the NO production by bone cells. Values are mean treatment-over-control ratios (T/C) \pm SEM. lo, low-amplitude (0.31 Pa); hi, high-amplitude (0.70 Pa).

DISCUSSION

The present study suggests that the bone cell response to fluid shear stress is rate- dependent, but that an initial stress kick is required for the cells to respond. Increasing either the shear stress amplitude or frequency, without increasing the average stress, enhanced NO production by bone cells *in vitro*. Bone cells responded similarly to similar rates of fluid shear stress, despite different frequencies (5 Hz, 21.99 Pa-Hz or 9Hz, 17.53 Pa-Hz). Hence, the rate of fluid shear stress (i.e., $2\pi \times f \times \tau$) is proportional to the product of the fluid shear stress amplitude and frequency (8).

Our *in vitro* results support the notion that bone formation *in vivo* is stimulated by dynamic rather than static loads (40), and that low-magnitude, high-frequency mechanical stimuli may be as stimulatory as high-amplitude, low-frequency stimuli, provided that the cells are “kicked” in a pre-conditioned state. The steady, non-dynamic shear stress gave a zero shear rate, but also elicited a significant NO response. When the steady shear stress was applied, the cells experienced a sudden increase of fluid stress from 0 to 0.70 Pa in less than a second, after the pump was switched on. This suggests that bone cells responded significantly to an initial rapid stress increase. The pre-treatment phase, eliminating the initial stress-kick, strongly decreased the NO response of bone cells to fluid shear stress. The initial stress condition seems to define how bone cells respond to the ensuing fluid shear stress regime. This suggests that bone can be pre-conditioned to the environmental stress state by impact loading, as e.g. during exercise like jogging. Conversely, lack of stress-kicks may impair the sensitivity of bone cells to stress, contributing to an insufficient maintenance of bone quality. This might play a role in disuse osteoporosis induced by prolonged bed rest or microgravity, where impact loading conditions are absent. The finding that the bone cell’s response to fluid shear stress is rate dependent provides an explanation why adaptive bone formation can occur despite the sporadic occurrence of high-amplitude strains in daily life (28).

The change in the sensitivity of bone cells to fluid shear stress in the absence of a stress-kick might be due to a cytoskeleton-mediated change in cellular mechanical properties. It has been shown that the ability of cells to respond to mechanical stimuli is mediated by its cytoskeleton (41), which is important for the fluid shear stress response of bone cells (38, 42). The cytoskeletal stiffness (ratio of stress to strain) was shown to increase in response to increasing mechanical stress (41). Furthermore, Pavalko and co-workers showed that MC3T3-E1 actin cytoskeleton rearranges in response to fluid flow stimulation (42). Therefore the transient pre-treatment phase to remove the initial stress-kick might have influenced bone cell cytoskeletal stiffness to make them less sensitive to the following fluid shear stress regime. Our results showed that the cells did not distinguish between a 1 min or 5 min pre-treatment phase (which removed the initial stress-kick) suggesting that the cellular sensitivity to stress might have been affected already within 1 min. However, the cells were also not affected by the application of a single pulse shear stress, i.e. a short duration stress-kick (10 sec, 0.7 Pa amplitude). Thus, the period between 10 sec and 1 min might be crucial for modulating the NO production by bone cells.

Interestingly, an initial stress-kick was shown to be essential for a stable response of bone cells. This corresponds to recent findings that low-frequency, high-amplitude loads and high-frequency, low-amplitude noise give a stronger response than the two signals alone (33). This might also indicate that bone cells have an initial activation barrier in terms of a loading threshold. The necessity of an initial stress kick for bone cells to respond to dynamic loading implies an essential non-linearity to the way bone cells respond to mechanical stress. This provides a cellular basis for stochastic resonance to occur in bone as a non-linear biological system (33). Based on our findings, we suggest that the history of stress pre-conditions the way bone cells respond to mechanical loading. Hence, the absence of high rate stresses might impair the mechanosensitivity of bone cells.

We conclude that NO production by bone cells subjected to fluid flow is dependent on the rate of fluid shear stress. The amplitude and frequency of stress as well as the initial stress conditions contribute to the flow-induced activation of bone cells. We hypothesize, that high rate stresses pre-condition the cells in such a way, that they become sensitive to mechanical loading.

ACKNOWLEDGEMENTS

The authors would like to thank C.M. Semeins and S.J. Dijcks for their technical assistance. The Space Research Organization of the Netherlands supported the work of R.G. Bacabac (SRON grant MG-055) who also received financial assistance from the Netherlands Organization For International Cooperation In Higher Education (Physics Development Project PHL-146). The European Community supported the work of J. Klein-Nulend (fifth framework grant QLK3-1999-00559).

REFERENCES

1. Burger EH, Klein-Nulend J 1999 Mechanotransduction in bone - Role of the lacuno-canalicular network. FASEB J 13(Supplement):S101-S112.
2. Piekarski K, Munro M 1977 Transport mechanism operating between blood supply and osteocytes in long bones. Nature 269(5623):80-82.
3. Weinbaum S, Cowin SC, Zeng Y 1994 A model for the excitation of osteocytes by mechanical loading-induced bone fluid shear stresses. J Biomech 27(3):339-360.

4. Knothe Tate ML, Niederer P, Knothe U 1998 In vivo tracer transport through the lacunocanicular system of rat bone in an environment devoid of mechanical loading. *Bone* 22(2):107-117.
5. Knothe Tate ML, Knothe U 2000 An ex vivo model to study transport processes and fluid flow in loaded bone. *J Biomech* 33(2):247-254.
6. Klein-Nulend J, van der Plas A, Semeins CM, Ajubi NE, Frangos JA, Nijweide PJ, Burger EH 1995 Sensitivity of osteocytes to biomechanical stress in vitro. *FASEB J* 9(5):441-445.
7. Smit TH, Burger EH, Huyghe JM 2002 A case for strain-induced fluid flow as a regulator of BMU-coupling and osteonal alignment. *J Bone Min Res* 17(11):2021-2029.
8. Bacabac RG, Smit TH, Mullender MG, Dijcks SJ, Van Loon JJWA, Klein-Nulend J 2004 Nitric oxide production by bone cells is fluid shear stress rate dependent. *Biochem Biophys Res Commun* 315:823-829.
9. Bakker AD, Soejima K, Klein-Nulend J, Burger EH 2001 The production of nitric oxide and prostaglandin E2 by primary bone cells is shear stress dependent. *J Biomech* 34(5):671-677.
10. Chen NX, Ryder KD, Pavalko FM, Turner CH, Burr DB, Qiu J, Duncan RL 2000 Ca(2+) regulates fluid shear-induced cytoskeletal reorganization and gene expression in osteoblasts. *Am J Physiol Cell Physiol* 278(5):C989-C997.
11. Frangos JA, Johnson D 1995 Fluid flow in bone: stimulated release at remodeling mediators. *Biorheology* 32(2-3):187.

12. Jacobs CR, Yellowley CE, Davis BR, Zhou Z, Cimbala JM, Donahue HJ 1998 Differential effect of steady versus oscillating flow on bone cells. *J Biomech* 31(11):969-976.
13. Johnson DL, McAllister TN, Frangos JA 1996 Fluid flow stimulates rapid and continuous release of nitric oxide in osteoblasts. *Am J Physiol* 271(1):E205-E208.
14. Klein-Nulend J, Roelofsen J, Sterck JGH, Semeins CM, Burger EH 1995 Mechanical loading stimulates the release of transforming growth factor-beta activity by cultured mouse calvariae and periosteal cells. *J Cell Physiol* 163(1):115-119.
15. Klein-Nulend J, Semeins CM, Ajubi NE, Nijweide PJ, Burger EH 1995 Pulsating fluid flow increases nitric oxide (NO) synthesis by osteocytes but not periosteal fibroblasts--correlation with prostaglandin upregulation. *Biochem Biophys Res Commun* 217(2):640-648.
16. Jacobs CR, Yellowley CE, Davis BR, Zhou Z, Cimbala JM, Donahue HJ 1998 Differential effect of steady versus oscillating flow on bone cells. *J Biomech* 31(11):969-976.
17. Bakker AD, Soejima K, Klein-Nulend J, Burger EH 2001 The production of nitric oxide and prostaglandin E(2) by primary bone cells is shear stress dependent. *J Biomech* 34(5):671-677.
18. Hung CT, Allen FD, Pollack SR, Brighton CT 1996 What is the role of the convective current density in the real-time calcium response of cultured bone cells to fluid flow? *J Biomech* 29(11):1403-1409.

19. Mullender M, El Haj AJ, Yang Y, Magnay J, van Duin MA, and Klein-Nulend J. Fluid flow and mechanical strain induce different responses in human bone cells. 28. 2003. Trans 49th Ann Meet Orth Res Soc.
20. Owan I, Burr DB, Turner CH, Qiu J, Tu Y, Onyia JE, Duncan RL 1997 Mechanotransduction in bone: osteoblasts are more responsive to fluid forces than mechanical strain. Am J Physiol 273(3 Pt 1):C810-C815.
21. Smalt R, Mitchell FT, Howard RL, Chambers TJ 1997 Induction of NO and prostaglandin E2 in osteoblasts by wall-shear stress but not mechanical strain. Am J Physiol 273(4 Pt 1):E751-E758.
22. Forwood MR 1996 Inducible cyclo-oxygenase (COX-2) mediates the induction of bone formation by mechanical loading in vivo. J Bone Miner Res 11(11):1688-1693.
23. Turner CH, Takano Y, Owan I, Murrell GA 1996 Nitric oxide inhibitor L-NAME suppresses mechanically induced bone formation in rats. Am J Physiol 270(4 Pt 1):E634-E639.
24. Cowin SC 1999 Bone poroelasticity. J Biomech 32(3):217-238.
25. Mosley JR, Lanyon LE 1998 Strain rate as a controlling influence on adaptive modeling in response to dynamic loading of the ulna in growing male rats. Bone 23(4):313-318.
26. Turner CH, Owan I, Takano Y 1995 Mechanotransduction in bone: role of strain rate. Am J Physiol 269(3 Pt 1):E438-E442.

27. Rubin CT, Sommerfeldt DW, Judex S, Qin YX 2001 Inhibition of osteopenia by low magnitude, high-frequency mechanical stimuli. *Drug Discov Tod* 6(16):848-858.
28. Fritton SP, McLeod J, Rubin CT 2000 Quantifying the strain history of bone: spatial uniformity and self-similarity of low-magnitude strains. *J Biomech* 33(3):317-325.
29. Nordstrom P, Pettersson U, Lorentzon R 1998 Type of physical activity, muscle strength, and pubertal stage as determinants of bone mineral density and bone area in adolescent boys. *J Bone Miner Res* 13(7):1141-1148.
30. Tanaka M, Ejiri S, Nakajima M, Kohno S, Ozawa H 1999 Changes of cancellous bone mass in rat mandibular condyle following ovariectomy. *Bone* 25(3):339-347.
31. Judex S, Zernicke RF 2000 High-impact exercise and growing bone: relation between high strain rates and enhanced bone formation. *J App Physiol* 88:2183-2191.
32. Williams JL, Iannotti JP, Ham A, Bleuit J, Chen JH 1994 Effects of fluid shear stress on bone cells. *Biorheology* 31(2):163-170.
33. Tanaka SM, Alam I, Turner CH 2002 Stochastic resonance in osteogenic response to mechanical loading. *FASEB J* :02-0561fje.
34. Gammaconi L, Hanggi P, Jung P, Marchesoni F 1998 Stochastic resonance. *Rev Mod Phys* 70:223-287.
35. Pierson D, Moss F 1995 Detecting periodic unstable points in noisy chaotic and limit cycle attractors with applications to biology. *Phys Rev Lett* 75(11):2124-2127.

36. Kondepudi DK 1991 Detection of gravity through nonequilibrium mechanisms. ASGB Bulletin 4:119-124.
37. Fox SW, Chambers TJ, Chow JWM 1996 Nitric oxide is an early mediator of the increase in bone formation by mechanical stimulation. Am J Physiol 33(6):E955-E960.
38. Bacabac RG, Smit TH, Cowin SC, Van Loon JJWA, Nieuwstadt FTM, Heethaar R, Klein-Nulend J 2005 Dynamic shear stress in parallel-plate flow chambers. J Biomech 38(1):159-167.
39. Bacabac RG, Smit TH, Heethaar RM, Van Loon JJWA, Pourquie MJMB, Nieuwstadt FTM, Klein-Nulend J 2004 Characteristics of the parallel-plate flow chamber for mechanical stimulation of bone cells under microgravity. J Gravit Physiol 9:P181-P182.
40. Rubin CT, Lanyon LE 1984 Regulation of bone formation by applied dynamic loads. J Bone Joint Surg Am 66(3):397-402.
41. Wang N, Butler JP, Ingber DE 1993 Mechanotransduction across the cell surface and through the cytoskeleton. Science 260(5111):1124-1127.
42. Pavalko FM, Chen NX, Turner CH, Burr DB, Atkinson S, Hsieh YF, Qiu J, Duncan RL 1998 Fluid shear-induced mechanical signaling in MC3T3-E1 osteoblasts requires cytoskeleton-integrin interactions. Am J Physiol 275(6 Pt 1):C1591-C1601.

CHAPTER 5

STOCHASTIC RESONANCE ENHANCES THE RAPID RESPONSE OF BONE CELLS TO FLUID SHEAR STRESS

Rommel G. Bacabac¹, Jack J.W.A. Van Loon^{1,2}, Theo H. Smit³, Jenneke Klein-Nulend¹

¹Department of Oral Cell Biology, Academic Centre for Dentistry Amsterdam-Universiteit van Amsterdam and Vrije Universiteit, Amsterdam, The Netherlands;

²Dutch Experiment Support Center, Vrije Universiteit, Amsterdam, The Netherlands;

³Department of Physics and Clinical Engineering, VU University Medical Center, Amsterdam, The Netherlands.

Submitted for publication

ABSTRACT

Stochastic resonance is manifest in non-linear systems, where the response to a small periodic signal is enhanced by noise. It is unknown whether bone cell mechanosensitivity is enhanced by a noisy loading environment as an alternative mechanism for an amplified response to stress. Since osteocytes are believed to be the mechanosensors in bone *par excellance*, we studied whether noise of varying intensities enhanced the mechanosensitivity of MLO-Y4 osteocytes in comparison with MC3T3-E1 osteoblasts. Nitric oxide (NO) and prostaglandin E₂ (PGE₂) production were measured as parameters for bone cell activation. Here we modeled the response of the cell culture to noisy fluid shear stress by an enhancement of the information content of the applied stress. We found that the NO response of MLO-Y4 osteocytes to a small periodic fluid shear stress was acutely enhanced by noise. MC3T3-E1 osteoblasts did not show an acutely enhanced NO response to noise. However, MC3T3-E1 osteoblasts showed noise-enhanced PGE₂ response, while MLO-Y4 osteocytes did not, compared to their responses to noise alone. The difference in responses by MLO-Y4 and MC3T3-E1 cells implied differences in stress-thresholds for the production of NO and PGE₂. Since NO and PGE₂ regulate bone formation as well as resorption, our results explain how noise might enhance the activity of osteocytes and osteoblasts *in vivo* in driving the mechanical adaptation of bone.

INTRODUCTION

Stochastic resonance (SR) is the phenomenon, in which non-linear systems show enhanced response at the output to noise-supplemented input signals. SR has been used to explain various phenomena in biological systems (1), including the activity of cells under microgravity (2). In another study, it was suggested that SR enhances bone formation (3). However, much is unknown about the role of noise for the response of different bone cell types to stress.

Living bone tissue is permeated by a fluid-filled microscopic network of lacunae and canaliculi. Bone cells are housed in lacunae, and are interconnected via gap-junctions connecting cellular extensions through the canaliculi (4-6). Bone is minutely deformed by mechanical loading due to exercise or normal daily activities (7). Although normal daily activities mostly induce strain deformations at $10 \mu\epsilon$ (7), it is believed that strains to the order of $3000 \mu\epsilon$, mediate the flow of interstitial fluid in bone (8-10). Han et al. (11) suggested a strain amplification mechanism at the cellular level to explain the paradox of sustained bone health and the persistence of very small strains in normal daily activities (7). It is unknown whether bone cells use other amplification mechanisms for sensing small strains in bone. Nevertheless, fluid shear stress induced by the loading-mediated flow of interstitial fluid through the lacuno-canicular network is a likely stimulus for bone cell adaptive responses (12-14).

Osteocytes, being most responsive to fluid shear stress (15, 16), are hypothesized to be the functional orchestrators of bone remodeling (5, 12). In response to fluid shear stress, osteocytes produce signaling molecules that are potent regulators of the activity of other bone cells, osteoblasts and osteoclasts (12, 15). The crucial balance between osteoblasts in depositing bone (osteoid and mineral), and that of osteoclasts in resorbing bone, determines the adaptive architecture of bone for efficient loading support (17-19). This phenomenon of bone cell activity has been hypothesized in the so-called “Bone mineralizing

unit” (BMU), where the release of signaling molecules in relation to local fluid shear stresses determine the mineralization process (20).

We have shown earlier that MC3T3-E1 osteoblasts' response to fluid shear stress is rate-dependent (21), and that this response necessitated an initial stress-kick (22). This suggests that bone cells have an initial activation barrier in terms of a stress-threshold. The necessity of an initial stress-kick for bone cells to respond to dynamic loading implies an essential non-linearity to the way bone cells respond to mechanical stress. This provides a cellular basis for stochastic resonance to occur in bone as a non-linear biological system.

Threshold detectors are unable to verify the presence of a signal below its threshold (1). The addition of noise at the input enables the detector to sense the small signal (1, 23, 24). A model for SR might use an information measure for the detectability of the input signal, at the output, by the addition of noise at the input. Models using the Fisher information as a measure for the detectability of the input signal in the presence of noise have been explored in detailed statistical analysis for single and multi-threshold systems for signals that are below or above the system threshold (25, 26).

This study investigated whether the activation of bone cells by a small periodic loading stimulus is enhanced by noise. A previous investigation on the NO response of MC3T3-E1 cells indicated a fluid shear stress rate of 0.11 Pa/s as a threshold for stimulation with an initial stress-kick due to the intial rise of the applied fluid shear stress from 0 to 0.7 Pa (21, 22). Here, we induced fluid shear stress regimes with an initial stress-kick due to a fluid shear stress rise from 0 to 1.4 Pa. To investigate the basic response of different bone cells to fluid shear stress, MLO-Y4 osteocytes and MC3T3-E1 osteoblasts were subjected to steady and dynamic fluid shear stress without noise. To investigate whether there is a difference to the response of different bone cell types to noisy stress, MLO-Y4 osteocytes and MC3T3-E1 osteoblasts, as models for primary osteocytes and osteoblasts, were subjected to a small periodic stimulus superposed with Gaussian white noise of different intensities. We then used

the results to propose differences in stress-thresholds for MLO-Y4 and MC3T3-E1 cells as modeled by noise-enhanced Fisher information about the small periodic stimulus input.

MATERIALS AND METHODS

Bone cell cultures

MLO-Y4 osteocytes were cultured up to near-confluence in 75 cm² cell culture flasks (Nunc, Roskilde, Denmark), using α -Modified Eagle's Medium (α -MEM; Gibco, Paisley, UK) supplemented with 5% fetal bovine serum (FBS; Gibco), 5% calf serum (CS; Gibco), penicillin (10 μ g/ml) and streptomycin (10 μ g/ml). The MLO-Y4 osteocytes were kindly provided by Dr. L. Bonewald (University of Missouri-Kansas City, Kansas City, MO, USA). MC3T3-E1 cells were cultured up to near-confluence in 75 cm² cell culture flasks (Nunc, Roskilde, Denmark), using α -Modified Eagle's Medium (α -MEM; Gibco, Paisley, UK) supplemented with 10% fetal bovine serum (FBS; Gibco), ascorbate (50 μ g/ml; Merck, Darmstadt, Germany), β -glycerophosphate disodium salt hydrate (10 mM; Sigma, St. Louis, MO, USA), l-glutamine (300 μ g/ml; Merck), gentamycine (50 μ g/ml; Gibco), and fungizone (1.25 μ g/ml; Gibco). The MC3T3-E1 osteoblasts were kindly provided by Dr. M. Kumegawa (Meikai University, Sakado, Japan). MLO-Y4 and MC3T3-E1 cells were then harvested and seeded at 1.5×10^5 cells per polylysine-coated (50 μ g/ml; poly-L-lysine hydrobromide; Sigma) glass slide (5 cm²), and incubated overnight to promote cell attachment, at 37°C with 5% CO₂ in air, prior to fluid shear stress experimental treatment as described below.

Parallel-plate flow chamber *in vitro* system

To study the effect of noise on the response of bone cells to fluid shear stress, Gaussian white noise $\eta(t)$ was added to the applied fluid shear stress:

$$\tau(t) \approx \tau_c + \tau_d TK \sin(\omega t) + \eta(t) \quad [1]$$

where τ_c is a constant offset to the periodic forcing term with amplitude τ_d , superposed with $\eta(t)$, a zero-mean Gaussian white noise of intensity D (i.e., $\langle \eta(t) \eta(s) \rangle = 2D\delta(t-s)$). The dimensionless product of the shear and flow factors TK attenuates the flow to 79% at frequencies above 89 Hz (for medium viscosity $\mu = 0.0069$ Poise, chamber height $h = 100$ μm). The factor TK theoretically ensures flow frequencies up to 22.3 Hz without phase difference between the applied pressure gradient and flow (see (27) for a description of the parallel-plate flow chamber). Considering flow frequency limitations, the applied noise had a spectrum band reaching up to 22.3 Hz. The applied noise intensity D was chosen between 0 Pa to 1.4 Pa (Table 1).

Fluid shear stress application

Pulsating fluid shear stress was generated using a flow apparatus containing a parallel-plate flow chamber (PPFC) as described earlier (15, 21). Fluid shear stress was induced for 5 min on the monolayer of cells by circulating 5 ml of CO₂-independent medium (Gibco) containing 2% FBS for MC3T3-E1 cells, 1% FBS and 1% CS for MLO-Y4 cells, plus supplements as described above, using a computer-controlled micro-annular gear pump (developed by HNP Mikrosysteme GmbH, Parchim, Germany). Precise flow regimes (Table 1) were implemented at room temperature (22.5°C) by controlling the pressure gradient using computer-mediated instrumentation (LabViewTM, National Instruments Corp., Austin, TX, USA). The flow was monitored online using a small animal blood flowmeter (T206, Transonic Systems Inc., Ithaca, NY, USA).

Table 1. Data of applied pulsating fluid shear stress (PFSS) regimes

D (Pa)	Mean Shear stress (Pa)	f (Hz)	A (Pa)	n (MLO-Y4)	n (MC3T3-E1)
0	1.4	0	0	9	6
0	1.4	9	0.12	10	6
0	1.4	9	1.4	6	6
0.25	1.4	0	0	6	--
0.70	1.4	0	0	--	6
0.04	1.4	9	0.12	4	5
0.07	1.4	9	0.12	5	5
0.11	1.4	9	0.12	4	6
0.14	1.4	9	0.12	7	7
0.25	1.4	9	0.12	5	5
0.32	1.4	9	0.12	5	5
0.42	1.4	9	0.12	5	5
0.70	1.4	9	0.12	4	5
1.09	1.4	9	0.12	4	5
1.40	1.4	9	0.12	5	6

f = frequency; A = amplitude; D = Noise intensity; n = number of experiments

Nitric oxide and prostaglandin E₂ determination

The conditioned medium was assayed for NO and prostaglandin E₂. NO was measured as nitrite (NO₂⁻) accumulation in the conditioned medium, using Griess reagent (1% sulfanilamide, 0.1% naphtylethelene-diamine-dihydrochloride, and 2.5 M H₃PO₄). The absorbance was measured at 540 nm. NO concentrations were determined using a standard curve derived from known concentrations of NaNO₂ in non-conditioned culture medium. PGE₂ was measured in conditioned medium by an enzyme immunoassay (EIA) system (Amersham, Buckinghamshire, UK) using an antibody raised against mouse PGE₂. The absorbance was measured at 450 nm.

Stochastic resonance by noise-enhanced Fisher information

To capture the essential features of the observed accumulated release of NO and PGE₂ as associated to the information content at the output, we use the

Fisher information I , which is a parameter for the estimation of the input signal τ (see (25) for a statistical description):

$$I(\theta, \tau, \sigma) = \frac{[f\left(\frac{\theta-\tau}{\sigma}\right)]^2}{\sigma^2 F\left(\frac{\theta-\tau}{\sigma}\right)[1 - F\left(\frac{\theta-\tau}{\sigma}\right)]} \quad [2]$$

where θ is the threshold, τ the apparent input signal recognized by the bone cell. The noise is taken to have a Gaussian distribution with the standard deviation σ , which is $D^{1/2}$ with normalized density f , such that $F(x)$:

$$F(x) = \int_{-\infty}^x f(x)dx \quad [3]$$

$$f(x) = (1/\sqrt{2\pi}) \exp(-x^2/2) \quad [4]$$

Our model takes the Fisher information as a measure for the ability of bone cells to detect the presence of a small periodic signal buried under noise. The released signaling molecules indicate the detectability of the input signal. The Fisher information predicts the presence of a peak response indicating the detectability of a signal with the presence of noise. Take for example, a signal = 1.0 (dimensionless), which is above the threshold; the peak in the Fisher information, increases as the threshold increases towards the signal value = 1.0 (Fig. 1). However, the peak decreases as the threshold increases further away, above the input signal value = 1.0. Note that for an input signal above the threshold, a higher peak response occurs at lower noise intensities for higher threshold values (Fig. 1).

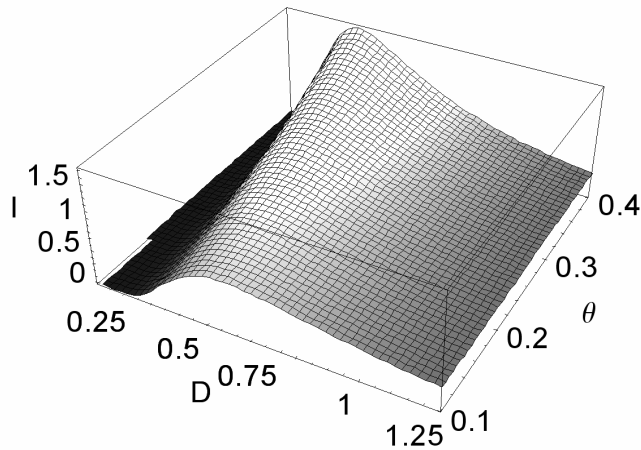


Figure 1. Fisher information I . The threshold θ is here taken to be above the input signal τ , that is, $\theta - \tau > 0$. D , noise intensity.

Statistics

Data were pooled from the results of at least four experiments for each fluid shear stress regime tested (Table 1). The effects of treatment with fluid shear stress were analyzed with the non-parametric Wilcoxon signed-rank sum test of the S-Plus 2000 package (release 1). Differences were considered significant at a p-value < 0.05 .

RESULTS

Application of fluid flow for 5 min to the MLO-Y4 and MC3T3-E1 cells did not result in visible changes in cell shape or alignment of the cells in the direction of the fluid flow. No cells were removed by any of the fluid shear stress regimes, as assessed by visually inspecting the cultures before and after fluid shear stress treatment.

The NO released by MLO-Y4 cells and MC3T3-E1 in response to steady fluid shear stress compared to the dynamic fluid shear stress regimes were similar (Fig. 2a). However, MLO-Y4 cells released more NO in response to the 9 Hz hi regime (Table 1, Fig. 2a). MLO-Y4 and MC3T3-E1 cells released the highest amount of PGE₂ in response to the 9 Hz hi regime (Fig. 2b). PGE₂ release by MLO-Y4 cells was significantly higher compared to the response of MC3T3-E1 cells in response to steady fluid shear stress, as well as to dynamic fluid shear stress at both the 9 Hz lo and hi regimes (Fig. 2b).

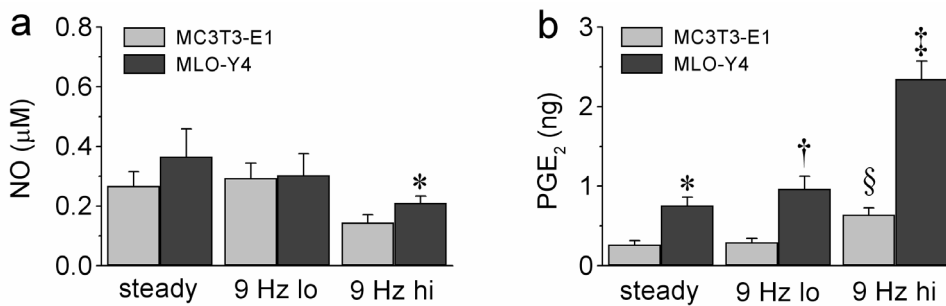


Figure 2. NO and PGE₂ production by MLO-Y4 and MC3T3-E1 cells. a. NO release by MLO-Y4 and MC3T3-E1 cells were similar in response to steady fluid shear stress (1.4 Pa) or 9 Hz lo regime (average 1.4 Pa, amplitude 0.12 Pa, frequency 9 Hz). NO release by MLO-Y4 cells was greater than the release by MC3T3-E1 cells at the 9 Hz hi regime (average 1.4 Pa, amplitude 1.4 Pa, frequency 9 Hz; * $p < 0.029$). b. PGE₂ release by MLO-Y4 was higher than MC3T3-E1 cells in response to steady fluid shear stress (1.4 Pa), (* $p < 0.016$), as well as, in response to 9 Hz lo regime (average 1.4 Pa, amplitude 0.12 Pa, frequency 9 Hz; at † $p < 0.001$) and in response to 9 Hz hi regime (average 1.4 Pa, amplitude 1.4 Pa, frequency 9 Hz; at ‡ $p < 0.016$). MLO-Y4 cell release of PGE₂ was most significant at the 9 Hz hi regime (‡ $p < 0.016$; higher than the response at steady or 9 Hz lo regime). MC3T3-E1 cells release of PGE₂ was significant at the 9 Hz hi regime (§ $p < 0.016$ greater than the response at 9 Hz lo regime; $p < 0.008$ greater than the response at steady fluid shear stress). Results are mean \pm SEM.

The NO released by the MLO-Y4 cells showed an optimum response to noisy stress with an intensity of 0.25 Pa (Fig. 3a). The NO response to 0.25 Pa

was significantly higher than the response to a very low noise intensity, 0.04 Pa, and to high noise intensities from 0.42 Pa, to a very high noise intensity, 1.4 Pa (Fig. 3a). NO release by MC3T3-E1 cells did not significantly reach an optimum at any noise intensity, although the trend suggests an optimum at a noise intensity of 0.7 Pa (Fig. 3a). Only MLO-Y4 cells released NO with a definitive peak response to noise, but not MC3T3-E1 cells.

The NO released in response to 9 Hz lo regime at the optimum noise intensity (0.25 Pa) by MLO-Y4 cells was significantly higher (Fig. 3b) than the response to noise alone (0.25 Pa), as well as to 9 Hz lo superposed with a very high intensity (Fig. 3b). However, this response was not higher than the NO release to the 9 Hz lo regime without noise. Similarly, NO release by MC3T3-E1 cells in response to 9 Hz lo regime at its optimum noise intensity (based on the trend, 0.70 Pa) was significantly different from the response to noise alone (noise intensity at 0.70 Pa; Fig. 3b). However, NO release by MC3T3-E1 osteoblasts, at the optimum noise level was not significantly higher than the release due to 9 Hz lo regime without noise, or with a very high noise (1.4 Pa) (Fig. 3b). Both MLO-Y4 and MC3T3-E1 cells released NO at their optimum noise level significantly higher than the response to noise alone.

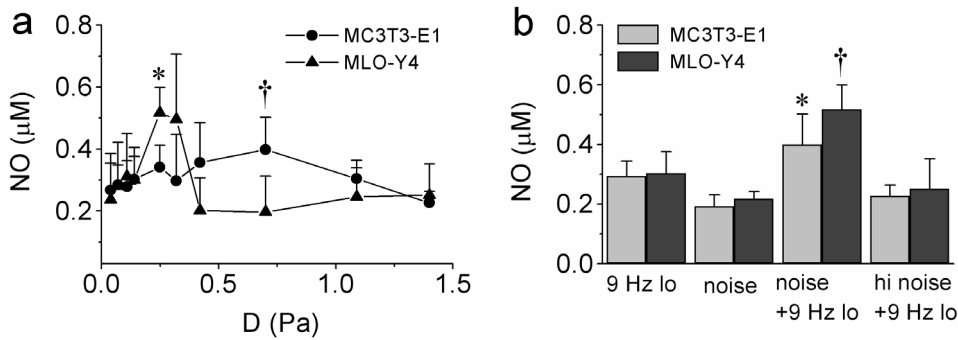


Figure 3. NO production by MLO-Y4 and MC3T3-E1 cells in response to noisy stress. a. NO release by MLO-Y4 cells in response to noisy stress was optimum at a noise intensity of 0.25 Pa (* $p < 0.047$, greater than the response at noise intensity 0.04 Pa; $p < 0.038$, greater than the response at noise intensity 1.40 Pa; $p < 0.023$, greater than the response at noise intensity 0.42 Pa). NO release by MC3T3-E1 cells in response to noisy stress does not result in a statistically significant optimum (†, probable peak at 0.70 Pa). b. NO release by MLO-Y4 cells at its optimum noise intensity (0.25 Pa noise intensity superposed with 9 Hz lo regime) is significantly larger than the response to noise alone (* $p < 0.030$, for 0.25 Pa noise alone) and to the highest noise intensity (* $p < 0.038$, for 1.4 Pa noise intensity superposed to 9 Hz lo). NO release by MC3T3-E1 cells at its possible optimum noise intensity (0.70 Pa noise intensity superposed with 9 Hz lo regime) is significantly higher than the response to noise alone († $p < 0.030$, for 0.70 Pa noise alone), but not to the highest noise intensity (1.4 Pa noise intensity superposed to 9 Hz lo). Results are mean \pm SEM.

The PGE₂ released by MLO-Y4 cells in response to noisy stress did not show a well defined peak response (Fig. 4a). However, the PGE₂ response of the MLO-Y4 cells to a noise intensity of 0.70 Pa was significantly higher than the response to its neighboring noise intensities 0.42 Pa and to 1.09 Pa (Fig. 4a). MC3T3-E1 cells released PGE₂ with a high level of variance in response to noise intensity of 0.42 Pa (Fig. 4a). This response is, however, not a statistically significant peak (Fig. 4a). Both cell types showed possible PGE₂ peak responses (Fig. 4a).

The PGE₂ released by MLO-Y4 cells at its possible optimum noise level, D = 0.70 Pa, was not significantly higher than the response to noise alone (D =

0.70 Pa), as well as to 9 Hz lo regime, or very high noise (Fig. 4b). However, MC3T3-E1 cells' release of PGE₂ at its supposed optimum ($D = 0.42$ Pa) was significantly higher than the response to noise alone ($D = 0.42$ Pa), and to 9 Hz lo regime without noise (Fig. 4b). Only MC3T3-E1 cells, but not MLO-Y4 cells, showed a peak PGE₂ response at the optimum noise that was significant compared to the response to noise alone.

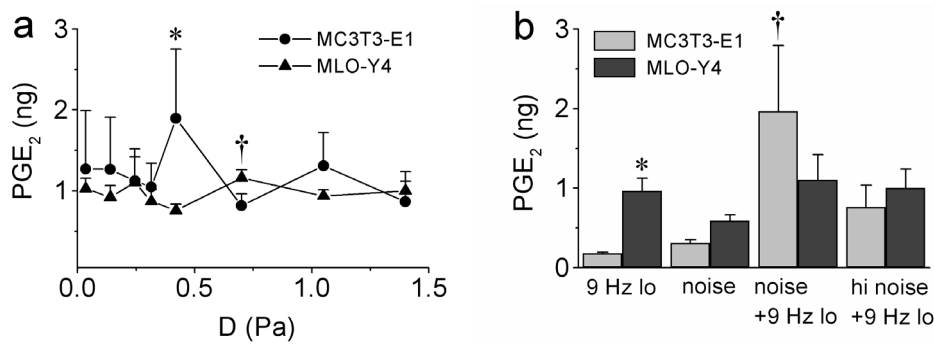


Figure 4. PGE₂ production by MLO-Y4 and MC3T3-E1 cells in response to noisy stress. a. MC3T3-E1 cells did not show a pronounced peak response to fluid shear stress although the trend implies a possible optimum at $D = 0.42$ Pa (* $p < 0.06$ higher than response at $D = 1.4$ Pa). MLO-Y4 cells release PGE₂ with a locally pronounced peak at noise intensity $D = 0.70$ Pa, which is significantly higher than response at $D = 0.42$ Pa, $p < 0.029$, and than the response at $D = 1.09$ Pa, † $p < 0.029$. b. PGE₂ release by MLO-Y4 was higher than MC3T3-E1 cells in response to 9 Hz lo regime (average 1.4 Pa, amplitude 0.12 Pa, frequency 9 Hz; at * $p < 0.001$). MC3T3-E1 cell release of PGE₂ at its supposed optimum ($D = 0.42$ Pa) was significantly larger than the response to noise alone ($D = 0.42$ Pa), and to 9 Hz lo regime without noise († $p < 0.032$). PGE₂ release by MLO-Y4 cells at its possible optimum noise level, $D = 0.70$ Pa, was not significantly higher than the response to noise alone ($D = 0.70$ Pa). Results are mean \pm SEM.

DISCUSSION

In this study, we used MLO-Y4 and MC3T3-E1 cells to model primary osteocytes and osteoblasts and found novel ways by which bone cells might

cooperate for influencing local changes in bone mass and structure. Our results confirmed that there is a fundamental difference in the response of osteocytes and osteoblasts in response to fluid shear stress (15), here modeled by MLO-Y4 osteocytes and MC3T3-E1 osteoblasts. While NO release by MLO-Y4 and MC3T3-E1 cells are similar in response to steady and a small dynamic fluid shear stress, PGE₂ release by MLO-Y4 cells was higher compared to that of MC3T3-E1 cells.

Previously, we showed a rate-dependent response to fluid shear stress, provided that the cells are “kicked” in a pre-conditioned state (22). In that study, bone cells were subjected to a sudden increase of fluid shear stress from 0 to 0.7 Pa (initial stress-kick). Our results here did not show a rate-dependent response to fluid shear stress in terms of NO production, because the initial stress-kick was high (increase from 0 to 1.4 Pa), and therefore induced a high NO baseline production. The high NO baseline production likely hid the rate-dependent response to fluid shear stress. We have shown in another study that the PGE₂ response to the fluid shear stress by MC3T3-E1 cells was not rate-dependent (28). In that study, bone cells were treated with regimes that have an initial stress-kick due to an initial fluid shear stress rise from 0 to 0.6 Pa. Here, we showed that the response to PGE₂ production for both cell types, was apparently rate dependent. Furthermore, MLO-Y4 cells released more PGE₂ compared to MC3T3-E1 cells. This difference can be attributed to our use of a higher intial stress-kick, which is due to an intial fluid shear stress rise from 0 to 1.4 Pa. It would seem that a fluid shear stress rate-dependent production of PGE₂ for MC3T3-E1 or MLO-Y4 cells requires a higher initial stress-kick (0 to 1.4 Pa) than what NO production requires (0 to 0.7 Pa). Thus, the initial threshold barrier for NO production is lower than the initial threshold barrier for PGE₂ production for both cell types (Table 2).

Table 2. Stress-threshold comparison between cells

	NO	PGE ₂
MLO-Y4	Higher threshold	Lower threshold
MC3T3-E1	Lower threshold	Higher threshold

The stress-threshold for NO is lower than PGE₂ for both MLO-Y4 and MC3T3-E1 cells

Our results showed different responsiveness to noisy stress, which suggests a difference in the stress-thresholds of the two bone cell types for NO production. The difference in stress-thresholds is predicted by our model using the Fisher information which fits the re-scaled peak NO responses of MLO-Y4 and MC3T3-E1 cells (Fig. 5). MC3T3-E1 cells did not show a definitive peak NO release because MC3T3-E1 cells have a lower stress-threshold for NO release compared to MLO-Y4 cells (Table 2). Although noise seems to enhance NO production by MLO-Y4 cells, our results indicated that noise alone, even at the optimum intensity (0.24 Pa), does not enhance NO production as noisy stress with a small periodic stimulus. This suggests that noisy stress conditions are stimulatory only in the presence of periodic loading as would be expected in exercise or sports with repetitive motions.

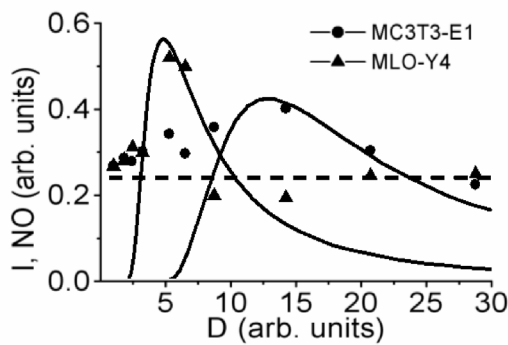


Figure 5. NO production by MLO-Y4 and MC3T3-E1 cells as a function of noise intensity plotted with the predicted peak from the Fisher Information, predicted with the input signal greater than the stress-threshold. Dashed line indicates NO production baseline. Arb. units., arbitrary units.

Previously, it has been shown that primary osteocytes produces more PGE₂ in response to fluid shear stress compared to primary osteoblasts and periosteal fibroblasts (29), confirming MLO-Y4 and MC3T3-E1 cells as plausible models for primary bone cells (osteocytes and osteoblasts, respectively). PGE₂ production in response to noisy stress was more significant for MC3T3-E1 cells compared to MLO-Y4 cells. No indicative PGE₂ peak was observed for both cell types, possibly because the small periodic signal (9 Hz lo regime), although above the PGE₂ stress-threshold, is too far from the PGE₂ stress-threshold. Using the Fisher information to predict the presence of a peak response to noise, it is possible that MC3T3-E1 cells have a higher stress-threshold for PGE₂ production compared to MLO-Y4 cells (Table 2). It is possible that MLO-Y4 cells are more sensitive to stress in terms of PGE₂ production, but MC3T3-E1 cells are more sensitive to stress in terms of NO production (as discussed above, see Table 2). While it might be observed that osteocytes produce more signaling molecules compared to osteoblasts or periosteal fibroblasts in response to stress (15, 29, 30), the loading threshold for specific signaling molecules (*e.g.* PGE₂, in this study) is not necessarily lower. MLO-Y4 cells produced more signaling molecules in response to fluid shear stress, compared to MC3T3-E1 cells. However, MLO-Y4 cells have a lower PGE₂ stress-threshold compared to MC3T3-E1 cells, while MC3T3-E1 cells have a lower NO stress-threshold compared to MLO-Y4 cells (Table 2).

Both NO and PGE₂ are important intercellular messenger molecules for bone cells. Studies on whole animals have show that they play a key role in the mechanical adaptation of bone, because inhibiting their synthesis inhibits bone adaptation to loading (31-33). NO is known to drive away osteoclasts *in vitro* (34). On the other hand, PGE₂ increases mRNA levels of osteoprotegerin ligand (OPG-L)/osteoclast differentiation factor (ODF), from osteoblastic lineage cells. OPG-L/ODF stimulates osteoclast differentiation and activity, further inhibiting osteoclast apoptosis (35). NO and PGE₂ regulate the activity of osteoclasts (34, 36). It would seem that osteocytes, deep in the bone matrix, drive away osteoclasts, preventing bone resorption in their regions by

producing NO at high stress conditions (since MLO-Y4 cells as model for osteocytes have a higher stress-threshold for NO production compared to MC3T3-E1 cells as model for osteoblasts; Table 2). At low stress conditions, our results indicate that osteocytes might promote the activity of osteoclasts by producing more PGE₂ and lesser NO (since the stress-threshold for PGE₂ is lower compared to NO for MLO-Y4 cells; Table 2). Since MC3T3-E1 cells produce less NO and PGE₂ compared to MLO-Y4 cells, given the same loading conditions, it would seem that *in vivo*, osteocytes are indeed more responsible for directing the activity of osteoclasts. However, osteoblasts might produce high levels of NO locally under conditions of high stress to drive away osteoclasts, towards regions of low stress where osteocytes are still able to produce PGE₂ to promote osteoclast activity.

The possibility of SR in bone cells further suggests that osteocytes and osteoblasts take advantage of noisy stresses as an alternative mechanism for the adaptation of bone to mechanical loading by tuning their different peak responses for specific signaling molecules. This explains the osteogenic benefits of dynamic stress to functional bone adaptation to mechanical loading. By a tuned nitric oxide and prostaglandin E₂ response to noisy stress, it is possible that osteocytes and osteoblasts locally recruit or inhibit osteoclasts, for a functional manipulation of bone mass and architecture.

ACKNOWLEDGEMENTS

The Space Research Organization of the Netherlands (SRON) supported the work of J.J.W.A. van Loon (DESC, MG-057 and SRON grant MG-055) and R.G. Bacabac (SRON grant MG-055), who also received financial assistance from the University of San Carlos, Cebu City, Philippines.

REFERENCES

1. Gammaconi L, Hanggi P, Jung P, Marchesoni F 1998 Stochastic resonance. *Reviews of Modern Physics* 70(1):223-287.
2. Konddepudi DK 1991 Detection of gravity through nonequilibrium mechanisms. *ASGB Bulletin* 4:119-124.
3. Tanaka SM, Alam I, Turner CH 2002 Stochastic resonance in osteogenic response to mechanical loading. *FASEB J* :02-0561fje.
4. Cowin SC, Moss-Salentijn L, Moss ML 1991 Candidates for the mechanosensory system in bone. *J Biomech Eng* 113(2):191-197.
5. Lanyon LE 1993 Osteocytes, strain detection, bone modeling and remodeling. *Calcif Tissue Int* 53(Supp 1):S102-S106.
6. Donahue HJ 2000 Gap junctions and biophysical regulation of bone cell differentiation. *Bone* 26(5):417-422.
7. Fritton SP, McLeod J, Rubin CT 2000 Quantifying the strain history of bone: spatial uniformity and self-similarity of low-magnitude strains. *J Biomech* 33(3):317-325.
8. Weinbaum S, Cowin SC, Zeng Y 1994 A model for the excitation of osteocytes by mechanical loading-induced bone fluid shear stresses. *J Biomech* 27(3):339-360.
9. Cowin SC, Weinbaum S, Zeng Y 1995 A case for bone canaliculi as the anatomical site of strain generated potentials. *J Biomech* 28(11):1281-1297.
10. Cowin SC 1999 Bone poroelasticity. *J Biomech* 32(3):217-238.

11. Han YF, Cowin SC, Schaffler MB, Weinbaum S 2004 Mechanotransduction and strain amplification in osteocyte cell processes. *Proc Natl Acad Sci USA* 101:16689-16694.
12. Burger EH, Klein-Nulend J 1999 Mechanotransduction in bone - Role of the lacuno-canalicular network. *FASEB J* 13(Supplement):S101-S112.
13. Knothe Tate ML, Knothe U 2000 An ex vivo model to study transport processes and fluid flow in loaded bone. *J Biomech* 33(2):247-254.
14. Kufahl RH, Saha S 1990 A theoretical model for stress-generated fluid flow in the canaliculi-lacunae network in bone tissue. *J Biomech* 23(2):171-180.
15. Klein-Nulend J, van der Plas A, Semeins CM, Ajubi NE, Frangos JA, Nijweide PJ, Burger EH 1995 Sensitivity of osteocytes to biomechanical stress in vitro. *FASEB J* 9(5):441-445.
16. Ajubi NE, Nijweide PJ, Klein-Nulend J, Burger EH, Semeins CM 1995 Pulsatile fluid flow stimulates nitric oxide (NO) production by osteocytes, but not periosteal fibroblasts. *Bone* 17(6):566.
17. Smit TH, Burger EH, Huyghe JM 2002 A case for strain-induced fluid flow as a regulator of BMU-coupling and osteonal alignment. *J Bone Min Res* 17(11):2021-2029.
18. Burger EH, Klein-Nulend J, Van der Plas A, Nijweide PJ 1995 Function of osteocytes in bone--their role in mechanotransduction. *J Nutr* 125(7 Suppl):2020S-2023S.

19. Burger EH, Klein-Nulend J, Smit TH 2003 Strain-derived canalicular fluid flow regulates osteoclast activity in a remodelling osteon - a proposal. *J Biomech* 36(10):1453-1459.
20. Smit TH, Burger EH 2000 Is BMU-coupling a strain-regulated phenomenon? A finite element analysis. *J Bone Miner Res* 15(2):301-307.
21. Bacabac RG, Smit TH, Mullender MG, Dijcks SJ, Van Loon JJWA, Klein-Nulend J 2004 Nitric oxide production by bone cells is fluid shear stress rate dependent. *Biochem Biophys Res Commun* 315:823-829.
22. Bacabac RG, Smit TH, Mullender MG, Van Loon JJWA, Klein-Nulend J 2005 Initial stress-kick is required for fluid shear stress-induced rate dependent activation of bone cells. *Ann Biomed Eng* 33(1):104-110.
23. Mcnamara B, Wiesenfeld K 1989 Theory of Stochastic Resonance. *Phys Rev A* 39(9):4854-4869.
24. Greenwood PE, Ward LM, Russell DF, Neiman A, Moss F 2000 Stochastic resonance enhances the electrosensory information available to paddlefish for prey capture. *Phys Rev Lett* 84(20):4773-4776.
25. Greenwood PE, Ward LM, Wefelmeyer W 1999 Statistical analysis of stochastic resonance in a simple setting. *Phys Rev E* 60(4 Pt B):4687-4695.
26. Muller UU, Ward LM 2000 Stochastic resonance in a statistical model of a time-integrating detector. *Phys Rev E* 61(4):4286-4294.

27. Bacabac RG, Smit TH, Cowin SC, Van Loon JJWA, Nieuwstadt FTM, Heethaar R, Klein-Nulend J 2005 Dynamic shear stress in parallel-plate flow chambers. *J Biomech* 38(1):159-167.
28. Mullender MG, Dijcks SJ, Bacabac RG, Semeins CM, Van Loon JJWA, Klein-Nulend J 2005 Release of Nitric Oxide, but not Prostaglandin E2 by bone cells depends on fluid flow frequency. submitted .
29. Westbroek I, Ajubi NE, Alblas MJ, Semeins CM, Klein-Nulend J, Burger EH, Nijweide PJ 2000 Differential stimulation of prostaglandin G/H synthase-2 in osteocytes and other osteogenic cells by pulsating fluid flow. *Biochem Biophys Res Commun* 268(2):414-419.
30. Klein-Nulend J, Semeins CM, Ajubi NE, Nijweide PJ, Burger EH 1995 Pulsating fluid flow increases nitric oxide (NO) synthesis by osteocytes but not periosteal fibroblasts--correlation with prostaglandin upregulation. *Biochem Biophys Res Commun* 217(2):640-648.
31. Chow JWM, Chambers TJ 1994 Indomethacin Has Distinct Early and Late Actions on Bone-Formation Induced by Mechanical Stimulation. *Am J Physiol* 267(2):E287-E292.
32. Fox SW, Chambers TJ, Chow JWM 1996 Nitric oxide is an early mediator of the induction of bone formation by mechanical stimulation. *Bone* 19(6):687.
33. Forwood MR 1996 Inducible cyclo-oxygenase (COX-2) mediates the induction of bone formation by mechanical loading in vivo. *J Bone Miner Res* 11(11):1688-1693.

34. Mancini L, Moradi-Bidhendi N, Brandi ML, MacIntyre I 1998 Nitric oxide superoxide and peroxynitrite modulate osteoclast activity. *Biochem Biophys Res Commun* 243(3):785-790.
35. Webster SSJ 2001 Integrated Bone Tissue Physiology: Anatomy and Physiology. In: Stephen C.Cowin (ed) *Bone Mechanics Handbook*, vol 1. CRC Press, Boca Raton, pp. 1-1-1-68.
36. Raisz LG 1999 Prostaglandins and bone: physiology and pathophysiology. *Osteoarthr Cartil* 7(4):419-421.

CHAPTER 6

BONE CELL RESPONSES TO HIGH-FREQUENCY VIBRATION STRESS: DOES THE NUCLEUS OSCILLATE WITHIN THE CYTOPLASM?

Rommel G. Bacabac¹, Theo H. Smit², Jack J.W.A. Van Loon^{1,3}, Jolanda M.A. de Blieck-Hogervorst¹, Cor M. Semeins¹, Behrouz Zandieh Doulabi¹, Marco Helder¹, Jenneke Klein-Nulend¹

¹Department of Oral Cell Biology, Academic Centre for Dentistry Amsterdam-Universiteit van Amsterdam and Vrije Universiteit, Amsterdam, The Netherlands

²Department of Clinical Physics and Informatics, VU University Medical Center, Amsterdam, The Netherlands

³Dutch Experiment Support Center, Vrije Universiteit, Amsterdam, The Netherlands

Submitted for publication

ABSTRACT

Mechanosensing by cells directs changes in bone mass and structure, in response to the challenges of mechanical loading. Low-amplitude, high-frequency loading stimulates bone growth by enhancing bone formation and inhibiting disuse osteoporosis. However, how bone cells sense vibration stress is unknown. Hence, we investigated bone cell responses to vibration stress at a wide frequency range (5-100 Hz). We used nitric oxide (NO) and prostaglandin E₂ (PGE₂) release, and COX-2 mRNA expression, as parameters for bone cell response, since these molecules regulate bone adaptation to mechanical loading. NO release positively correlated, while PGE₂ release negatively correlated to the maximum acceleration rate of the vibration stress. COX-2 mRNA expression increased in a frequency-dependent manner, which relates to increased NO release at high frequencies confirming our previous results. The anti-correlated release of NO and PGE₂ suggests that these signaling molecules play different roles in bone adaptation to high-frequency loading. The maximum acceleration rate is proportional to ω^3 (frequency = $\omega/2\pi$), which is commensurate with the Stokes-Einstein relation for modeling cell nucleus motion within the cytoplasm due to vibration stress. Correlations of NO and PGE₂ with the maximum acceleration rate then relate to nucleus oscillations, providing a physical basis for cellular mechanosensing of high-frequency loading.

INTRODUCTION

Bone is an obvious biological system that exhibits the interplay of mechanical stress and adaptive response both at the tissue and cellular levels(1-3). Bones adapt their mass and structure in response to the demands of mechanical loading (4). Furthermore, it has been suggested that the rate rather than the magnitude alone of the applied loading stimulus correlates to bone formation *in vivo* (5, 6). This suggests that both the frequency and amplitude of applied stresses are important for the osteogenic response of bone.

We have recently found in another study that the NO production by MC3T3-E1 cells was linearly dependent on the rate of fluid shear stress, which depended on both the amplitude and frequency of stress (7). In that study however, the applied fluid shear stress was only up to a maximum of 9 Hz. Nitric oxide (NO) and prostaglandin E₂ production are essential for the induction of new bone formation in response to mechanical loading *in vivo* (8-10). The constitutional, endothelial form of nitric oxide synthase (eNOS), one of the three NOS enzyme isoforms responsible for the synthesis of NO, is prominently expressed in osteocytes and upregulated by mechanical loading (11). Blocking of either cyclooxygenase-2 (COX-2), the key enzyme for mechanically-induced PG production, or NOS could prevent mechanically induced bone formation (8, 12, 13). Since osteoblasts respond to fluid shear stress as osteocytes, although to a lesser extent, osteoblasts could provide a practical model for osteocyte response to stress.

Using animal models, low magnitude (< 10 μe) high-frequency (10 - 100 Hz) mechanical stimuli have been shown to be capable of stimulating bone growth by doubling bone formation rates and inhibiting disuse osteoporosis (14). Thus, it would seem that higher frequencies are also stimulatory to bone cells. Much is unknown however, about how high frequency loading might permeate bone despite the presence of soft tissues. We have shown earlier that external loading from exercise could involve frequencies reaching 9 Hz (7). Frequencies experienced by cells beyond 10 Hz might occur at much lower

amplitudes considering the damping effects of soft tissue. Regardless of frequency range, the applied rate of loading, which is dependent on both frequency and magnitude, seems to be a decisive factor in bone formation and maintenance.

Paradigms for understanding mechanosensing by cells include models for the mechanical properties of the cytoplasm as predominantly a continuum (15) or as composed of linked polymers that transfer forces through the cytoskeleton to the nucleus (16). Cellular activation by mechanical loads in general or vibration in particular, leading to a biochemical cascade requires some form of cellular deformation as a mechanism for sensing forces. Although there is evidence that bone cells respond to dynamic loading, how bone cells might sense mechanical vibration is unknown. Therefore, we studied the response of bone cells to mechanical vibration over a wide frequency range (5 Hz up to 100 Hz), at different magnitudes. We tested whether vibration stress applied with varying frequencies and amplitudes affects the nitric oxide (NO) and prostaglandin E₂ (PGE₂) production, and mRNA expression for COX-2 by MC3T3-E1 osteoblastic cells. Based on the results, we empirically derived a model to propose an alternative mechanism by which cells might sense high-frequency mechanical loading.

MATERIALS AND METHODS

Bone cell cultures

MC3T3-E1 cells (Kodama, et al, 1981; kindly provided by Dr. Kumegawa, Mekai University School of Dentistry, Sakado, Saitama, Japan) were cultured up to near-confluence in 75 cm² cell culture flasks (Nunc, Roskilde, Denmark), using α -Modified Eagle's Medium (α -MEM; Gibco, Paisley, UK) supplemented with 10% fetal bovine serum (FBS; Gibco), ascorbate (50 μ g/ml; Merck, Darmstadt, Germany), β -glycerophosphate disodium salt hydrate (10 mM; Sigma, St. Louis, MO, USA), l-glutamine (300 μ g/ml; Merck),

gentamycine (50 µg/ml; Gibco), fungizone (1.25 µg/ml; Gibco), at 37°C with 5% CO₂ in air. Cells were then harvested using 0.25% trypsin (Difco Laboratories, Detroit, MI, USA) and 0.1% EDTA (Sigma) in PBS, and seeded at 0.7x10⁵ cells per well in a 24-well plate, then incubated overnight in α-MEM with 10% FBS to promote cell attachment prior to vibration stress treatment as described below.

Application of vibration stress

For vibration stress treatment, the culture medium was changed to CO₂-independent medium (Gibco, USA) with 2% FBS, and incubated for 5 min in the presence of mechanical vibration at varying frequencies and amplitudes (see Table 1). Vibration stress was implemented on attached cells by sinusoidal displacement of the 24-well plate along the cells' plane of attachment using a voltage controlled linear actuator (fig. 1A). Conditioned medium was sampled after 5 min of vibration stress treatment to measure accumulated NO in medium produced by MC3T3-E1 cells.

Table 1. *Data of applied vibration stress*

Regime frequency	5 Hz	30 Hz	60 Hz	100 Hz
Amplitude (mm)	5	4.5	1.75	0.75
Maximum acceleration rate (km/s ³)	0.15	30.1	93.8	186
Maximum velocity (m/s)	0.15	0.85	0.66	0.47

$\omega = 2\pi \times \text{frequency}$; Maximum velocity = amplitude × ω ;

Maximum acceleration = amplitude × ω^3

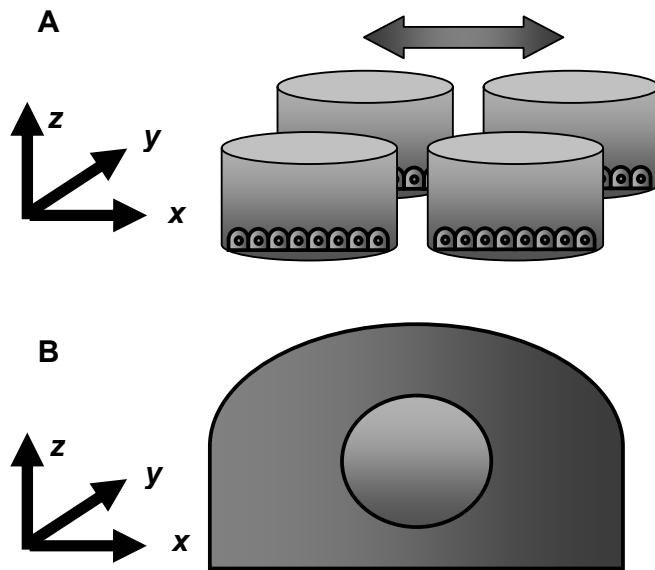


Figure 1. Vibration stress application. A. Cells were seeded onto the bottom surface of the 24-wells plate (as described in Methods). Sinusoidal motion is along the x-axis (arrow). B. Simplified model of a cell with an approximately rigid spherical nucleus compared to its viscoelastic cell body.

Nuclear oscillations induced by vibration stress

We take a minimalist approach to understand how the cells are possibly receiving stress by translational oscillation. We consider the nucleus to be spherical and embedded in the viscoelastic medium of the cell body. The source of mechanical stimulus is then attributed to the possible motion of the cellular nucleus (modeled to be a sphere, figure 1B) inside the cell. Based on the Generalized Stokes-Einstein relation we estimated the displacement of the nucleus in the cell $x_n(\omega)$, modeled as a rigid sphere compared to the cytoplasm, as proportional to the applied force F :

$$x_n(\omega) \propto \frac{F(\omega)}{R_n G(\omega)} \quad [1]$$

where $G(\omega)$, is here considered to be the elastic modulus of the cell cytoplasm (at the order of 100 Pa) (17), and the acting force is due to the mass of the nucleus $\rho_n V_n$, with a volume V_n , and radius R_n , considering a relative acceleration of the nucleus with respect to the cell body. In this approximation, we neglect the time dependence of the modulus, so, $G(\omega) \rightarrow G_o$. The nucleus is considered to be four times more rigid compared to the cytoplasm (e.g., the elastic modulus of the nucleus is at the order of 400 Pa) (18). The force acting on the nucleus is due to the acceleration it experiences due to the applied sinusoidal vibration, with amplitude x_o and frequency = $\omega/(2\pi)$:

$$F = -\rho_n V_n \frac{d^2}{dt^2} [x_o \sin(\omega t)] = \rho_n V_n x_o \omega^2 \sin(\omega t) \quad [2]$$

Thus, the absolute maximum force due to the nucleus F_{max} , is related to the maximum acceleration of the entire plate:

$$F_{max} = \rho_n V_n x_o \omega^2 \quad [3]$$

where $x_o \omega^2$ is the maximum acceleration of the plate. The maximum velocity of the plate is related to nuclear velocity v_n , which in turn is related to ω :

$$v_n(\omega) \propto \left(\frac{\rho'_n V_n}{R_n G_o} \right) x_o \omega \quad [4]$$

where ρ'_n is the density difference between the cell nucleus and the surrounding cytoplasm. Here, we approximate the elastic modulus to be constant G_o . The maximum rate of acceleration by the plate is related to the rate of acceleration ra_n by the nucleus at ω :

$$ra_n(\omega) \propto \left(\frac{\rho'_n V_n}{R_n G_o} \right) x_o \omega^3 \quad [5]$$

Using this *in vitro* system, for a non-negligible density difference between the cell nucleus and the surrounding cytoplasm, we are able to mechanically stimulate cells by inducing body forces by vibration stress. Hence, by correlating the amount of released signaling molecules to the maximum

velocity or rate of acceleration of the plate we characterized the effect of vibration stress to bone cell mechanosensitivity.

Nitric Oxide and Prostaglandin E₂ determination

The conditioned medium was assayed for NO, which was measured as nitrite (NO_2^-) accumulation in the conditioned medium, using Griess reagent (1% sulfanilamide, 0.1% naphtylethelene-diamine-dihydrochloride, and 2.5 M H_3PO_4). The absorbance was measured at 540 nm. NO concentrations were determined using a standard curve derived from known concentrations of NaNO_2 in non-conditioned culture medium. PGE₂ was measured in conditioned medium by an enzyme immunoassay (EIA) system (Amersham, Buckinghamshire, UK) using an antibody raised against mouse PGE₂. The detection limit was 16 pg/ml. Absorbance was measured at 450 nm.

Total DNA, RNA and total protein determination

DNA, RNA and protein were isolated from the bone cell cultures using Trizol reagent according to the manufacturer's instructions. The amount of protein was determined using a BCA protein Assay Reagent Kit (Pierce, Rockford, IL, USA), the absorbance was read at 570 nm. The RNA and DNA content were determined by measuring absorbance in water at 260 nm using an Ultraspec III spectrophotometer (Amersham).

RNA isolation and Reverse transcription

Total RNA from the cells was isolated using Trizol® reagent with one modification; 5 µg of glycogen (Roche Diagnostics, Mannheim, Germany) was added to RNA and isopropanol solution prior to centrifuge step to increase RNA yield. Total RNA concentration was quantified spectrophotometrically. cDNA synthesis was performed using 0.5-1 µg total RNA in a 20 µl reaction mix consisting of 5 Units of Transcriptor Reverse Transcriptase according to the manufacturer's instructions (Roche Diagnostics) with 0.08 A₂₆₀ units random primers (Roche Diagnostics), 1 mM of each dNTP (Invitrogen), and

Transcriptor RT reaction buffer. cDNA was diluted 5 times and stored at -80 °C prior to real-time PCR.

Real-time PCR

Real-time PCR reactions were performed using the SYBRGreen reaction kit according to the manufacturer's instructions (Roche Diagnostics) in a LightCycler (Roche Diagnostics). cDNA (2 µl each) was diluted to a volume of 20 µl with PCR mix (Light Cycler DNA Master Fast start ^{plus} Kit, Roche Diagnostics) containing a final concentration of 0.2 pmol of primers. Relative housekeeping gene expression (18S; which its expression was not subjected to time and or treatment related variations) and relative target gene expression (COX-2) were determined. Primers (Invitrogen) used for real-time PCR are listed in Table 2 were designed using Clone manager suite software program version 6 (Scientific & Educational Software, NC, USA) and the amplified PCR fragment had extension over at least one exon-border except for 18S which gene is encoded only by one exon. Values of relative target gene expression were normalized for relative 18S housekeeping gene expression.

Table 2. Primers used for real time PCR

Target gene	Oligonucleotide sequence	Expected product size, bp
18s forward	5'-gtaacccgttgaaccccatt-3'	151
18s reverse	5'-ccatccaatcggttagtagcg-3'	
COX-2 forward	5'-geattcttgccccagcactt-3'	299
COX-2 reverse	5'-agaccaggcaccagaccaaaga-3'	

Real Time PCR Data analyses

With the Light Cycler software (version 2), the crossing points were assessed and plotted versus the the serial dilution of known concentrations of the standards derived from each gene. PCR efficiency (E) was obtained by the formula: $E=10^{-1/\text{slope}}$ and the data were used if and only if the PCR efficiency was calculated between 1.85-2.0.

Statistics

Data were pooled from the results of at least 5 experiments for each vibration stress regime. The effects of vibration stress regimes were analyzed with the non-parametric Wilcoxon signed rank sum test of the S-Plus 2000 package (release 1). Differences between total DNA, RNA, and protein expressions for different vibration stress regimes were tested using one-way ANOVA. The relation between the release of NO or PGE₂ against the peak rate acceleration by the vibration stress, and against each other, was characterized by linear regression. Significant differences were considered at a p-value < 0.05.

RESULTS

Application of vibration stress for 5 min to the MC3T3-E1 cells did not result in visible changes in cell shape or alignment of the cells to any orientation (data not shown). No cells were removed by any of the vibration stress regimes, as assessed by visually inspecting the cultures before and after vibration stress treatment, and by measuring the total amount of DNA, RNA and protein (table 3).

Table 3. Total DNA, RNA, and Protein.

	5 Hz	30 Hz	60 Hz	100 Hz
DNA (μg/μl)	0.045 ± 0.021	0.035 ± 0.012	0.029 ± 0.009	0.041 ± 0.012
RNA (μg/μl)	0.200 ± 0.064	0.163 ± 0.038	0.170 ± 0.048	0.203 ± 0.055
Protein (μg/ml)	108 ± 5	98 ± 11	84 ± 10	94 ± 8

One-way ANOVA test indicated that the means are not significantly different at p < 0.05.

The rapid response to vibration stress by bone cells was measured as the accumulation of NO released in the medium after 5 min of treatment with the different vibration stress regimes (table 1). NO production in rapid response to treatment with vibration stress linearly correlated with the applied maximum

acceleration rate, (fig. 2A; $p < 0.05$, $R = 0.95$). However, this response did not correlate linearly to the applied maximum velocity. The highest response was due to the 100 Hz regime (see table 1), which was significantly larger than the response to 5 Hz and 60 Hz regimes (fig. 2A and B, $p < 0.03$).

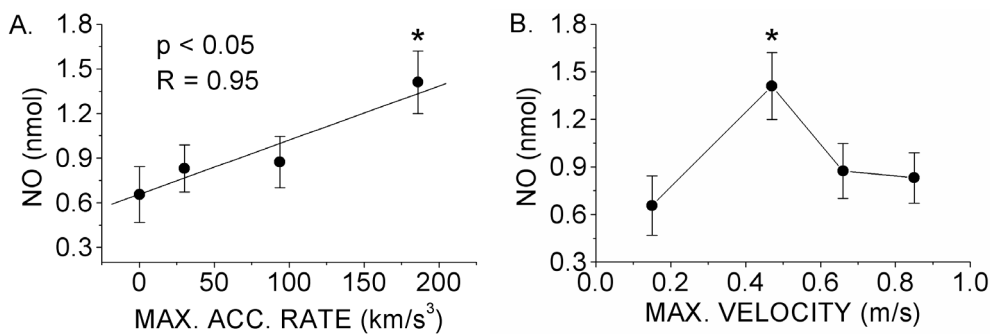


Figure 2. Effect of vibration stress on NO production by bone cells. A. Bone cells respond in positive correlation to the applied maximum acceleration rate (max. acc. rate) of vibration stress immediately after 5 min ($p < 0.05$). B. The response to mechanical vibration does not correlate linearly to the applied maximum velocity (max. velocity). The response to vibration stress of 100 Hz was significantly larger than the response to 5 Hz and 60 Hz (* $p < 0.03$). Values are mean total amount \pm SEM.

The late response to vibration stress by bone cells was measured as the accumulation of PGE₂ released in the medium after 5 min of treatment with the different vibration stress regimes (table 1). PGE₂ was assayed in the conditioned medium after 30 min of post incubation at 37°C without vibration stress. The PGE₂ released by bone cells in response to vibration stress anti-correlated with the applied peak acceleration rate (fig. 3A, $p < 0.006$). However, the response to mechanical vibration did not correlate linearly to the applied maximum velocity (fig. 3B). The highest response to vibration stress was due to the 5 Hz regime (see table 1), which was significantly larger than the response to 100 Hz (fig. 3, $p < 0.003$).

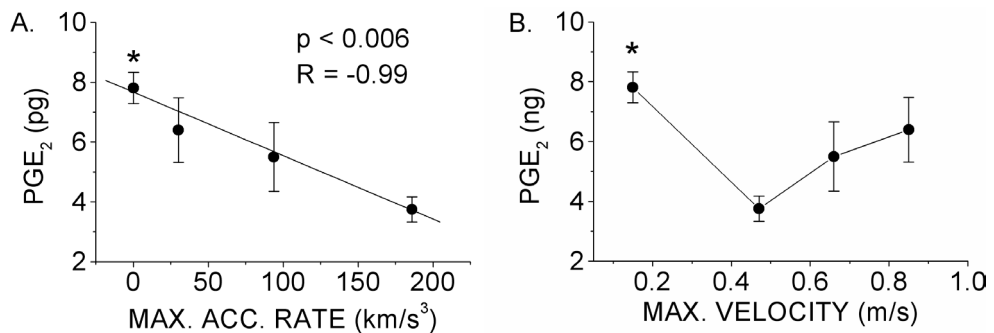


Figure 3. Effect of vibration stress on PGE₂ production by bone cells. A. Bone cells respond in negative correlation to the applied maximum acceleration rate (max. acc. rate) of vibration stress ($p < 0.006$). B. The response to mechanical vibration does not correlate linearly to the applied maximum velocity (max. velocity). The response to vibration stress of 5 Hz was significantly larger than the response to 100 Hz (* $p < 0.003$). PGE₂ was assayed from medium harvested after 30 min of post-incubation subsequent to 5 min of vibration stress. Values are mean total amount \pm SEM.

To investigate whether the production of NO and PGE₂ was related, the measured release of these signaling molecules to corresponding increasing frequencies of the vibration stress were correlated by linear regression. The NO and PGE₂ released by bone cells in response to vibration stress at varying frequencies, were found to be anti-correlated (fig. 4, $p < 0.013$, $R = -0.99$).

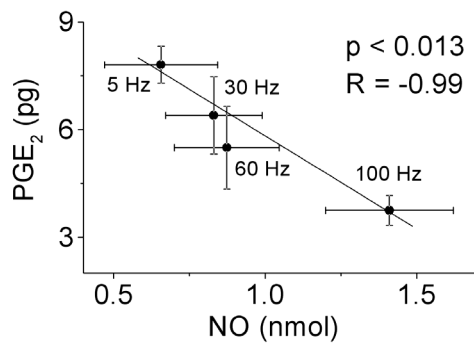


Figure 4. Anti-correlated release of NO and PGE₂ by bone cells in response to vibration stress.

To investigate the long-term effect of vibration stress on bone cells, the mRNA expression for COX-2 was measured in relation to PGE₂ release, at 30 min subsequent to 5 min vibration stress. The bone cells were harvested for COX-2 mRNA expression after 2.5 hours of post-incubation subsequent to 5 min of vibration stress. The mRNA expression for COX-2 was found most upregulated in response to 100 Hz vibration stress, which was significantly higher than the response to all the other regimes (fig. 5). The mRNA expression for COX-2 in response to 100 Hz was 2-fold higher than the response to 5 and 30 Hz. Also, the mRNA expression for COX-2, in response to 60 Hz vibration was found to be 1.5 times higher than the response to the 30 Hz regime (fig. 5, p < 0.047).

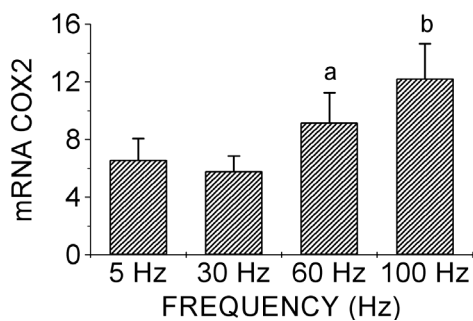


Figure 5. Vibration stress upregulates mRNA for COX-2 expression by bone cells. mRNA expression for COX-2, was 2-fold regulated in response to 100 Hz vibration stress (b, higher than the response to 5 Hz, p < 0.028, higher than 30 Hz, p < 0.011, and higher than 60 Hz, p < 0.05). mRNA expression for COX-2, in response to 60 Hz vibration was 1.5 times higher than the response to 30 Hz (^ap < 0.047). Cells were harvested for measuring mRNA expression for COX-2 after 2 hours of post-incubation subsequent to 5 min of vibration stress. Values are mean total amount ± SEM. mRNA values were normalized relative to the 18S housekeeping gene expression.

DISCUSSION

The membrane-bound soluble enzyme called endothelial cell NOS (ecNOS or NOS III, one of three members of the NOS family) is involved in the NO response of bone cells to mechanical stress (19, 20). NO production is an essential step for mechanical loading-induced bone formation as observed in rats *in vivo* (8). We have found earlier that mRNA expression for ecNOS in bone cells (osteocytes isolated from chicken calvaria) is upregulated in response to fluid shear stress (21). Prostaglandins are generated by the release of arachidonic acid from phospholipids in the cell membrane, followed by conversion of arachidonic acid into prostaglandin G₂ and subsequently H₂. Prostaglandin H₂ is further isomerized to the biological active prostanoids, prostaglandin E₂ (PGE₂). The *in vivo* acute prostaglandin production by loading-stimulated bone cells seems to be more important than the sustained prostaglandin release (10, 13). Hence, NO and PGE₂ production, in response to fluid shear stress, are meaningful parameters for measuring bone cell activation.

NO and PGE₂ production by bone cells linearly correlated at opposing signs, with the maximum applied acceleration rate, at opposing signs, which is third order or cubic in frequency dimension (see Table 1). This suggests that the bone cell response to vibration stress treatment is highly dependent on the applied frequency of loading. The response however, did not linearly correlate with the applied maximum velocity, which is a joint effect of the applied amplitude and frequency, both at first order. The most likely effect of the vibration stress might be the movement of the cell nucleus through the cell body induced by the acceleration of the plate. NO release and PGE₂ release correlated with the rate of acceleration, which is proportional to the rate of the force on the nucleus. The rate of force is proportional to the rate of stress experienced by the cell through nuclear motion directly. This supports our earlier finding that bone cell response is linear to the applied fluid shear stress rate (7). In our model for the mechanical effect of vibration stress, the

acceleration rate corresponds to the rate of the force acting on the cell nucleus. Since stress is the amount of force about a cross-sectional area, the consistent signature for bone cell response to mechanical loading seems to be linear stress-rate dependence. Fluid shear stress, which is contact stress primarily acting on the cell membrane, might be linearly rate-dependent only for low frequencies (< 10 Hz), since fluid flow might attenuate at high frequencies (> 10 Hz). Thus, our model for the motion of the cell nucleus for vibration stress at high frequencies, involving body forces, explains the different way how bone cells might sense loading at high frequencies (> 10 Hz) or at high impact loading.

The anti-correlation of NO and PGE₂ release is closely linked to the rate of stress experienced by the bone cells at a wide range of frequencies induced by vibration. These opposing trends of molecular release suggest different roles for NO and PGE₂ in regulating the mechanical adaptation of bone. It has been shown *in vitro* that osteoclasts migrate away from NO (22, 23). PGE₂ increases mRNA levels of osteoprotegerin ligand (OPG-L)/osteoclast differentiation factor (ODF), from osteoblastic lineage cells. OPG-L/ODF stimulates osteoclast differentiation and activity, further inhibiting osteoclast apoptosis (22). NO and PGE₂ regulate the activity of osteoclasts (23, 24). Since at higher frequencies, MC3T3-E1 tends to increase NO release but tends to decrease PGE₂ release, this suggests an acute tendency for bone cells to oppose the presence of osteoclasts at high frequency loading. It is possible that *in vivo*, osteoblasts enhance their rejection of osteoclasts when stimulated with high frequencies. This might in turn, stimulate osteoblast activity in the absence of osteoclasts. Indirectly, osteoclasts are possibly recruited onto regions not experiencing high frequency loading. Since materials of higher density are expected to favor force transfer at high frequencies, it is possible that in bone, regions that are less dense (hence not responsive to high frequencies) are more prone to being degraded by osteoclasts, while regions of higher densities are strategically maintained. Furthermore, since the release of signaling molecules correlates strongly to ω^3 , the absence of high strains in normal daily activities

does not necessarily correspond to bone loss. High frequencies in the spectrum of loading are expected during movements of high impact activity, as in exercise and sports, which have been shown to be beneficial for bone health (25-27). Thus, it would seem that the loss in strain amplitude can be compensated by the application of higher frequency loading.

Our results might also provide further insight on the effects of a broad band of frequencies on bone formation (6, 28). Our model for predicting the motion of the nucleus through the cell body during vibration stress application, might relate to the reported osteogenic benefits of vibration-related stimulation. For example, the use of low-intensity ultrasound has been shown to stimulate a higher occurrence of spinal fusion compared to cases without low-intensity ultrasound application (29). There is much unknown on the mechanisms responsible for the transfer of forces in bone as imparted by loading of minute magnitudes, at high frequencies. It is possible that high frequency vibration attenuate through soft-tissue surrounding the bone mineralized matrix. However, it is also likely that high frequencies are able to survive in the denser mineralized matrix of bone. In this case, our model for the motion of the cell nucleus is a possible mechanism for bone cells to sense high frequency loading.

The increased mRNA expression for COX-2, in relation to increasing frequencies of vibration stress suggests a memory response for high frequency loading. In this study, the vibration stress was applied for only 5 min, however, after 2.5 hours of post-incubation without stress, the upregulation of mRNA expression for COX-2 occurred. Despite a decreased PGE₂ release at high frequencies, after 30 min of post-incubation, subsequent to the 5 min vibration stress, bone cells maintain the capacity for producing PGE₂. This suggests that bone cells compensate for a short-term PGE₂ production (after 30 min) by increasing mRNA levels for COX-2 for a possible delayed response (or memory effect).

Interestingly, bone cells do respond to high frequency vibration stress (i.e., 100 Hz) although fluid shear stresses *in vivo* might involve lower frequencies (7). In this study we have not considered in detail the physical differences of

the effects of fluid shear stress or vibration stress on bone cell deformation. However complicated the transfer of forces at the cellular level might be, in terms of fluid shear stress or vibration stress, our results imply that the joint effect of the frequency and amplitude of loading might play similar roles for different types of stresses on bone cells. Our results suggest that the joint effect of the frequency (at third order) and amplitude (at first order) of loading correlates to the biochemical response of bone cells that contribute to sustained bone metabolism. Furthermore, this response might involve mechanisms that contribute to a specific behavior of bone cells in response to vibration stress enabling recognition of high frequency loading.

ACKNOWLEDGEMENTS

The authors would like to thank R.M. Heethaar for critically reading the manuscript. The Space Research Organization of the Netherlands supported the work of J.J.W.A. van Loon (DESC, MG-057 and SRON grant MG-055) and R.G. Bacabac (SRON grant MG-055) who also received financial assistance from the Netherlands Organization For International Cooperation In Higher Education (Physics Development Project PHL-146).

REFERENCES

1. Burger EH, Klein-Nulend J 1999 Mechanotransduction in bone - Role of the lacuno-canalicular network. *FASEB J* 13(Supplement):S101-S112.
2. Frost HM 2003 Bone's mechanostat: a 2003 update. *Anat Rec A Discov Mol Cell Evol Biol* 275(2):1081-1101.

3. Huiskes R, Ruimerman R, van Lenthe GH, Janssen JD 2000 Effects of mechanical forces on maintenance and adaptation of form in trabecular bone. *Nature* 405:704-706.
4. Wolff J 1892 *Gesetz der transformation der knochen*, Hirschwald, Berlin.
5. Turner CH, Owan I, Takano Y 1995 Mechanotransduction in bone: role of strain rate. *Am J Physiol* 269(3 Pt 1):E438-E442.
6. Tanaka SM, Li J, Duncan RL, Yokota H, Burr DB, Turner CH 2003 Effects of broad frequency vibration on cultured osteoblasts. *J Biomech* 36(1):73-80.
7. Bacabac RG, Smit TH, Mullender MG, Dijcks SJ, Van Loon JJWA, Klein-Nulend J 2004 Nitric oxide production by bone cells is fluid shear stress rate dependent. *Biochem Biophys Res Commun* 315:823-829.
8. Turner CH, Takano Y, Owan I, Murrell GA 1996 Nitric oxide inhibitor L-NAME suppresses mechanically induced bone formation in rats. *Am J Physiol* 270(4 Pt 1):E634-E639.
9. Pitsillides AA, Rawlinson SC, Suswillo RF, Bourrin S, Zaman G, Lanyon LE 1995 Mechanical strain-induced NO production by bone cells: a possible role in adaptive bone (re)modeling? *FASEB J* 9(15):1614-1622.
10. Chow JWM, Chambers TJ 1994 Indomethacin Has Distinct Early and Late Actions on Bone-Formation Induced by Mechanical Stimulation. *Am J Physiol* 267(2):E287-E292.

11. Jones DB, Nolte H, Scholubbers JG, Turner E, Veltel D 1991 Biochemical signal transduction of mechanical strain in osteoblast-like cells. *Biomater* 12(2):101-110.
12. Forwood MR 1996 Inducible cyclo-oxygenase (COX-2) mediates the induction of bone formation by mechanical loading *in vivo*. *J Bone Miner Res* 11(11):1688-1693.
13. Li J, Burr DB, Turner CH 2002 Suppression of prostaglandin synthesis with NS-398 has different effects on endocortical and periosteal bone formation induced by mechanical loading. *Calcif Tiss Internat* 70(4):320-329.
14. Rubin CT, Sommerfeldt DW, Judex S, Qin YX 2001 Inhibition of osteopenia by low magnitude, high-frequency mechanical stimuli. *Drug Discov Tod* 6(16):848-858.
15. Karcher H, Lammerding J, Huang HD, Lee RT, Kamm RD, Kaazempur-Mofrad MR 2003 A three-dimensional viscoelastic model for cell deformation with experimental verification. *Biophys J* 85(5):3336-3349.
16. Wang N, Butler JP, Ingber DE 1993 Mechanotransduction across the cell surface and through the cytoskeleton. *Science* 260(5111):1124-1127.
17. Kamm, R. D., McVittie, A. K., and Bathe, M. On the role of continuum models in mechanobiology. 242, 1-9. 2000. ASME Internat Cong - Mech Biol.
18. Guilak F, Tedrow JR, Burgkart R 2000 Viscoelastic properties of the cell nucleus. *Biochem Biophys Res Commun* 269:781-786.

19. Klein-Nulend J, Helfrich MH, Sterck JG, MacPherson H, Joldersma M, Ralston SH, Semeins CM, Burger EH 1998 Nitric oxide response to shear stress by human bone cell cultures is endothelial nitric oxide synthase dependent. *Biochem Biophys Res Commun* 250(1):108-114.
20. Fox SW, Chambers TJ, Chow JWM 1996 Nitric oxide is an early mediator of the increase in bone formation by mechanical stimulation. *Am J Physiol* 33(6):E955-E960.
21. Klein-Nulend J, Semeins CM, Ajubi NE, Nijweide PJ, Burger EH 1995 Pulsating fluid flow increases nitric oxide (NO) synthesis by osteocytes but not periosteal fibroblasts--correlation with prostaglandin upregulation. *Biochem Biophys Res Commun* 217(2):640-648.
22. Webster SSJ 2001 Integrated Bone Tissue Physiology: Anatomy and Physiology. In: Stephen C.Cowin (ed) *Bone Mechanics Handbook*, vol 1. CRC Press, Boca Raton, pp. 1-1-1-68.
23. Mancini L, Moradi-Bidhendi N, Brandi ML, MacIntyre I 1998 Nitric oxide superoxide and peroxynitrite modulate osteoclast activity. *Biochem Biophys Res Commun* 243(3):785-790.
24. Buttery LDK, Hukkanen MVJ, O'Donnell A, Polak JM, Hughes FJ 1995 Nitric oxide dependent and independent induction of prostaglandin synthesis in osteoblasts. *Bone* 17(6):560.
25. Hara S, Yanagi H, Amagai H, Endoh K, Tsuchiya S, Tomura S 2001 Effect of physical activity during teenage years, based on type of sport and duration of exercise, on bone mineral density of young, premenopausal Japanese women. *Calcif Tissue Int* 68(1):23-30.

26. Honda A, Sogo N, Nagasawa S, Shimizu T, Umemura Y 2003 High-impact exercise strengthens bone in osteopenic ovariectomized rats with the same outcome as Sham rats. *J Appl Physiol* 95(3):1032-1037.
27. Taaffe DR, Robinson TL, Snow CM, Marcus R 1997 High-impact exercise promotes bone gain in well-trained female athletes. *J Bone Miner Res* 12(2):255-260.
28. Rubin CT, Lanyon LE 1984 Regulation of bone formation by applied dynamic loads. *J Bone Joint Surg Am* 66(3):397-402.
29. Cook SD, Salkeld SL, Mse, Patron LP, Ryaby JP, Whitecloud TS 2001 Low-intensity pulsed ultrasound improves spinal fusion. *Spine J* 1(4):246-254.

CHAPTER 7

MICRORHEOLOGY OF MECHANOSENSITIVE BONE CELLS

Rommel G. Bacabac¹, Daisuke S. Mizuno², Theo H. Smit³, Jack J.W.A. Van Loon^{1,4}, Christoph Schmidt², Fred MacKintosh⁵, Jenneke Klein-Nulend¹

¹Department of Oral Cell Biology, Academic Centre for Dentistry Amsterdam-Universiteit van Amsterdam and Vrije Universiteit, Amsterdam, The Netherlands

²Department of Physics of Complex Systems, Vrije Universiteit, Amsterdam, The Netherlands

³Department of Clinical Physics and Informatics, VU University Medical Center, Amsterdam, The Netherlands

⁴Dutch Experiment Support Center, Vrije Universiteit, Amsterdam, The Netherlands

⁵Department of Theoretical Physics, Vrije Universiteit, Amsterdam, The Netherlands

In preparation for publication

ABSTRACT

To understand how the mechanosensing by bone cells might relate to cellular metabolism and mechanical properties, a physical portrait of cell viscoelasticity is needed. Thus, we developed a novel application of two-particle microrheology using fibronectin-coated spherical probes to characterize the viscoelasticity, mechanically stimulate, and probe the mechano-activity of various cell types. We found that the elastic modulus of MLO-Y4 osteocytes was below 500 Pa, as well as for MC3T3-E1 osteoblasts, and primary osteocytes and osteoblasts. Interestingly, the nitric oxide released by MLO-Y4 cells increased after a mechanical stimulation at 5 pN, with cell-attached integrin-bound probes. This suggests that bone cells respond to forces at a similar range as for deforming integrins. MLO-Y4 cells interacted with the integrin-bound probes by changing their shape from spherical to being polar at 37°C. However, the same shape change at 22°C was acquired by stimulation with 5-20 pN forces. This suggests that temperature has a significant effect on cell morphology. To probe the mechano-activity of bone cells, we measured the fluctuation of force $\langle f f^* \rangle$ induced by the cells on the integrin-bound probes. $\langle f f^* \rangle$ induced by MLO-Y4 cells were proportional to ω^2 (where frequency = $\omega/(2\pi)$) at frequencies < 3 Hz at 22°C. However, the force fluctuation was proportional to ω^2 for frequencies < 10 Hz at 37°C. Thus, temperature change possibly induces a sharp non-linear metabolic increase underlining the significant effect of the mechanical environment to cellular metabolism. Compared to MLO-Y4 cells, CCL-224 fibroblasts had a higher $\langle f f^* \rangle$ magnitude at 37°C, as might be expected considering the motility of fibroblastic cells. The linear relation of $\langle f f^* \rangle$ with ω^2 is a signature expected for continuums with slowly evolving internal processes. Hence, microrheology is a useful tool for understanding the varied set of observations on mechanosensing by bone cells and its implications on the osteogenic response of bone to mechanical loading.

INTRODUCTION

Cellular activity in response to stress stimuli has long been recognized. Previous reports have shown that cells respond to near zero gravity, fluid shear stress, strain stimuli, and vibration stress (1-4). Activation by mechanical loading has been shown to trigger chemical cascades that have significant roles for the metabolic maintenance of a global tissue to which the cell belongs. Mechanosensing, is the ability of cells to perceive forces, which includes the activity of different types of cells for transducing sound, for example, or for relaxing blood vessels at high fluid shear stress (5-7). The stress response of bone cells that direct osteogenic adaptation of bone to mechanical loading is an obvious example where mechanosensing by cells direct local changes that govern a global adaptation of the overall tissue. In bone, osteocytes are generally believed to sense the strain-induced fluid flow in the lacuno-canicular system. In response to stress, osteocytes produce signaling molecules, e.g., nitric oxide (NO) and prostaglandin E₂ (PGE₂), that regulate the activity of other cells for building or resorbing bone (8-10).

The cytoskeleton of the cell has been acknowledged as one of the key factors in mechanosensing (11). The cytoskeleton is crucial for various cellular mechanisms, including the internal transport of vesicles (12), motility (13), and the fundamental support of cell shape. To understand the underlying mechanisms for the metabolic responses of cells to mechanical stress, a physical portrait of the viscoelastic properties of the cell is needed. Recent techniques in microrheology might prove crucial for probing the viscoelasticity of cells and its relevance to mechanosensing. For instance, the two-particle microrheology technique has been extended for characterizing inter-cellular force generators (14, 15).

In vitro, cells attach to substrates via focal adhesion centers for anchorage (16). Interestingly, some cells adapt to environmental stress by inducing contractile forces in relation to the stiffness of surrounding material (17). By induction of traction forces, possibly at focal adhesion centers, cells match

environmental stress and adapt morphology accordingly. Thus, mechanically-induced adaptation might be as important as chemically-mediated metabolic cascades. By probing changes in mechanical properties of cells, we might be able to understand mechanisms of cellular interaction with its stress environment.

Mechanical properties of soft materials, such as cells, can be studied by using techniques from microrheology. The two general approaches in microrheology pertain to the measurement of probe particle displacements embedded in the material investigated. The approach is either by inducing external forces on the probes (active mode) or by monitoring the thermal fluctuations of the probes (passive mode). Materials in thermal equilibrium are subject to a measurement of the complex shear modulus (G^*) due to the Fluctuation-dissipation theorem (18). For our purpose in this study, the cell is taken as a non-thermal system, that is, a complex material that is able by itself to induce forces while interacting with its environment. Recently, using intracellular probes, it was shown that cells exhibit internally slow evolving processes characterized by ω^{-2} power-law for internal force fluctuation (14, 19). Cells also show enhanced diffusion scaling as $t^{3/2}$ at short times by SV80 fibroblasts, of phagocytized or endogenous particles demonstrating the non-thermal activity of cells (12).

Paradigms taken for understanding cellular activation might include models for the mechanical properties of the cytoplasm as predominantly a continuum (20) or as composed of linked polymers that transfer forces through the cytoskeleton to the nucleus (11). A model linking cellular deformation to a chemical response by cells, might explain the significance of interconnectivity between the extra-cellular matrix, trans-membrane proteins and the cytoskeleton as a direct link to the cell nucleus (11, 21). An initial activation might involve the stretching of a protein, thereby exposing a cryptic section of the unfolded protein that reacts to immediately trigger a biochemical cascade (21). Thus, a continuous force transfer from the site of mechanical stimulation to the nucleus is not necessary. Regardless of the actual mechanisms that

induce a meaningful biochemical cascade, the mechanical property of the cell is important for mechanosensing since the mechanical property determines how the cell will deform.

The aim of this study is to investigate events occurring at the onset of mechanical stimulation. Thus, we developed here a two-particle assay for measuring the viscoelastic properties of cells and characterizing the chemical and mechanical activation of cells in response to stress. We extended the Hertz model for the deformation of an elastic (and viscoelastic) sphere upon the indentation of a rigid spherical probe to measure the elastic (and viscoelastic) response of a cell. Using the same two-particle assay, we measured nitric oxide release as a parameter for bone cell mechanosensitivity in response to sinusoidal forces. The mechanoactivity of bone cells was studied by measuring the morphological changes while being attached to the probe particles, and the force traction induced by the cells on the probes. Finally, the mechanoactivity of bone cells was characterized by inferring the fluctuation of the induced force traction of the cells on the probes.

MATERIALS AND METHODS

The elastic modulus of MLO-Y4, MC3T3-E1, primary osteocytes and osteoblasts, were measured at 22°C, using a two-particle assay for microrheology by attaching fibronectin-coated beads at opposite ends of the cells using an optical trap setup (bead attachment diagram shown in fig 1). The cell was deformed by sinusoidal movements of one of the attached beads, and the elastic modulus was determined as described in the section “Hertz model extended for viscoelastic spheres”.

The elastic modulus of an MLO-Y4 cell, as a function of indentation depth, was measured at 22°C using an atomic force microscope (AFM) with a bead attached to the cantilever tip of the AFM using the Hertz model for round cells (for an application on thin regions of fibroblasts see (22)). The AFM

measurement was performed for a round MLO-Y4 cell that was partially attached to the substrate.

Nitric oxide released by MLO-Y4 cells was measured at 22°C. Morphological changes of bone cells, as well as the force traction induced by cells on the attached beads, were measured at 37°C. The apparent compliance measured by active and passive modes, at 22°C, was compared for MLO-Y4 cells to illustrate the difference between the active and passive mode measurements. The apparent compliance of MLO-Y4, MC3T3-E1, primary osteocytes and osteoblasts, were measured at 22°C and characterized by the force fluctuation. The force fluctuation of MLO-Y4 osteocytes was compared to that of CCL-224 fibroblasts at 37°C.

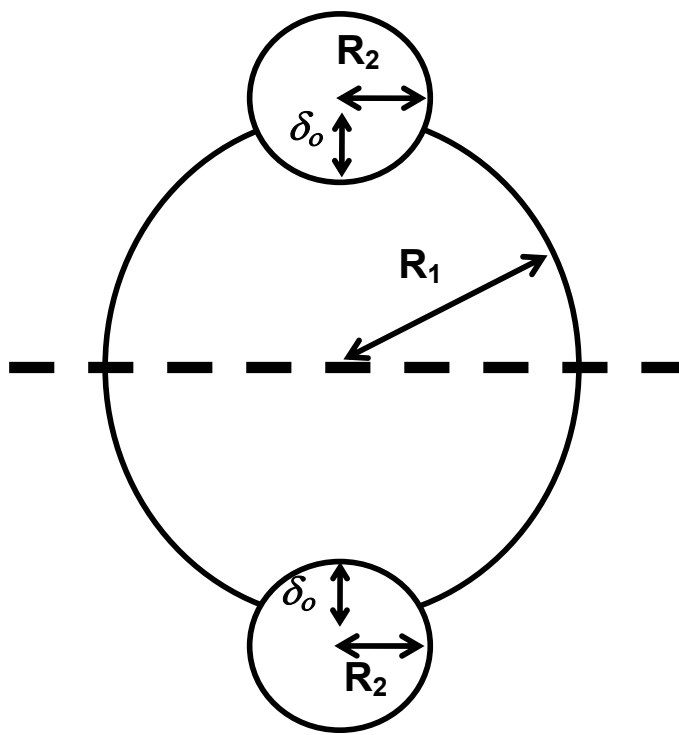


Figure 1. Hertz model for viscoelastic sphere indented with rigid spheres. Dashed line indicates the symmetry of the model.

Cell cultures

MLO-Y4 osteocytes were cultured at 37°C, up to near-confluence in 75 cm² cell culture flasks (Nunc, Roskilde, Denmark), using α-Modified Eagle's Medium (α-MEM; Gibco, Paisley, UK) supplemented with 5% fetal bovine serum (FBS; Gibco), 5% calf serum (CS; Gibco), penicillin (10μg/ml) and streptomycin (10μg/ml). The MLO-Y4 osteocytes were kindly provided by Dr. L. Bonewald (University of Missouri-Kansas City, Kansas City, MO, USA).

MC3T3-E1 cells were cultured at 37°C, up to near-confluence in 75 cm² cell culture flasks (Nunc), using α-MEM supplemented with 10% FBS, ascorbate (50 μg/ml; Merck, Darmstadt, Germany), β-glycerophosphate disodium salt hydrate (10 mM; Sigma, St. Louis, MO, USA), l-glutamine (300 μg/ml; Merck), gentamycine (50 μg/ml; Gibco), and fungizone (1.25 μg/ml; Gibco). The MC3T3-E1 osteoblasts were kindly provided by Dr. M. Kumegawa (Meikai University, Sakado, Japan).

CCL-224 fibroblasts were cultured at 37°C, up to near-confluence using α-MEM supplemented with 10% FBS, penicillin (10μg/ml) and streptomycin (10μg/ml). The CCL-224 cells were kindly provided by Dr. J. Boonstra, (Utrecht University, Utrecht, the Netherlands).

MLO-Y4, MC3T3-E1, and CCL-224 cells were harvested by 10 min treatment with 0.05% trypsin/0.01% EDTA in PBS at 37°C. These cells were incubated in ice-water water bath after harvesting. Prior to experiments, these cells were equilibrated to 22°C or 37°C in CO₂-independent medium (Gibco) without supplements.

Primary bone cell isolations

Fetal chicken calvarial cells were isolated as described by Ajubi *et al.* (23). Calvariae were aseptically dissected from 18-day-old chicken fetuses. A mixed population of osteocytes and osteoblasts was obtained from the calvariae by sequential treatments of 1 mg/ml collagenase (Sigma, St. Louis, MO, USA)

and 4 mM EDTA. Osteocytes were identified from the mixed population of cells using a specific anti-body OB 7.3 directed to antigens on the cytoplasmic membrane (24). Using an immunodissection method based on Van der Plas and Nijweide, 1992 (25), osteocytes were isolated and purified from the mixed cell population of osteocytes and osteoblasts. After isolation, Osteocytes and osteoblasts were cultured separately in 75 cm² cell culture flasks (Nunc) with α-MEM, containing 2% chicken serum (Gibco), 200 µg/ml glutamine (Sigma), 50 µg/ml gentamycin sulfate (Sigma), 50 µg/ml L-ascorbic acid (BDH, Brunschwig Chemie, Amsterdam, The Netherlands), and 1 mg/ml D-glucose. After one day, the osteocytes and osteoblasts were harvested by 5 min treatment with 0.05% trypsin/0.01% EDTA in PBS at 37°C. These cells were incubated in ice-water water bath after harvesting. Prior to experiments, these cells were equilibrated to 22°C or 37°C in CO₂-independent medium (Gibco) without supplements.

DAR4M loading for nitric oxide fluorescence

For nitric oxide determination, MLO-Y4 cells were treated with a membrane-permeable fluorescent indicator Diaminorhodamine-4M AM (DAR-4M AM; Daiichi Pure Chemicals, Tokyo, Japan) (26). The intracellular DAR-4M AM treatment of cells lasted for 1 hr while the cells were incubated in ice-water bath. Prior to experiments, the cells were equilibrated to 22°C in CO₂-independent medium (Gibco) without supplements. To test whether an increase of fluorescence signal is induced by the presence of NO, 20 mM of the NO donor S-nitroso-N-acetylpenicillamine (SNAP; Sigma) was added to MLO-Y4 cells treated with DAR-4M AM.

Preparation of fibronectin-coated microspheres (beads)

Carboxyl-modified 4 µm diameter-polystyrene microspheres (beads; Bangs Laboratories, Inc., Fishers, IN, USA) were cleaned and coated with fibronectin

(Gibco) according to the manufacturer's instructions (Bangs Laboratories, Inc.). The fibronectin-coated beads were suspended in phosphate buffered saline (PBS; Gibco) with 0.1% bovine serum albumin (BSA; Gibco). For the experiments, the fibronectin-coated beads were cleaned with PBS and sonicated for 5 min to remove aggregations. The beads were then re-suspended in CO₂-independent medium and equilibrated to 22°C or 37°C.

Preparation of dichloro-dimethyl-silane coated cover slips

24 x 50 mm cover slips (Menzel-Glaser, Braunschweig, Germany) used as the bottom surface of the culture chamber for observation in the optical trap setup were made hydrophobic by coating them with dichloro-dimethyl-silane (DDS; Acros Organics, USA). The cover slips were sequentially treated with KOH (30 g/200 ml ethanol) for 30 min and sequentially rinsed in distilled water (3 s), HCl (5% in distilled water for 3 s), and ethanol (3 s). After completely drying the cover slips, they were treated with DDS in trichloroethylene (TCE; Acros Organics, Morris Plains, NJ, USA) for 5 min. The treated cover slips were rinsed with ethanol for 2-5 min under sonic bath before overnight annealing at 80°C.

Preparation of Atomic force microscope cantilever

12 µm diameter-polystyrene microspheres (beads; Bangs Laboratories, Inc.) were attached to an atomic force microscope cantilever (stiffness 0.05 N/m, resonance frequency 18 kHz). The cantilever was cleaned with toluene and acetone. The cantilever tip was then treated with ultraviolet-hardened glue (UV-glue, 1 part in 5 parts toluene), and was left to dry. The treated cantilever was attached to a micropipette tip at the end opposite the tip, with grease. The cantilever was subsequently immersed in a suspension of beads. After a bead was conveniently located at the cantilever tip, it was irradiated with UV to permanently attach the bead to the cantilever tip.

Hertz model extended for viscoelastic spheres

To measure cell viscoelasticity, we extended the Hertz model (reference Hertz) for viscoelastic spheres. The force-indentation relation for contact between two elastic spheres has been described by Timoshenko and Goodier (27). Here we extend this model for a rigid spherical probe indenting a viscoelastic sphere, the force F is related to a 3/2 scaling-law due to the indentation depth d :

$$F = \frac{4}{3} \sqrt{\frac{R_1 R_2}{R_1 + R_2}} \left(\frac{E_o}{1 - \nu^2} d^{3/2} \right) \quad [1]$$

where R_1 and R_2 , are the radii of the cell and the probe (fig 1), the homogenous elastic modulus E_o and the Poisson ratio ν . Since we attach the probe to the cell, we induce a constant indentation depth of d_o and perturb about this value sinusoidally at amplitude d . By a Taylor expansion about d_o , we find a complex modulus E^* :

$$F = \frac{4}{3} \sqrt{\frac{R_1 R_2}{R_1 + R_2}} \left(\frac{E_o}{1 - \nu^2} d_o^{3/2} + \frac{3E^*}{2(1 - \nu^2)} \sqrt{d_o} d \right) \quad [2]$$

where E_o is an elastic contribution due to a constant force F_o (see also Mahaffy et al. for an application for flat cells using “atomic force microscopy” or AFM (22)). By setting F_o to zero, i.e., by assuring that the applied force oscillates about zero, the complex modulus E^* is found as follows:

$$F = F_o + F^* \quad [3]$$

setting $F_o = 0$, the applied force F^* becomes linear with the indentation d (provided $d < d_o$):

$$F^* = 2 \sqrt{\frac{R_1 R_2}{R_1 + R_2}} \left(\frac{E^*}{1 - \nu^2} \right) (\sqrt{d_o}) d \quad [4]$$

Hence, the complex modulus is:

$$E^* = E' + iE'' \quad [5a]$$

where the loss and storage moduli are E' and E'' , respectively. The elastic modulus is then calculated as $|E^*|/(1-\nu^2)$ or simply $E/(1-\nu^2)$:

$$\frac{|E^*|}{(1 - \nu^2)} = \frac{E}{(1 - \nu^2)} = \frac{|F^*|}{2d} \sqrt{\frac{R_1 + R_2}{R_1 R_2 d_o}} \quad [5b]$$

which is related to the shear modulus:

$$|G^*| = \frac{E}{2(1+\nu)} \quad [5c]$$

The cell stiffness k_{12} is related to the trap stiffnesses, k_1 and k_2 , in our two-particle assay, constituting a three-spring series (fig 2). The force-balance equations, with the forces at the probes, f_1 and f_2 , the displacements of the beads x_1 and x_2 , and the stiffnesses, are as follows:

$$\begin{pmatrix} f_1 \\ f_2 \end{pmatrix} = \begin{pmatrix} k_1 + k_2 & -k_{12} \\ -k_{12} & k_2 + k_{12} \end{pmatrix} \begin{pmatrix} x_1 \\ x_2 \end{pmatrix} \quad [6]$$

Hence the apparent compliance A_{ij} (mutual compliance for $i \neq j$) is simply the inverse of the stiffness matrix k_{ij} above, at the quasi-steady regime:

$$\begin{pmatrix} x_1 \\ x_2 \end{pmatrix} = \begin{pmatrix} A_{11} & A_{12} \\ A_{21} & A_{22} \end{pmatrix} \begin{pmatrix} f_1 \\ f_2 \end{pmatrix} \quad [7a]$$

$$\begin{pmatrix} A_{11} & A_{12} \\ A_{21} & A_{22} \end{pmatrix} = \frac{1}{(k_1 + k_{12})(k_2 + k_{12}) - (k_{12})^2} \begin{pmatrix} k_1 + k_{12} & k_{12} \\ k_{12} & k_2 + k_{12} \end{pmatrix} \quad [7b]$$

The apparent compliance was measured in the active mode directly from the movement of the particles at 0.1 Hz and 0.5 Hz. At higher frequencies, we used a lock-in amplifier technique referenced from the frequency at the acousto-optical device in the optical trap setup (see fig 3 for a diagram of the setup).

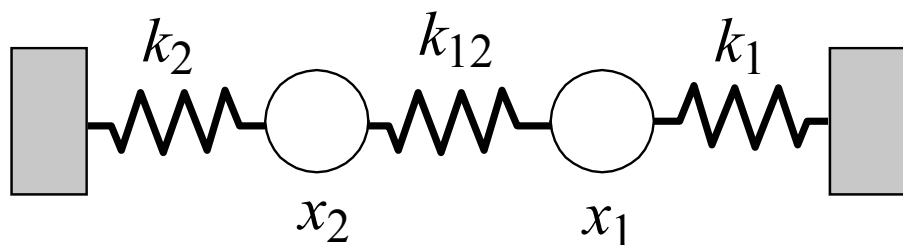


Figure 2. Spring series model for two-particle microrheology assay for cells. k_1 , k_2 are optical trap stiffnesses; k_{12} , cell stiffness; x_1 and x_2 , particle displacements.

Passive microrheology

By observing the fluctuations of each probe and the mutual fluctuations of the beads, the complex compliances are calculated from the auto-correlations and cross-correlations of the particles. Details of the techniques for both one and two-particle microrheology has been described previously (15, 28, 29). Based on the fluctuation-dissipation theorem, the imaginary component of the compliance α_{ij}'' (mutual apparent compliances where $i \neq j$) is related to the thermal energy $k_B T$ as follows:

$$\langle x_i(\omega)x_j(\omega) \rangle = 4k_B T \alpha_{ij}''(\omega) / \omega \quad i=1,2 \quad [8]$$

where, k_B is the Boltzmann constant, T is the absolute temperature, and the frequency $= \omega/(2\pi)$. The Kramers-Kronig relation is used to find the real component of the apparent compliance α_{ij}' :

$$\alpha_{ij}'(\omega) = \frac{2}{\pi} P \int_0^\infty \frac{\chi \alpha_{ij}''}{\chi^2 - \omega^2} d\chi \quad i,j=1,2 \quad [9]$$

For the quasi-steady regimes, the cell compliance α_{12} is calculated by setting $1/k_{12} = \alpha_{12}$ in [7]. The components of the complex compliance of the cell α_{12} are linear to the corresponding components of the apparent compliance A_{12} :

$$\alpha_{12} = \alpha' + i\alpha'' \quad [10a]$$

$$\alpha_{12} = \left(\frac{A_{12}'}{|A_{12}|^2 k_1 k_2} - \frac{k_1 + k_2}{k_1 k_2} \right) + i \left(\frac{-A_{12}''}{|A_{12}|^2 k_1 k_2} \right) \quad [10b]$$

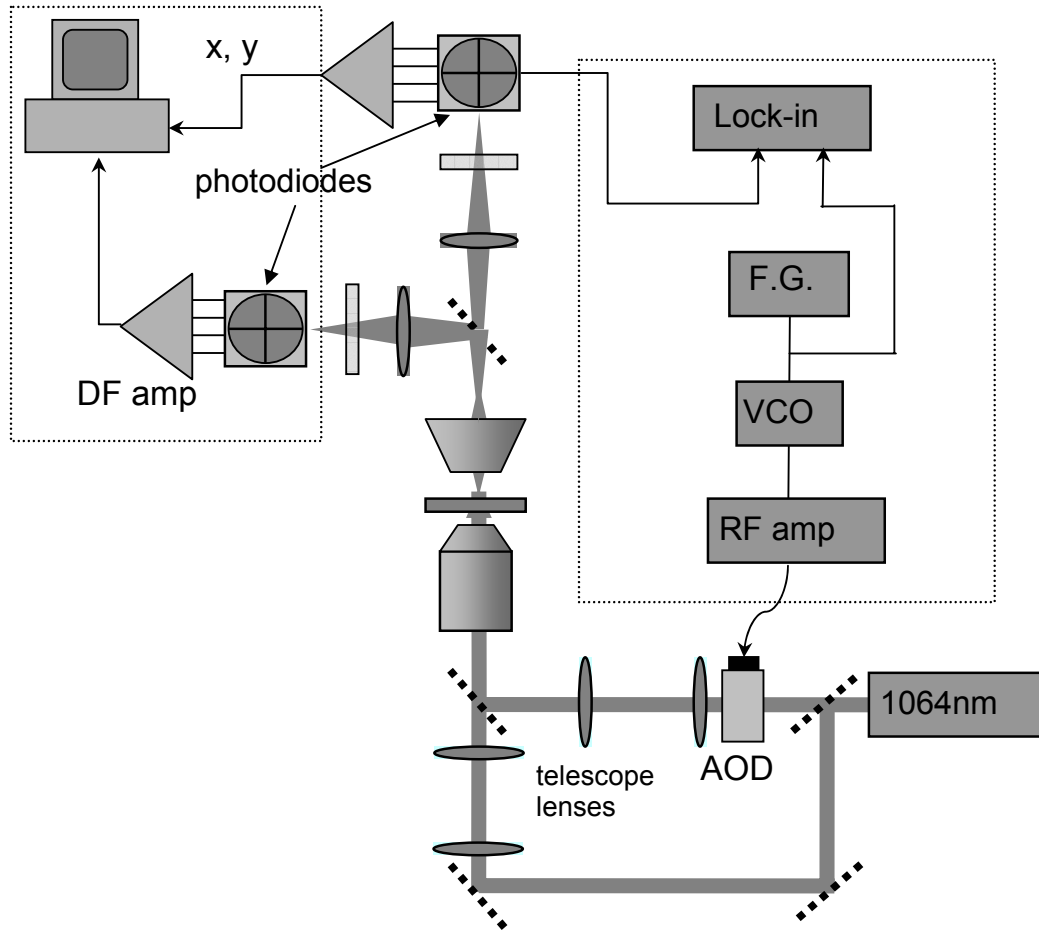


Figure 3. Schematic diagram of experimental setup. 1064 nm laser beam is diverted in two paths for trapping two particles. One of the beams is manipulated by using an acoustic optical device (AOD). A lock-in amplifier is used for measurements of the frequency response. DF amp, differential amplifier; F.G., function generator; VCO, voltage controlled oscillator; RF amp, radio frequency amplifier.

Non-thermal force fluctuation

A Generalized Langevin equation is used to model the force-balance in our two-particle assay for the microrheology of cells. The force on a small thermal particle with velocity u_i is related to a memory friction $\xi_{ij}(t)$ (mutual memory friction for $i \neq j$) of the complex material:

$$m_i \frac{du_i(t)}{dt} = f_{Ri}(t) - \int_{-\infty}^t \xi_{ij}(t-t') u_i(t') dt' \quad [11a]$$

where f_{Ri} represents all forces acting on particle i , including an inter-particle force f_I (in this case, comprising non-thermal forces from the cell), forces from the laser traps with stiffness $k_i x_i$, and stochastic Brownian forces K_i :

$$f_{Ri} = -k_i x_i + K_i + f_I \quad [11b]$$

Zero resultant force is expected in our two-particle assay, thus the coupled force-balance equations are:

$$\int_{-\infty}^t \xi_{11}(t-t') u_1(t') dt' = - \int_{-\infty}^t \xi_{12}(t-t') u_2(t') dt' - k_1 x_1 + K_1 + f \quad [12a]$$

$$\int_{-\infty}^t \xi_{22}(t-t') u_2(t') dt' = - \int_{-\infty}^t \xi_{21}(t-t') u_1(t') dt' - k_2 x_2 + K_2 - f \quad [12b]$$

Where the thermal force fluctuation is:

$$\langle K_i(t) K_j(t') \rangle = 2k_B T \xi_{ij}(t-t') \quad [13]$$

The non-thermal force fluctuation is then simply the difference between the total force fluctuation in the assay based on the displacement fluctuation of the probe particles $\langle x_1 x_2^* \rangle$, and the thermal force fluctuation. The power spectrum of the non-thermal fluctuation $\langle x_1 x_2^* \rangle$ is:

$$\langle x_1 x_2^* \rangle - \frac{4k_B T \alpha_{12}''}{\omega} = -\Delta(\omega) \{ (A_{11}'' - A_{12}'')^2 + (A_{11}' - A_{12}')^2 \} \quad [13]$$

where $\Delta(\omega)$ represents the power spectrum of the fluctuation. Alternately, the force fluctuation is directly measured as:

$$\langle f(t) f(t') \rangle = 2k_B T \Delta(t-t') \quad [14]$$

with the power spectrum:

$$\langle f f^* \rangle = \frac{2k_B T}{\sqrt{2\pi}} \Delta(\omega) \quad [15]$$

RESULTS

The typical force-displacement curves for MLO-Y4 cells and primary osteocyte cells showed a linear relation between the applied force and the cell

diameter change (2d, fig 4A and B). This shows that our model is accurate for determining the elastic modulus of cells for the quasi-steady regime (here taken at 0.1 Hz). The elastic moduli ($E/(1-\nu^2)$) of the bone cells were all similarly below 1 kPa, except for one osteocyte cell, which had an elastic modulus about 1.4 kPa (fig 5A). The MLO-Y4 modulus varied between 35 Pa and 430 Pa (fig 5A). Using AFM with the Hertz model for round cells, the elastic modulus of a MLO-Y4 osteocyte was shown to vary from 65 Pa to 230 Pa, for indentation depths varying between 4800 to 7900 nm (fig 5B).

To investigate the effects of mechanical loading on cell using pN forces, the accumulated nitric oxide (NO) released by MLO-Y4 cells were monitored. A typical MLO-Y4 cell treated with DAR-4M-AM indicated continued fluorescence increase with the addition of 20 nM SNAP (data shown for 60 s, fig 6A). The effect of small changes in force amplitudes was investigated by stimulating MLO-Y4 cells with sinusoidal force at amplitudes 5, 7.5, 10, and 12.5 pN, all at 0.1 Hz (each regime taken at durations of 60s). Total fluorescence intensity increase was found simultaneous to force application at 0.1 Hz (fig 6B and C). Fluorescence intensity increased from the basal level upto 60 s as a force amplitude of 5pN was applied (fig 6B). An abrupt increase was observed when a force amplitude of 7.5 pN was applied (at about the 60 s time point); afterwards, the intensity was nearly stable beyond 200 s of force application. The sharp increase with the application of 10 pN force amplitude is attributed to a possible artifact by perturbation of the cell position disturbing the fluorescence intensity, as the intensity went back to the stable level (fig 6B). Simultaneous with the observation of fluorescence intensity increase, the cellular traction force was found to increase from 0 to 60 pN in the period of 4 min (fig 6 B). Another MLO-Y4 cell was stimulated with sinusoidal loading at 0.1 Hz with amplitudes 5, 10, 15 pN at one-min intervals. After 1 min of 5 pN stimulation, the fluorescence intensity increased from the basal level and remained stable (fig 6C). This increase occurred while the cell was stimulated with 10 pN sinusoidal force, and remained at a stable value despite further stimulation with 15 pN (fig 6C).

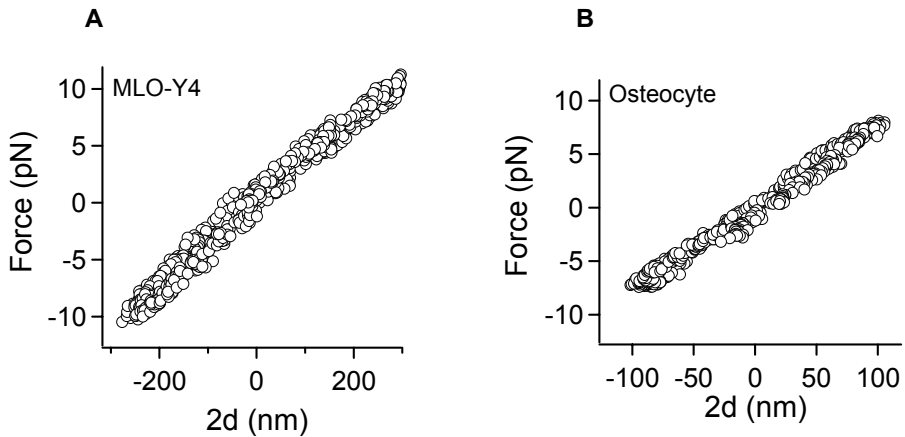


Figure 4. Force-displacement curves. A. MLO-Y4. B. Osteocyte. $2d$, change in cell diameter.

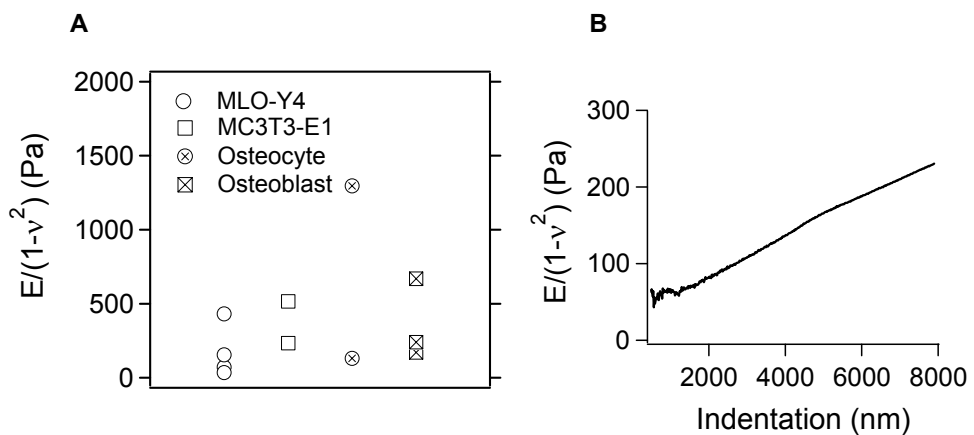


Figure 5. Elastic moduli E . A. Elastic moduli for bone cells. B. Elastic modulus change of a round MLO-Y4 cell in relation to indentation depth by atomic force microscopy.

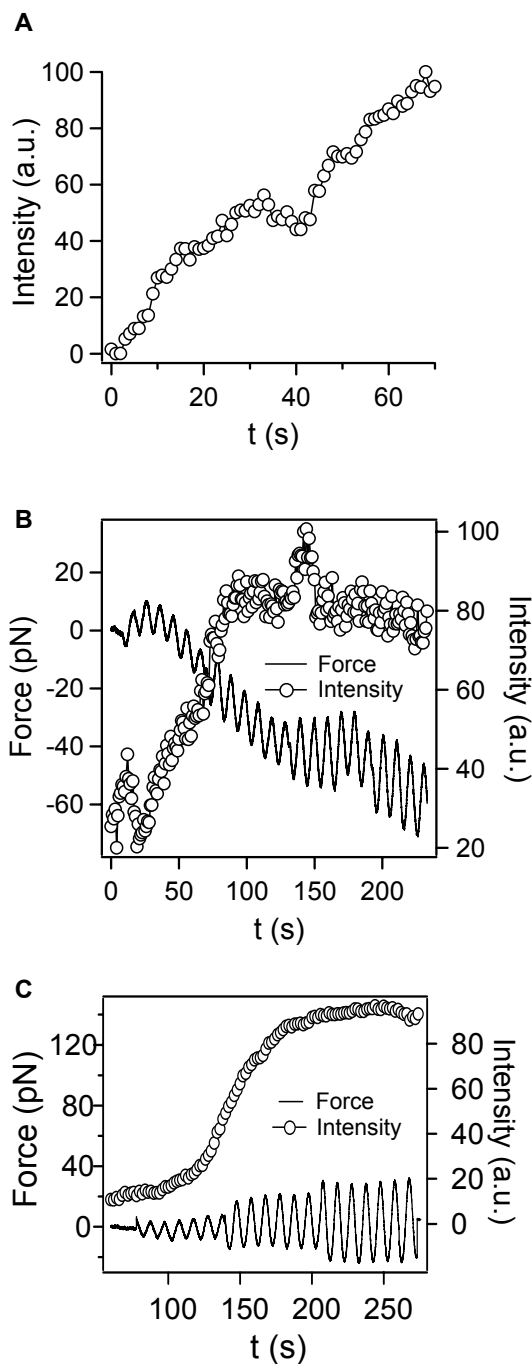


Figure 6. Nitric oxide release. A. Fluorescence intensity increase in MLO-Y4 cell treated with 20 mM SNAP solution. B. Nitric oxide release and MLO-Y4 cell induction of contractile force while stimulated with 0.1 Hz sinusoidal force with increasing amplitudes at 22°C. C. Nitric oxide release of MLO-Y4 cell while stimulated with sinusoidal force at 0.1 Hz, at increasing amplitudes.

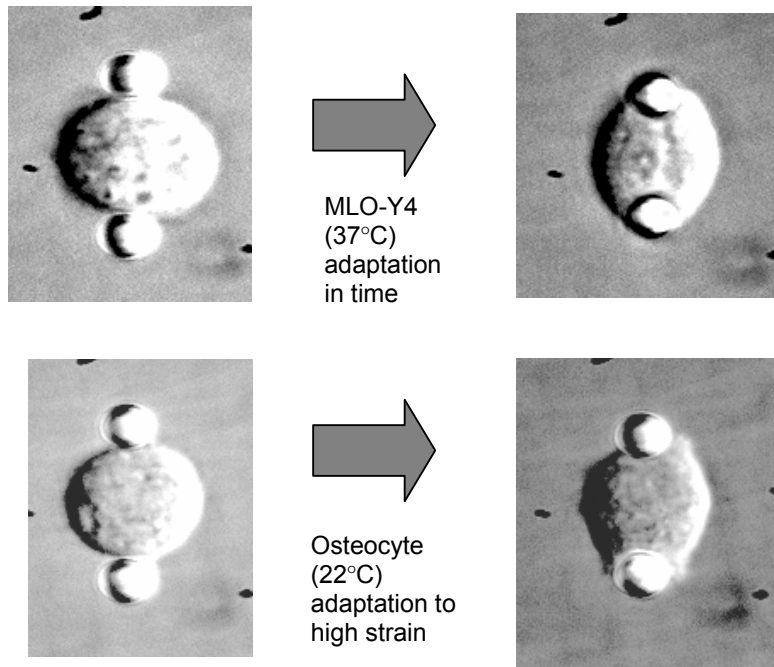


Figure 7. Morphology adaptation. A. MLO-Y4 cell changed morphology from spherical to polar shape at 37°C, without force stimulation. B. Osteocyte cell changed morphology from spherical to polar shape at 22°C, after stimulation with sinusoidal force at 0.1 Hz, with increasing amplitudes from 5pN to nearly 30pN.

MLO-Y4 cells, while attached to two particles, showed morphological adaptation within ~ 20 min at 37°C (typical change shown in fig 7). The cell changed from a spherical to a polar shape at the attachment sites (fig 7). At 22°C, an osteocyte cell was subjected to sinusoidal forces at 0.1 Hz, at increasing amplitudes (between 5 to 20 pN). The tension was released after each sinusoidal force stimulation, every 30s. The osteocyte adapted by changing shape from spherical to being polar at the attachment sites (fig 7). At 37°C the contractile force of an MLO-Y4 cell on the attached particle was found to increase to 30 pN in 60s (fig 8A). For another MLO-Y4 cell, also at 37°C, the contractile force varied periodically and reached a peak at 30 pN in 30s (fig 8B). The contractile forces on the attached particles appeared to be

consistently anti-correlating, as the experiment configuration is symmetric (fig 8A and B).

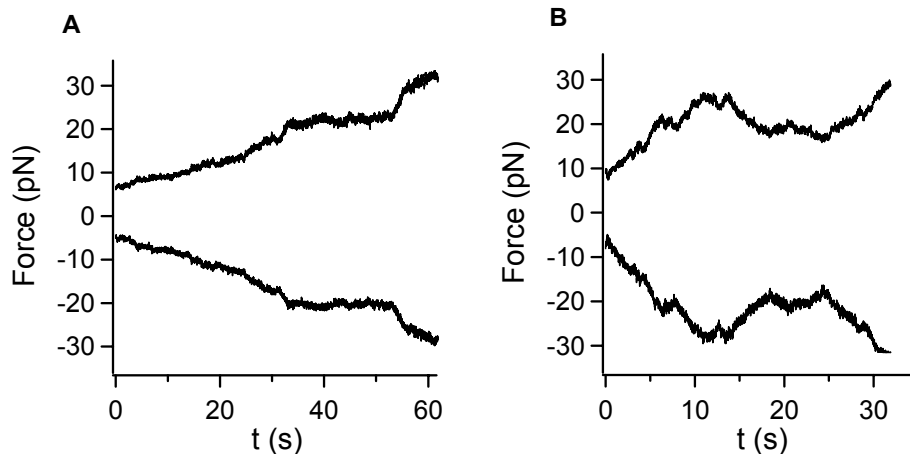


Figure 8. MLO-Y4 cell induction of contractile force. A. at 22°C. B. at 37°C.

The apparent compliance of osteocytes, and MLO-Y4 cells measured by active or passive modes were compared for measurements performed at 22°C and 37°C, respectively. At 22°C the real component of the apparent compliance, A_{12}' of osteocytes measured by active or passive modes was similar (fig 9A). However, the imaginary component of the apparent compliance, A_{12}'' , measured by passive mode was negative and much lower compared to A_{12}'' measured by active mode until around 3 Hz (fig 9A). At 37°C A_{12}' measured by active and passive modes for MLO-Y4 cells, were similar in value, but A_{12}'' measured by active and passive modes differed (fig 9B). Whereas, A_{12}'' by active mode was nearly zero, A_{12}'' by passive mode was negative until about 10 Hz.

To compare the mechanical activity of different cell types, the force fluctuation $\langle f f^* \rangle$, based on equation [15] was measured for MLO-Y4, MC3T3-E1 cells, primary osteocytes and primary osteoblasts at 22°C, and for MLO-Y4 and CCL-224 fibroblasts at 37°C. At 22°C, the force fluctuation for all cell-types was found proportional to ω^2 for frequencies ≤ 3 Hz (fig 10). The force fluctuation for MLO-Y4 cells were found higher than MC3T3-E1 cells (fig 10).

Also, osteocytes exhibited higher force fluctuation compared to osteoblasts (fig 10). The force fluctuation of MC3T3-E1 cells was found relatively similar to osteocytes (fig 10). At 37°C the force fluctuation of CCL-224 fibroblasts was a decade higher than MLO-Y4 cells (fig 11). However, the force fluctuation of both MLO-Y4 and CCL-224 cells were proportional to ω^{-2} for frequencies ≤ 10 Hz.

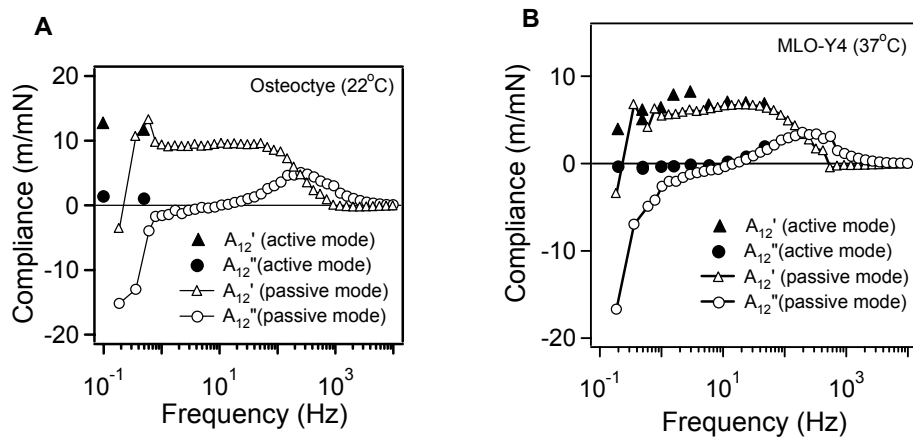


Figure 9. Apparent compliance. A. Osteocyte cell at 22°C. B. MLO-Y4 at 37°C

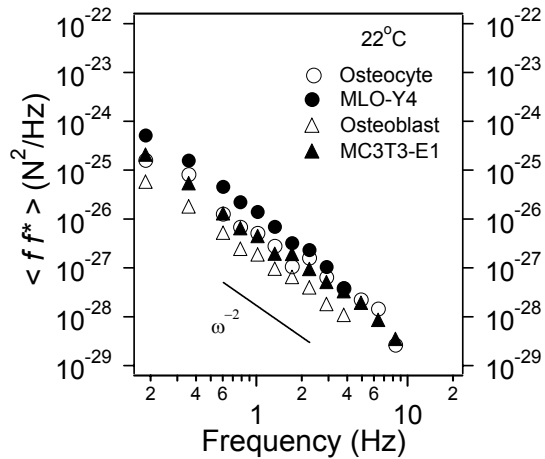


Figure 10. Force fluctuation at 22°C by bone cells

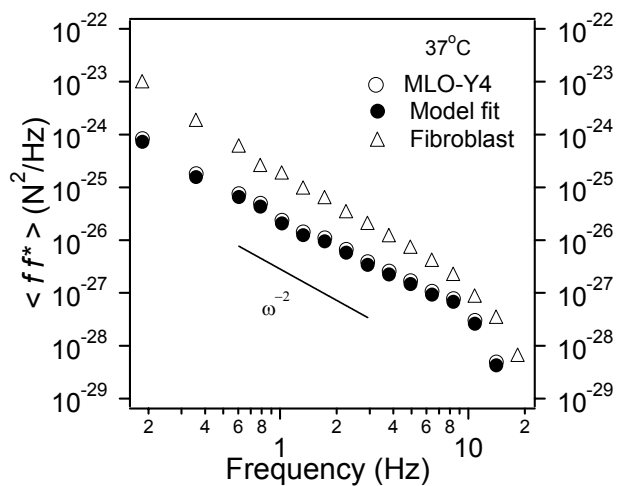


Figure 11. Force fluctuation at 37°C by MLO-Y4 osteocytes and CCL-224 fibroblasts.

DISCUSSION

The elastic moduli of the bone cells were similarly below 1 kPa, except for one osteocyte with an elastic modulus nearly 1.4 kPa. The elastic modulus of MLO-Y4 cells, as measured by optical tweezers, were confirmed to be within a similar range of values, as measured by AFM on a round MLO-Y4 cell. However, the AFM results also showed that the elastic modulus of a round MLO-Y4 cell varied with increasing indentation depth by the AFM cantilever. Thus, the elastic modulus of a cell is strongly dependent to the applied stress. Previously, we showed that osteocytes are more mechanosensitive than osteoblasts (1). Since the elastic modulus of the different bone cell types were similar, this might indicate that differences in mechanosensitivity between cells might be more related to how cells change moduli in relation to deformation.

MLO-Y4 cells showed an increased release of NO (by increase in fluorescence intensity) after about 1 min mechanical stimulation of 5 pN. Simultaneous with increased NO release was the observed increased force traction on the attached bead. Continued morphological adaptation by MLO-Y4 cells during bead attachment, supports the notion that morphology and force induction by cells are related. Since, force traction is simultaneous with

morphological changes and morphological changes is directly related to the elasticity of the cell, the release of NO is possibly related to changes in the elastic modulus of the cell. Furthermore, we have shown that force traction of the cells increased up to nearly 30 pN, which is within the order of force values necessary for activating integrins (30, 31), which was interestingly within the order of the forces we used to stimulate NO release. Cells might adapt their elasticity in relation to their stress environment, in a strong relation to their physiological activity, *e.g.*, the release of a signaling molecule.

The apparent compliance is linear to the actual compliance as indicated in equation [10], provided, within negligible momentum effects due to the surrounding fluid. Our apparent compliance measurements, indicate that the MLO-Y4 cells change viscoelasticity in strong relation to temperature. Since A_{12}' is proportional to the cross-correlation of the fluctuations of the two attached beads, this difference measures the force traction of the cells below a cross-over frequency (3 Hz for 22°C, 10 Hz for 37°C). The cross-over frequency, separates the non-thermal activity (or cellular activity) from thermal activity. The difference between 22°C and 37°C is negligible (in the Kelvin scale). Hence, an order of difference between cross-over frequencies might indicate a non-linear transition due to temperature for the activity of cells. This further illustrates the importance of temperature for directing metabolic activities of the cell and the non-linear properties of cells. In general, the mechanical stress environment of a cell strongly influences its behavior.

The proportionality between the cellular force fluctuation with ω^2 , indicates a quantifiable signature for non-thermal related activity by bone cells. This signature is expected in continuums with slowly evolving internal processes (14). All cells in this study exhibited this signature. However, the magnitude of the force fluctuations $\langle f f^* \rangle$ varied across cell types at 22°C and 37°C. It is interesting that this variation across cell types indicates that osteocytes have a higher mechanoactivity than osteoblasts. However, we also showed that the force fluctuation by CCL-224 is an order higher than that of osteocytes. This

supports the notion that fibroblasts have a high metabolism, which is necessary for motility.

The force fluctuation is indicative of internal metabolic processes. Our results have shown that osteocytes are also more mechanoactive compared to osteoblasts. However, fibroblasts, are even more mechanoactive than osteocytes. This, however, does not correlate with our earlier result showing that fibroblasts are least mechanosensitive compared to osteocytes and osteoblasts (32). Thus, mechanoactivity and mechanosensitivity, though related might not necessarily correlate.

In conclusion, we have shown the use of microrheology to probe the possible novel correlations between mechanosensitivity, mechano-activity, and the viscoelasticity of bone cells. Our results might prove useful for numerical models for cells in relation to their functional activity in bone. Techniques in microrheology provide quantifiable measures for explaining the varied set of observations in studying the response of bone cells to stress and its implications for the osteogenic response of bone to mechanical loading.

ACKNOWLEDGEMENTS

The authors would like to thank R.M. Heethaar for critically reading the manuscript, A. Vatsa for the intracellular NO detection, and C.M. Semeins for his technical assistance and discussion. The Space Research Organization of the Netherlands supported the work of R.G. Bacabac (SRON grant MG-055 and MG-057) who also received financial assistance from the Netherlands Organization For International Cooperation In Higher Education (Physics Development Project PHL-146).

REFERENCES

1. Klein-Nulend J, van der Plas A, Semeins CM, Ajubi NE, Frangos JA, Nijweide PJ, Burger EH 1995 Sensitivity of osteocytes to biomechanical stress in vitro. *FASEB J* 9(5):441-445.
2. Owan I, Burr DB, Turner CH, Qiu J, Tu Y, Onyia JE, Duncan RL 1997 Mechanotransduction in bone: osteoblasts are more responsive to fluid forces than mechanical strain. *Am J Physiol* 273(3 Pt 1):C810-C815.
3. Judex S, Boyd S, Qin YX, Turner S, Ye K, Muller R, Rubin C 2003 Adaptations of trabecular bone to low magnitude vibrations result in more uniform stress and strain under load. *Ann Biomed Eng* 31(1):12-20.
4. Cogoli A, Tschopp A, Fuchsblislin P 1984 Cell Sensitivity to Gravity. *Science* 225(4658):228-230.
5. Haidekker MA, Stevens HY, Frangos JA 2004 Cell membrane fluidity changes and membrane undulations observed using a laser scattering technique. *Ann Biomed Eng* 32(4):531-536.
6. White CR, Haidekker M, Bao X, Frangos JA 2001 Temporal gradients in shear, but not spatial gradients, stimulate endothelial cell proliferation. *Circulation* 103(20):2508-2513.
7. Kros C 2005 Hearing: aid from hair force. *Nature* 433(7028):810-811.
8. Burger EH, Klein-Nulend J 1999 Mechanotransduction in bone - Role of the lacuno-canalicular network. *FASEB J* 13(Supplement):S101-S112.

9. Burger EH, Klein-Nulend J, Van der Plas A, Nijweide PJ 1995 Function of osteocytes in bone--their role in mechanotransduction. *J Nutr* 125(7 Suppl):2020S-2023S.
10. Klein-Nulend J, Semeins CM, Ajubi NE, Nijweide PJ, Burger EH 1995 Pulsating fluid flow increases nitric oxide (NO) synthesis by osteocytes but not periosteal fibroblasts--correlation with prostaglandin upregulation. *Biochem Biophys Res Commun* 217(2):640-648.
11. Wang N, Butler JP, Ingber DE 1993 Mechanotransduction across the cell surface and through the cytoskeleton. *Science* 260(5111):1124-1127.
12. Caspi A, Granek R, Elbaum M 2000 Enhanced diffusion in active intracellular transport. *Phys Rev Lett* 85(26):5655-5658.
13. Kole TP, Tseng Y, Jiang I, Katz JL, Wirtz D 2005 Intracellular mechanics of migrating fibroblasts. *Mol Biol Cell* 16(1):328-338.
14. Lau AW, Hoffman BD, Davies A, Crocker JC, Lubensky TC 2003 Microrheology, stress fluctuations, and active behavior of living cells. *Phys Rev Lett* 91(19):198101-1-198101-4.
15. Crocker JC, Valentine MT, Weeks ER, Gisler T, Kaplan PD, Yodh AG, Weitz DA 2000 Two-point microrheology of inhomogeneous soft materials. *Phys Rev Lett* 85(4):888-891.
16. Petit V, Thiery JP 2000 Focal adhesions: structure and dynamics. *Biol Cell* 92(7):477-494.

17. Pelham RJ, Wang YL 1997 Cell locomotion and focal adhesions are regulated by substrate flexibility. *Proc Natl Acad Sci USA* 94(25):13661-13665.
18. Chaikin PM, Lubensky TC 1995 Principles of condensed matter physics, Cambridge University Press, New York.
19. Fabry B, Maksym GN, Butler JP, Glogauer M, Navajas D, Fredberg JJ 2001 Scaling the microrheology of living cells. *Phys Rev Lett* 87(14):148102.
20. Karcher H, Lammerding J, Huang HD, Lee RT, Kamm RD, Kaazempur-Mofrad MR 2003 A three-dimensional viscoelastic model for cell deformation with experimental verification. *Biophys J* 85(5):3336-3349.
21. Janmey PA, Weitz DA 2004 Dealing with mechanics: mechanisms of force transduction in cells. *Tren Biochem Sci* 29(7):364-370.
22. Mahaffy RE, Park S, Gerde E, Kas J, Shih CK 2004 Quantitative analysis of the viscoelastic properties of thin regions of fibroblasts using atomic force microscopy. *Biophys J* 86(3):1777-1793.
23. Ajubi NE, Klein-Nulend J, Nijweide PJ, Vrijheid-Lammers T, Alblas MJ, Burger EH 1996 Pulsating fluid flow increases prostaglandin production by cultured chicken osteocytes--a cytoskeleton-dependent process. *Biochem Biophys Res Commun* 225(1):62-68.
24. Nijweide PJ, Mulder RJ 1986 Identification of osteocytes in osteoblast-like cell cultures using a monoclonal antibody specifically directed against osteocytes. *Histochem* 84(4-6):342-347.

25. van der PA, Nijweide PJ 1992 Isolation and purification of osteocytes. *J Bone Miner Res* 7(4):389-396.
26. Kojima H, Hirotani M, Nakatubo N, Kikuchi K, Urano Y, Higuchi T, Hirata Y, Nagano T 2001 Bioimaging of nitric oxide with fluorescent indicators based on the rhodamine chromophore. *Anal Chem* 73(9):1967-1973.
27. Timoshenko SP, Goodier JN 1970 Theory of elasticity, 3rd ed, McGraw-Hill Book Company, Singapore.
28. Levine AJ, Lubensky TC 2000 One- and two-particle microrheology. *Phys Rev Lett* 85(8):1774-1777.
29. Levine AJ, Lubensky TC 2001 Response function of a sphere in a viscoelastic two-fluid medium. *Phys Rev E* 6304(4):041510-1-041510-12.
30. Gao M, Craig D, Lequin O, Campbell ID, Vogel V, Schulten K 2003 Structure and functional significance of mechanically unfolded fibronectin type III1 intermediates. *Proc Natl Acad Sci USA* 100(25):14784-14789.
31. Oberhauser AF, Badilla-Fernandez C, Carrion-Vazquez M, Fernandez JM 2002 The mechanical hierarchies of fibronectin observed with single-molecule AFM. *J Mol Biol* 319(2):433-447.
32. Ajubi NE, Nijweide PJ, Klein-Nulend J, Burger EH, Semeins CM 1995 Pulsatile fluid flow stimulates nitric oxide (NO) production by osteocytes, but not periosteal fibroblasts. *Bone* 17(6):566.

CHAPTER 8

MICROGRAVITY AND BONE CELL MECHANOSENSITIVITY

Rommel G. Bacabac¹, Jack J.W.A. Van Loon^{1,2}, Jolanda M.A. de Blieck-Hogervorst¹, Cor M. Semeins¹, Djien Tan¹, Aviral Vatsa¹, Theo H. Smit³, Jenneke Klein-Nulend¹

¹Department of Oral Cell Biology, Academic Centre for Dentistry Amsterdam-Universiteit van Amsterdam and Vrije Universiteit, Amsterdam, The Netherlands;

²Dutch Experiment Support Center, Vrije Universiteit, Amsterdam, The Netherlands;

³Department of Physics and Medical Technology, VU University Medical Center, Amsterdam, The Netherlands

ABSTRACT

Stress derived from bone loading which affects bone cells is likely the strain-induced flow of interstitial fluid along the surface of osteocytes and lining cells. The response of bone cells in culture to fluid flow includes prostaglandin (PG) synthesis and expression of prostaglandin G/H synthase inducible cyclooxygenase (COX-2). Cultured bone cells also rapidly produce nitric oxide (NO) in response to fluid flow as a result of activation of endothelial nitric oxide synthase (ecNOS), the enzyme which also mediates the adaptive response of bone tissue to mechanical loading. Earlier studies have shown that the disruption of the actin-cytoskeleton abolishes the response to stress, suggesting that the cytoskeleton is involved in cellular mechanotransduction.

Microgravity, or near weightlessness, is associated with the loss of bone in astronauts, and has catabolic effects on mineral metabolism in bone organ cultures. This might be explained as resulting from an exceptional form of disuse under near weightlessness conditions. We found earlier that the transduction of mechanical signals in bone cells also involves the cytoskeleton and is related to PGE₂ production. Therefore it is possible that the mechanosensitivity of bone cells is altered under near weightlessness conditions, and that this abnormal mechanosensation contributes to disturbed bone metabolism observed in astronauts.

In the experiment “FLOW”, we tested the hypothesis of altered cell bone mechanosensitivity using an *in vitro* model developed for space flight experiments. The specific aim of FLOW was to test whether the production of early signaling molecules that are involved in the mechanical load-induced osteogenic response (NO and PGE₂) by bone cells is changed under microgravity conditions compared to 1xg conditions. FLOW was one of the Biological experiment entries to the Dutch Soyuz Mission “DELTA” (Dutch Expedition for Life Science, Technology and Atmospheric Research). FLOW was flown by the Soyuz craft, which was launched on April 19, 2004, on its way to the International Space Station (ISS).

Osteocytes, osteoblasts, and periosteal fibroblasts were isolated from chicken skull and incubated in plunger boxes, developed by Centre for Concepts in Mechatronics (Nuenen, The Netherlands), using plunger activation events for single pulse fluid shear stress stimulations. Cultures in-flight were subjected to microgravity and simulated 1xg level by centrifugation. Ground controls were subjected to identical culture environment and fluid shear stress stimulations. Due to unforeseen hardware complications, results from in-flight cultures are considered lost. Ground control experiments showed an accumulative increase of NO in medium for osteocytes (as well as for osteoblasts and periosteal fibroblasts). Data from the online-NO sensor showed that the NO produced in medium by osteocytes increased sharply after pulse shear stress stimulations. COX-2 mRNA expression revealed high levels in osteoblasts compared to the other cell types tested. In conclusion, preparations for the FLOW experiment and preliminary ground results indicate that the FLOW setup is viable for a future flight opportunity.

INTRODUCTION

It has been well documented that bone tissue is sensitive to its mechanical environment. Subnormal mechanical stress as a result of bedrest or immobilization results in decreased bone mass and disuse osteoporosis (1). Spaceflight produces a unique condition of skeletal unloading as a result of the near absence of gravity. Studies of animals and humans subjected to spaceflight agree that near weightlessness negatively affects the mass and mechanical properties of bone (for a review, see (2)). Although the exact mechanism whereby bone loss as a result of spaceflight occurs is still unknown, recent *in vivo* studies suggest that bone cells are directly sensitive to near weightlessness. Using organ cultures of living bone rudiments from embryonic mice, Van Loon *et al.* (1995) showed that 4 days of spaceflight inhibited matrix mineralization, while stimulating osteoclastic resorption of mineralized matrix (3). Monolayer cultures of the human osteoblastic cell line MG-63 responded to 9 days of near weightlessness with reduced expression of osteocalcin, alkaline phosphatase, and collagen I α 1 mRNA (4). Reduced prostaglandin production was found in cultures of MC3T3-E1 osteoblastic cells exposed to 4 days of near weightlessness, probably due to inhibition of serum-induced growth activation (5). In addition near weightlessness induced prostaglandin E₂ (PGE₂) and interleukin-6 production in rat bone marrow stroma cultures, an observation that may be related to alterations in bone resorption (6). These results suggest that mineral metabolism and bone cell differentiation are modulated by near weightlessness, and that bone cells are directly responsive to microgravity conditions.

Direct responses of bone cells to mechanical stimuli have been studied using several methods to apply mechanical stress *in vivo* (for a review, see (7)). Stretching or bending of the cell substratum has been widely used, but recent evidence indicates that fluid flow over the cell surface may better simulate the cellular effect of mechanical loading of bone *in vivo* (8-15). Strain (deformation) of the bone matrix as a result of mechanical stress *in vivo* causes flow of

interstitial fluid through the network of osteocyte lacunae and canaliculi (16, 17). Weinbaum *et al.* (1994) used Biot's porous media theory to relate loads applied to a whole bone to the flow of canicular interstitial fluid. Their calculations predict fluid shear stresses of 0.8 to 3 Pa as a result of peak physiological loading regimes (12). We have shown earlier that osteocytes are sensitive to fluid shear stress *in vitro*, and release signaling molecules such as NO and PGE₂ in response to fluid shear stress (18).

FLOW was our entry to the Biological experiments carried by the Dutch Soyuz Mission "DELTA" (Dutch Expedition for Life Science, Technology and Atmospheric Research). Through DELTA, FLOW was flown by the Soyuz craft, which was launched on April 19, 2004, on its way to the International Space Station (ISS). The main scientific objective of the FLOW experiment was to test whether the production of early signaling molecules that are involved in the mechanical loading-induced osteogenic response (NO and PGE₂) by osteocytes is changed under microgravity conditions compared to 1xg conditions. Since we argue that especially the osteocyte, and not the osteoblast, is the mechanosensitive cell type within bone involved in mechanotransduction, the production of signaling molecules by osteocytes were compared to osteoblasts. Periosteal fibroblasts were used as negative controls. Chicken osteocytes, osteoblasts, and periosteal fibroblasts were incubated in plunger boxes developed by the Centre for Concepts in Mechatronics, using plunger activation events for single pulse fluid shear stress stimulations. Cultures in-flight were subjected to microgravity (μ -g) and simulated 1xg level by centrifugation. Ground controls were subjected to identical culture environment and fluid shear stress stimulations.

GROUND PREPARATIONS AND HARDWARE DEVELOPMENT

Dutch Soyuz Mission – FLOW hardware development

The experiment FLOW made use of plunger box units (PBU) (figure 1) developed by the Centre for Concepts in Mechatronics (CCM). One module contained two culture compartments, each holding a glass slide containing about 5×10^4 cells each (fig 1A). For each culture compartment fresh culture medium or RNA stabilization solution (RNALater, Ambion Inc., USA) were stored in three fluid reservoirs. The fluid was forced into the culture compartment by releasing a spring-loaded plunger by scorching a nylon thread by a heat wire at preset times. The fluid was led to the cultures via a system of internal channels and valves (as indicated by arrows in fig 1A). The spent medium was forced out of the culture compartment and found its way to the, now void, volume behind the just released plunger. These units were accommodated with a small NO probe and associated electronics for automated activation and digital data storage, during the experiment time-line for the Dutch Soyuz Mission (fig 1B).

The FLOW equipment for flight made use of 16 Type I experiment containers, which were installed in the KUBIK incubator facility, containing a centrifuge, built by COMAT Aerospace (Toulouse, France) for the European Space Agency (ESA) (fig 1C). A total of 6 containers in the flight centrifuge as 1xg controls, and 6 flight static (microgravity) containers were used. We designed the experiment to carry 4 units per cell type / g-level. This means that 12 cell cultures at 1xg and 12 cell cultures at μ -g were accommodated. An additional 2 containers per g-level were needed to command the experiment timeline and acquire and store the NO measurements.

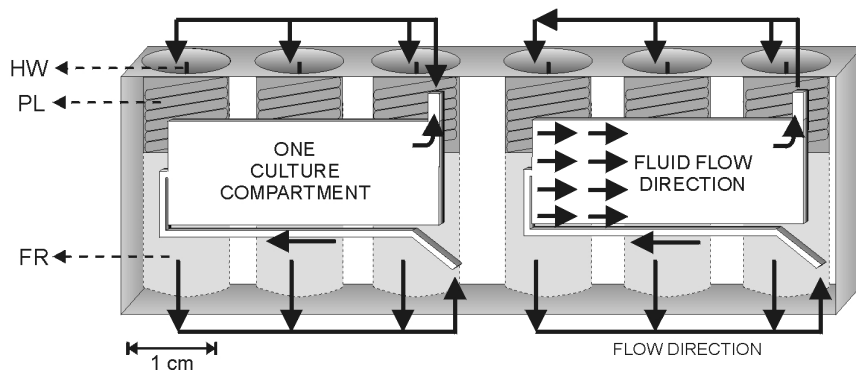
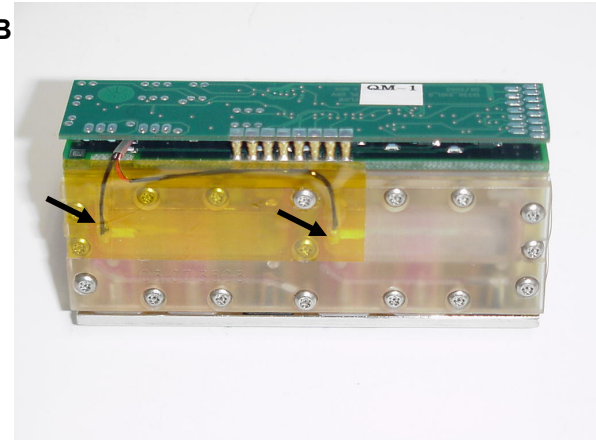
A**B****C**

Figure 1. Plungerbox. A. schematic representation of an automated tissue culture module (20x40x80 mm) made of a single block of polysulphone (PSU) as it was developed by the Centre for Concepts in Mechatronics (CCM; diagram courtesy of Dr. van Loon; HW, waste or sample holder; PL, plunger; FR, fluid reservoir). B. Plunger box unit with nitric oxide (NO) sensor (arrow). C. KUBIK incubator and centrifuge facility. Pictures courtesy of Centre for Concepts in Mechatronics (CCM).

Dutch Soyuz Mission – FLOW hardware fluid flow characterization

The present laboratory hardware set-up as used for our regular research was scaled down and manufactured in compliance with space flight requirements. A characterization of the parallel-plate flow chamber was performed using analytical and numerical calculations assuming laminar viscous flow under isothermal conditions ((19); see chapter 2 of this thesis). The parallel-plate flow chamber was downscaled from a width-to-height ratio of 80.0 to 33.3 (fig 2A). In order to validate this downscaled flow chamber, immortalized mouse calvarial osteoblast-like cells (MC3T3-E1) were used. These cells were cultured to near confluence in α -MEM with 10% fetal bovine serum (FBS). For fluid shear stress treatment, cells were plated at 2×10^5 cells/glass slide (5 cm^2), and incubated for 5 min in the presence of dynamic fluid shear stress with amplitude 0.7 Pa, average 0.7 Pa, and frequency of 5 Hz. Bone cell cultures showed similar mechanosensitivity (i.e., increased NO production) in response to dynamic wall shear stress averaging 0.7 Pa for a parallel-plate chamber width-to-height ratio of 80.0 reduced to 33.3 (fig 2B). Thus, our design conditions for downscaling the parallel-plate chamber for space flight requirements do not introduce artifacts for measuring the mechanosensitivity of bone cells. The NO produced was measured in the harvested media, as well as online with NO sensor probes incorporated in the PBU's (see fig. 1B).

Fluid flow patterns in the actual geometry of the PBU's developed by CCM for FLOW were simulated using Computational Fluid Dynamics software in the Technical University of Delft (flow chamber diagram, fig 2C). This work was done in collaboration with Prof. Frans Nieuwstadt and Dr. Mathieu Pourquie of the Hydrodynamics and Aerodynamics laboratory of the Technical University in Delft (The Netherlands). We found that the inclusion of an NO sensor in the PBU did not affect a homogenous fluid shear stress profile under laminar flows at the cell monolayer to induce a peak shear stress of 1.4 Pa, the stress needed to stimulate bone cells (fig 2D). The chamber height of the flight PBU's were adjusted in order to achieve fluid shear stress pulse stimulations on the cells reaching a peak of 1.4 Pa.

NO sensor characterization and cell culture test on plunger boxes

An online NO sensor, manufactured by Innovative Instruments, Inc. (Tampa, FL, USA) has been characterized for its use in the FLOW experiment (fig 3A). The online NO sensor was found to exhibit a linear relation between its current signals to the increase of NO in solution. The temperature dependence of the sensor could be corrected by software; however, since the Dutch Soyuz Mission experiment involved a constant temperature environment, such a correction procedure was not necessary.

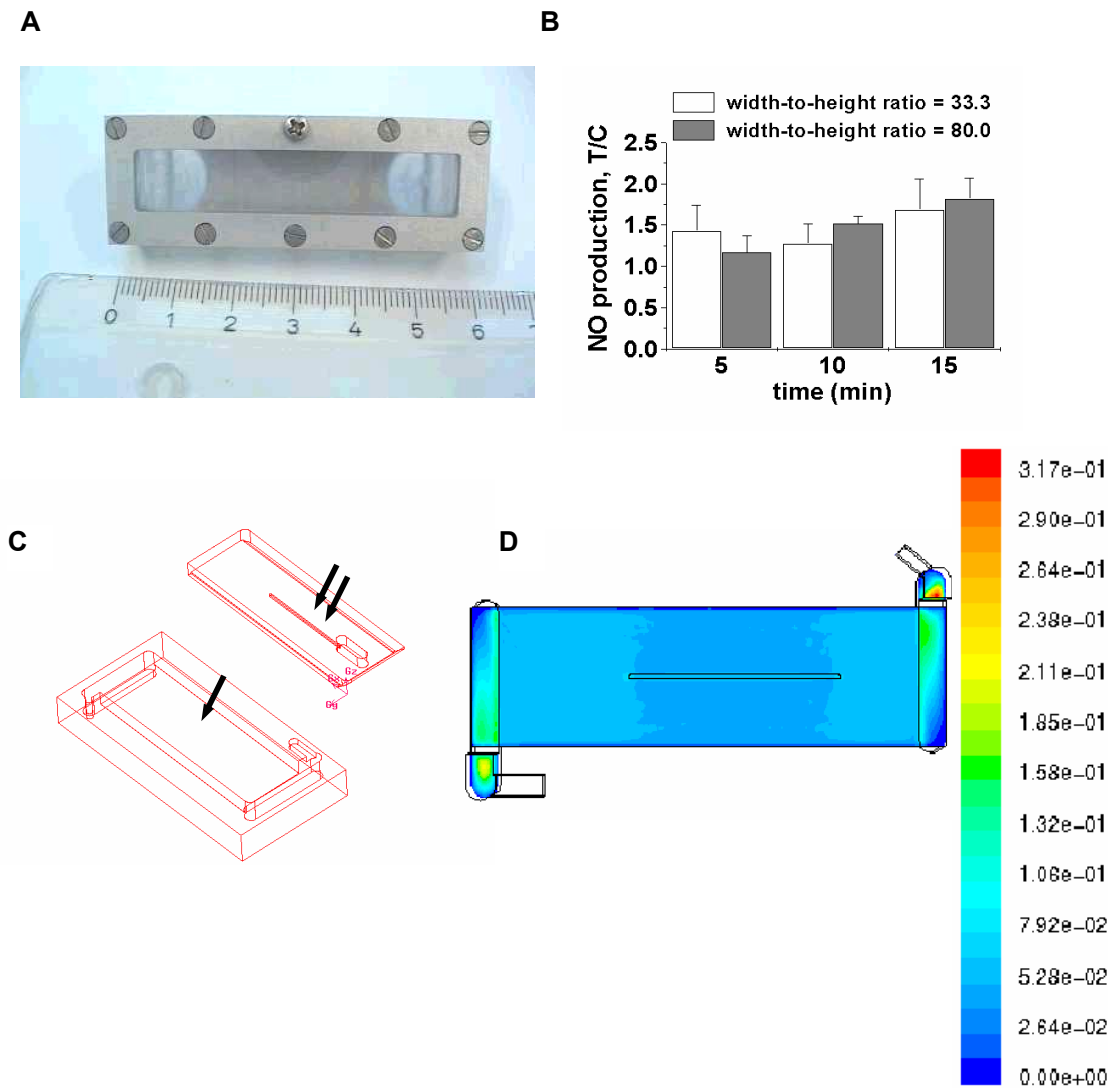


Figure 2. Parallel-plate flow chamber *in vitro* system. A. The parallel-plate flow chamber system was downscaled to have a width-to-height ratio of 33.3 from a previous ratio of 80.0 to fit into the space flight experiment requirements. B. Bone cells respond similarly to the same flow regime (PFSS, average shear stress = 0.7 Pa, 5Hz), for different flow chamber width-to-height ratios (33.3 and 80.0) up to nearly 2-fold NO production. T/C, PFF treatment over control ratio. C. Plunger box unit: culture chamber (single arrow), lid with online nitric oxide sensor (two arrows). D. Homogenous velocity patterns in the plunger box unit implies a homogenous wall shear stress at 1.4 Pa (fluid velocity in arbitrary units).

Cell viability for the FLOW experiment was tested by using primary bone cells (chicken-derived osteocytes, osteoblasts, and periosteal fibroblasts), and back-up cell-lines (MLO-Y4 osteocyte-like cells, MC3T3-E1 osteoblast-like cells, and CCL-226 fibroblast-like cells) in a simulated experiment time-line for the actual space experiment, including ground preparations and transport duration and environment from Amsterdam to the hand-over at Baikonur, Kazakhstan. These tests showed that the cells survived prolonged culture at ambient temperatures for transport using a CO₂-independent medium (fig 3B and C). This viability test also indicated that the presence of the NO sensor was not harmful to the cell cultures.

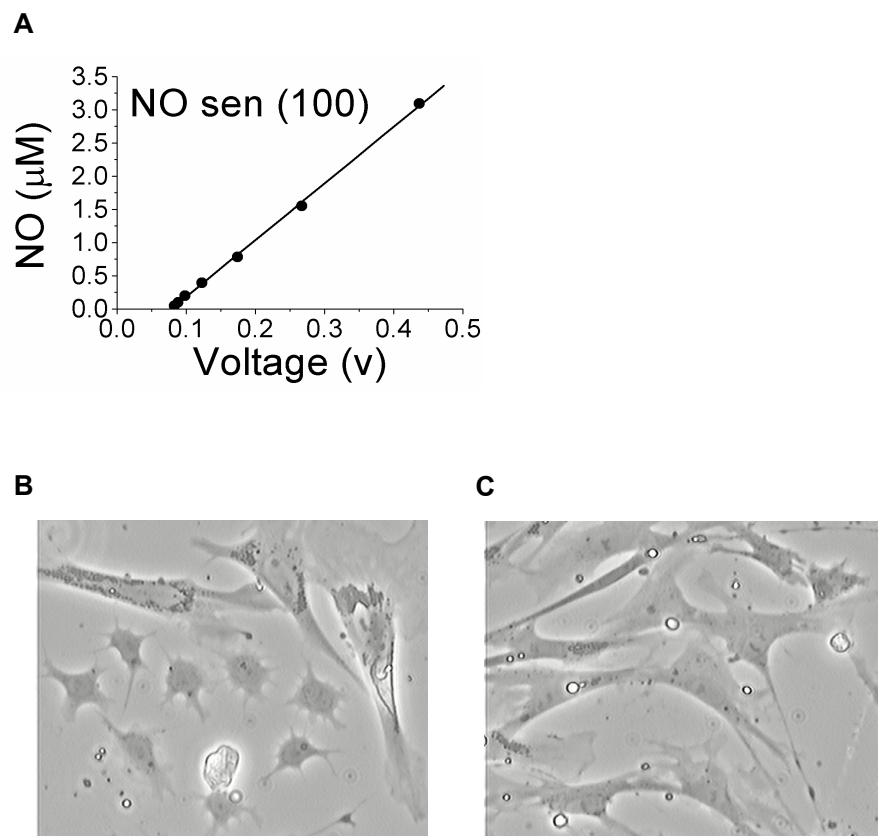


Figure 3. Nitric oxide sensor calibration and cell cultures in the plunger box units (PBU). A. inNO 100 by Innovative Instruments, Inc. (Tampa, FL, USA) indicated linear increase in voltage in relation to sequential increase of nitric oxide concentration in solution. B. Osteocytes after 6 days of room temperature. C. Periosteal fibroblasts after 6 days at room temperature.

FLIGHT EXPERIMENT “FLOW” ON THE DUTCH SOYUZ MISSION

In this FLOW experiment, we tested the hypothesis of changed bone cell mechanosensitivity under near-weightlessness conditions. Gravity was applied using an onboard centrifuge. The response of the cells to flow stimulation was measured using online NO sensors. At the end of the experiment conditioned medium was tested for prostaglandin and NO production. Semi-quantitative polymerase chain reactions was performed to study COX-2 mRNA expression.

Bone cell cultures

Osteocytes were isolated from avian bone, using immunoseparation with a chicken osteocyte-specific antibody (gift from Dr. Nijweide, Leiden University, The Netherlands). Primary chicken osteocytes, osteoblasts and periosteal fibroblasts were harvested from calvariae as described by Ajubi *et al.* (20).

Primary cell cultures were prepared in Amsterdam, and transported at late access to Baikonur in Kazachstan. In this regard, a ground laboratory venue for handling primary cell cultures was set up for preparations in Baikonur. The following conditions were required for transport and storage conditions: temperature: ambient, 4-8°C or lower; pressure: ambient (normal environmental conditions on earth or in flight); shock: minimum at post-launch, storage and after re-entry; humidity: ambient.

Experimental groups

The experiment consisted of six different groups (where $g = 9.8 \text{ m/s}^2$, acceleration due to gravity).

Group 1: $1 \times g$, osteocytes (OCY)

Group 2: $1 \times g$, osteoblasts (OB)

Group 3: $1 \times g$, fibroblasts (PF)

Group 4: $\mu\text{-}g$, osteocytes

Group 5: $\mu\text{-}g$, osteoblasts

Group 6: $\mu\text{-}g$, fibroblasts

Expected results

According to our working hypothesis the mechanosensitivity of bone cells under near weightlessness conditions is disturbed compared to unit gravity control conditions. If this hypothesis is correct and if there is a direct effect of near weightlessness on the cell, then the results as depicted in table 1 may be expected compared to control Group 1.

Table 1. *Expected results*

		Medium components (PGs, NO)	mRNA (COX-2, ecNOS)	mRNA (COX-1)
Group 1 (OCY)	$1 \times g$	++	++	0
Group 2 (OB)		+	+	0
Group 3 (PF)		0	0	0
Group 4 (OCY)	$\mu\text{-}g$	0	0	0
Group 5 (OB)		0	0	0
Group 6 (PF)		0	0	0

PGs, prostaglandins; NO, nitric oxide; COX-2, cyclooxygenase-2; ecNOS, endothelial cell nitric oxide synthase. ++, highest response; +, response; 0, no response.

Experiment hardware

We employed “standard” experiment container units based on “plunger boxes” developed by CCM. The only change was that these units had to be accommodated with the small NO probe and associated electronics for automated activation and digital data storage during experiment time line, and some minor technical changes were implemented in order to achieve a peak shear stress stimulation of 1.4 Pa. Automated activation and digital data storage were dependent on a suitable power source provided by the KUBIK facility.

Brief flight experiment protocol

During the complete experiment time-line the medium was changed three times: the medium was refreshed two times, while during the last step RNA stabilization liquid was added. The experiment (phase B-C-D of experiment time-line, see fig 4) was conducted in the Soyuz using Type I Experiment containers, and had a microgravity group with an in-flight 1xg control group using a centrifuge and a ground control group. We used closed Type I containers with two extra type I containers used as electronics boxes for each group (in-flight microgravity group, 1xg-control group, ground control group). These two electronics boxes were needed for 1) experiment activation, and 2) online NO sensor signal processing. We required having power on all the experiment containers in the Kubik even before launch, since online NO detection was already interesting during the launch period (phase A of experiment time-line, see fig 4). However, during launch, centrifuge operation was not strictly necessary.

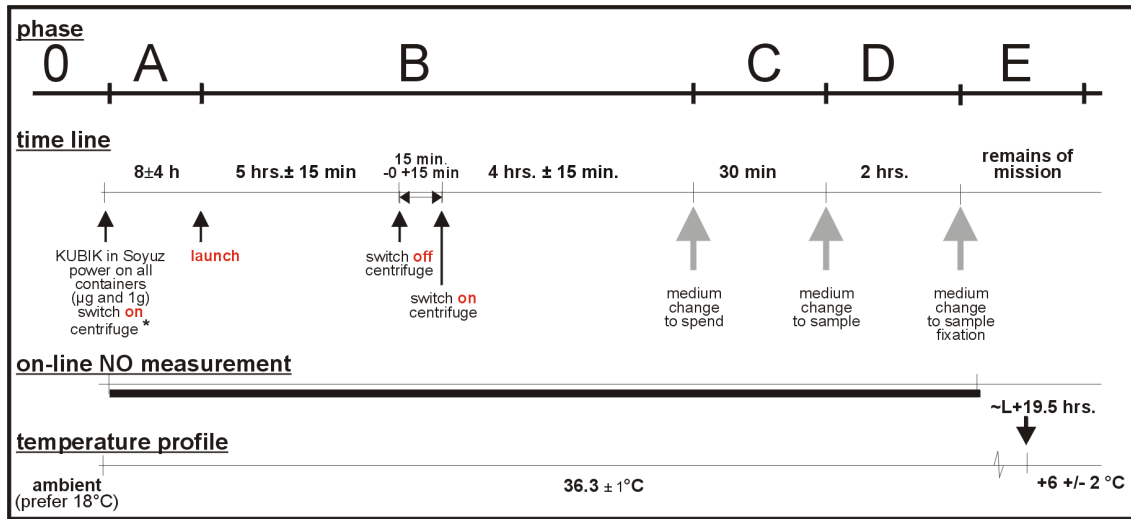


Figure 4. Schematic diagram of experiment protocol.

Experiment phases (fig 4)

0. Pre- launch period: samples were shipped to launch site and integrated into facility / launcher.
- A. Pre-launch period: the experiment containers, now in the Kubik, were integrated into Soyuz and all experiment containers for FLOW (total 16: 8 on static and 8 on centrifuge positions) were powered via the Kubik. In this period we started to log the NO data from the cells. This phase needed to be as short as possible.
- B. Post-launch period in which all containers were under microgravity until the crew was able to switch on the centrifuge. The centrifuge was turned on as soon as possible after launch. Estimated time to start the centrifuge was about 3 hours. Two hours after switch on the centrifuge it was temporarily switched off for about 15 minutes. The remaining part of this phase (i.e. 4 hours) was designated for the culture to overcome any possible disturbing effects of launch acceleration and vibration and start / stop of the centrifuge.
- C. Experiment phase 1. This is the experiment phase in which the cells were exposed to near weightlessness or 1×g conditions. In this ‘early response period’ we measured on-line NO levels starting from baseline (i.e. fresh medium), and sampled this medium for on-ground

- prostaglandin levels. The replaced medium needed to be collected separately.
- D. This is the extended experiment phase in which the cells were still exposed to near weightlessness or $1\times g$ conditions. During this period we measured on-line NO levels starting from baseline (i.e. fresh medium), and sampled this medium for on-ground prostaglandin levels. At the end of this phase the medium was replaced by mRNA extraction fluid to “stabilize” the cellular mRNA. The replaced medium needed to be collected separately. The experiment containers were then left in place / stored until landing.
- E. Post-experiment / storage phase.

Temperature requirements for the International Space Station (ISS)

Since the space experiment (phase B-C-D, fig 4) was anticipated to be finished in the Soyuz spacecraft, the ISS was the venue for sample storage. The optimum temperature range for storage was required to fall between 4°C to 8°C .

Materials returned to earth

All samples, spent media, digital NO sensor data were returned to earth. The preferred storage temperature was between 4°C to 8°C , hence early access was also required for retrieving all units as soon as possible after landing.

Requirements for the station crew

Step 1: Before launch: FLOW units were transferred to KUBIK incubator: to “centrifuge” or “static” condition as labelled on units (end of Phase A, fig 4)

Step 2: Before launch: KUBIK incubator should have been activated. It was required that activation of KUBIK relays an electronic signal to activate our automated experiment (Phase A-B-C-D) and use the online NO sensor after integration, to monitor NO production already before launch.

NO determination

The conditioned medium was assayed for NO. NO was measured as nitrite (NO_2^-) accumulation in the conditioned medium, using Griess reagent (1% sulfanilamide, 0.1% naphtylethelene-diamine-dihydrochloride, and 2.5 M H_3PO_4). The absorbance was measured at 540 nm. NO concentrations were determined using a standard curve derived from known concentrations of NaNO_2 in non-conditioned culture medium.

RNA isolation and Reverse transcription

Total RNA from the cells was isolated using Trizol® reagent with one modification, i.e. 5 µg of glycogen (Roche Diagnostics, Mannheim, Germany) was added to RNA and isopropanol solution prior to a centrifuge step to increase the RNA yield. Total RNA concentration was quantified spectrophotometrically. cDNA synthesis was performed using 0.5-1 µg total RNA in a 20 µl reaction mix consisting of 5 Units of Transcriptor Reverse Transcriptase according to the manufacturer's instructions (Roche Diagnostics) with 0.08 A₂₆₀ units random primers (Roche Diagnostics), 1 mM of each dNTP (Invitrogen), and Transcriptor RT reaction buffer. cDNA was diluted 5 times and stored at -80°C prior to real-time PCR.

Real-time PCR

Real-time PCR reactions were performed using the SYBRGreen reaction kit according to the manufacturer's instructions (Roche Diagnostics) in a LightCycler (Roche Diagnostics).

cDNA (2 µl each) was diluted to a volume of 20 µl with PCR mix (Light Cycler DNA Master Fast start ^{plus} Kit, Roche Diagnostics) containing a final concentration of 0.2 pmol of primers. Relative housekeeping gene expression (18S; which expression was not subjected to time and/or treatment related variations) and relative target gene expression (COX-2) were determined.

Primers (Invitrogen) used for real-time PCR are listed in Table 2, and were designed using Clone manager suite software program version 6 (Scientific &

Educational Software, NC, USA). The amplified PCR fragment showed extension over at least one exon-border except for 18S, which gene is encoded only by one exon. Values of relative target gene expression were normalized for relative 18S housekeeping gene expression.

Table 2. Primers used for real time PCR

Target gene	Oligonucleotide sequence	Expected product size, bp
18s forward	5'-gtaacccgttgaaccccatt-3'	151
18s reverse	5'-ccatccaatcggttagtagcg-3'	
COX-2 forward	5'-gcattttgcccgactt-3'	299
COX-2 reverse	5'-agaccaggcaccagaccaaaga-3'	

Real Time PCR data analyses

With the Light Cycler software (version 2), the crossing points were assessed and plotted versus the serial dilution of known concentrations of the standards derived from each gene. PCR efficiency (E) was obtained by the formula: $E=10^{-1/\text{slope}}$ and the data were used if and only if the PCR efficiency was calculated between 1.85-2.0.

Statistics

Data were pooled from the results of at least four experiments for each cell culture group tested (Table 1). The differences between groups were analyzed with the non-parametric Wilcoxon signed-rank sum test of the S-Plus 2000 package (release 1). Differences were considered significant at a p-value < 0.05.

RESULTS AND DISCUSSION

Due to unforeseen hardware complications as a result of a lack of electronic power, the results from in-flight cultures are considered lost. However some

data were measured from the ground control experiments. Ground control experiments showed an accumulative increase of nitric oxide in medium for osteocytes (as well as for osteoblasts and periostial fibroblasts, figure 5). Data from the online-nitric oxide sensor showed that the nitric oxide produced in medium by osteocytes increased sharply after the pulse shear stress stimulations (figure 6, shows data from one culture). The mRNA expression for COX-2 was higher in osteoblasts than in osteocytes and in periosteal fibroblasts (fig 7). It was expected that osteocytes would show the highest COX-2 mRNA expression as a result of the pulse flow stimulations, since these cells are the most mechanosensitive bone cells. At this moment the question remains unanswered as to why osteocytes did not show a higher COX-2 mRNA expression than periosteal fibroblasts and osteoblasts. These ground control results will determine the experiment design for the next opportunity for a flight experiment in the next Soyuz missions. Despite the setback from the flight experiment complications, the preparations for the FLOW experiment and preliminary ground results indicate that the FLOW setup is viable for a future flight opportunity.

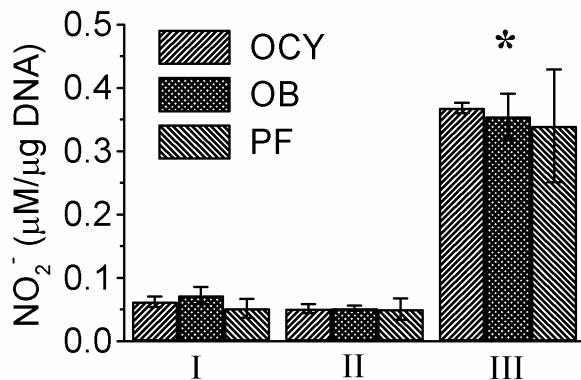


Figure 5. Accumulative nitrite concentration in the medium. Nitrite, the stable metabolite of nitric oxide, increased for all cell types 2½ hrs (III) after the 1st (I) and 2nd (II) pulse shear stress stimulations (*, p < 0.05, increase greater than I and II, for all cell types). Values are mean ± SEM, n=4. OCY, osteocytes; OB, osteoblasts; PF, periosteal fibroblasts.

FLOW has been considered as a potential candidate by the European Space Agency (ESA) for one of the next Soyuz missions in October, 2006. We were able to meet all necessary requirements in order to properly implement the FLOW experiment in the October, 2006 Soyuz mission.

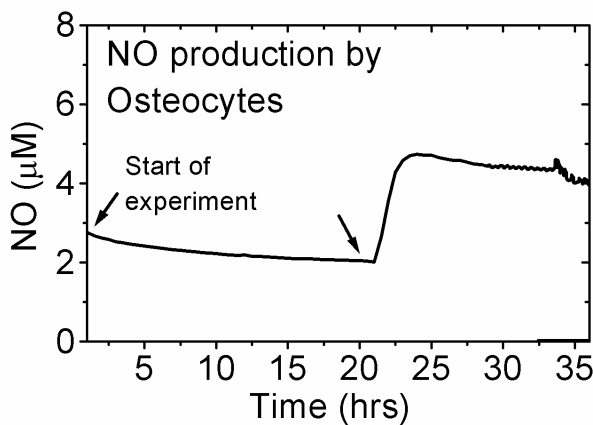


Figure 6. Nitric oxide (NO) production by osteocytes, at the first and second pulse fluid shear stress stimulations by plunger activation (arrow) as monitored by the online-nitric oxide sensor.

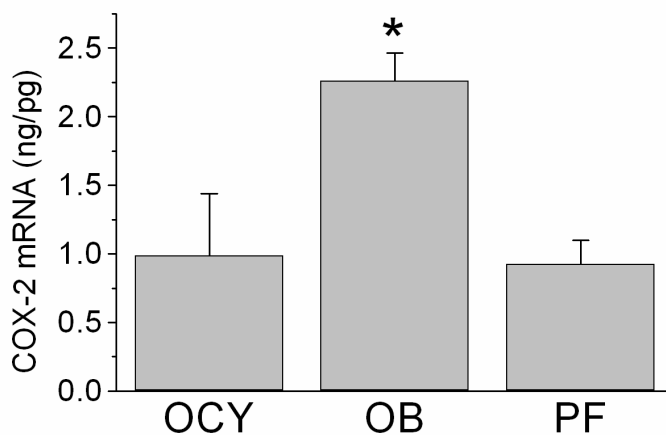


Figure 7. COX-2 mRNA expression. Osteoblasts expressed higher mRNA expression for COX-2 compared to osteocytes and periosteal fibroblasts. Values are mean \pm SEM, n=4.

*Significantly higher than periosteal fibroblasts and osteocytes, $p < 0.05$. OCY, osteocytes; OB, osteoblasts; PF, periosteal fibroblasts.

ACKNOWLEDGEMENTS

The authors would like to thank B. Zandieh Doulabi and M.N. Helder for their help in performing the RT-PCR measurements, F.T.M. Nieuwstadt and M.J.B.M. Pourquie for numerically testing some of our analytical results, and R.M. Heethaar for critically reading the manuscript. The Space Research Organization of the Netherlands supported the work of J.J.W.A. van Loon (DESC, MG-057 and SRON grant MG-055) and R.G. Bacabac (SRON grant MG-055) who also received financial assistance from the Netherlands Organization For International Cooperation In Higher Education (Physics Development Project PHL-146). The Centre for Concepts in Mechatronics (CCM, Nuenen, The Netherlands) manufactured hardware for the FLOW experiment. The Dutch Expedition for Life Science, Technology and Atmospheric Research (DELT A) mission to the International Space Station was made possible, in part, by the Dutch Ministry of Economic Affairs and the Ministry of Education, Culture and Science. Dr. Mark Heppener, of the European Space Agency (ESA), was responsible for the scientific implementation in DELTA.

REFERENCES

1. Houde JP, Schulz LA, Morgan WJ, Breen T, Warhold L, Crane GK, Baran DT 1995 Bone mineral density changes in the forearm after immobilization. *Clin Orthop* 57(317):199-205.
2. Van Loon JJWA, Veldhuijzen JP, Burger EH 1996 Bone and space flight: an overview, in Biological and medical research in space. In: Moore D, Bie P, Oser H (eds) Springer, Berlin, Germany, pp. 259-299.

3. van Loon JJ, Bervoets DJ, Burger EH, Dieudonne SC, Hagen JW, Semeins CM, Doulabi BZ, Veldhuijzen JP 1995 Decreased mineralization and increased calcium release in isolated fetal mouse long bones under near weightlessness. *J Bone Miner Res* 10(4):550-557.
4. Carmeliet, G., Nys, G., and Bouillon, R. Differentiation of human osteoblastic cells (MG-63) in vivo is decreased under microgravity conditions. SP-390, 279-282. 1996. Proc 6th Eur Symp Life Sci Res Space.
5. Hughes-Fulford M, Lewis ML 1996 Effects of microgravity on osteoblast growth activation. *Exp Cell Res* 224(1):103-109.
6. Kumei Y, Shimokawa H, Katano H, Hara E, Akiyama H, Hirano M, Mukai C, Nagaoka S, Whitson PA, Sams CF 1996 Microgravity induces prostaglandin E(2) and interleukin-6 production in normal rat osteoblasts: Role in bone demineralization. *J Biotech* 47(2-3):313-324.
7. Burger EH, Veldhuijzen JP 1993 Influence of mechanical factors on bone formation. In: Hall BK (ed) 7 ed, CRC Press, Boca, Raton, Florida, pp. 37-56.
8. Cowin SC, Moss-Salentijn L, Moss ML 1991 Candidates for the mechanosensory system in bone. *J Biomech Eng* 113(2):191-197.
9. Klein-Nulend J, van der Plas A, Semeins CM, Ajubi NE, Frangos JA, Nijweide PJ, Burger EH 1995 Sensitivity of osteocytes to biomechanical stress in vitro. *FASEB J* 9(5):441-445.

10. Reich KM, Gay CV, Frangos JA 1990 Fluid shear stress as a mediator of osteoblast cyclic adenosine monophosphate production. *J Cell Physiol* 143(1):100-104.
11. Turner CH, Forwood MR, Otter MW 1994 Mechanotransduction in bone: do bone cells act as sensors of fluid flow? *FASEB J* 8(11):875-878.
12. Weinbaum S, Cowin SC, Zeng Y 1994 A model for the excitation of osteocytes by mechanical loading-induced bone fluid shear stresses. *J Biomech* 27(3):339-360.
13. Owan I, Burr DB, Turner CH, Qiu J, Tu Y, Onyia JE, Duncan RL 1997 Mechanotransduction in bone: osteoblasts are more responsive to fluid forces than mechanical strain. *Am J Physiol* 273(3 Pt 1):C810-C815.
14. Smalt R, Mitchell FT, Howard RL, Chambers TJ 1997 Induction of NO and prostaglandin E2 in osteoblasts by wall-shear stress but not mechanical strain. *Am J Physiol* 273(4 Pt 1):E751-E758.
15. Bakker AD, Soejima K, Klein-Nulend J, Burger EH 2001 The production of nitric oxide and prostaglandin E2 by primary bone cells is shear stress dependent. *J Biomech* 34(5):671-677.
16. Kufahl RH, Saha S 1990 A theoretical model for stress-generated fluid flow in the canaliculi-lacunae network in bone tissue. *J Biomech* 23(2):171-180.
17. Piekarski K, Munro M 1977 Transport mechanism operating between blood supply and osteocytes in long bones. *Nature* 269(5623):80-82.

18. Klein-Nulend J, Semeins CM, Ajubi NE, Nijweide PJ, Burger EH 1995 Pulsating fluid flow increases nitric oxide (NO) synthesis by osteocytes but not periosteal fibroblasts--correlation with prostaglandin upregulation. *Biochem Biophys Res Commun* 217(2):640-648.
19. Bacabac RG, Smit TH, Cowin SC, Van Loon JJWA, Nieuwstadt FTM, Heethaar R, Klein-Nulend J 2005 Dynamic shear stress in parallel-plate flow chambers. *J Biomech* 38(1):159-167.
20. Ajubi NE, Klein-Nulend J, Nijweide PJ, Vrijheid-Lammers T, Alblas MJ, Burger EH 1996 Pulsating fluid flow increases prostaglandin production by cultured chicken osteocytes- a cytoskeleton-dependent process. *Biochem Biophys Res Commun* 225(1):62-68.

CHAPTER 9

GENERAL DISCUSSION

GENERAL DISCUSSION

Mechanotransduction in bone

Bone is an obvious biological system that exemplifies the interplay of mechanical stress and adaptive response both at the tissue and cellular levels (1-4). It is currently thought that osteocytes do not directly sense the loading of the bone matrix, but rather respond to the strain-induced flow of interstitial fluid along the network of osteocytes (5, 6). Several studies suggested that the rate of the applied mechanical strain is related to bone formation rather than the magnitude of strain (for example see (7, 8)). Low magnitude ($< 10 \mu\epsilon$), high frequency (10 - 100 Hz) loading has been shown to be capable of stimulating bone growth and inhibiting disuse osteoporosis (9). Also, high-amplitude, low-frequency stimuli are quite rare in the activities of daily life, whereas high-frequency, low-amplitude stimuli are quite common (10). High rates of loading also increased bone mass and strength after jumping exercises in middle-aged osteopenic ovariectomized rats (11). The rate of loading seems to be a decisive factor in bone formation and maintenance. However, the underlying physical picture for understanding how the rate of stress might relate to a meaningful physiological response remains poorly understood.

Rate-dependent response by bone cells

In this thesis we found that bone cells release increased amounts of NO linearly correlated to the rate of fluid shear stress. This supports the notion that bone formation *in vivo* is stimulated by dynamic rather than static loads (12), and that low-magnitude, high-frequency mechanical stimuli may be as stimulatory as high-amplitude, low-frequency stimuli. This rate-dependent response was found to occur, provided that the cells are “kicked” in a pre-conditioned state (13). The finding that the bone cell’s response to fluid shear stress is rate dependent provides an explanation why adaptive bone formation can occur despite the sporadic occurrence of high-amplitude strains in daily life (14). Based on theoretical analysis, it was shown that strain-induced flow in the

canalicular system, in turn induces fluid drag across the extra-cellular matrix on osteocyte processes, that are amplified to two-orders of magnitude (15, 16). This also provides an explanation for sustained bone formation despite the sporadic occurrence of high amplitude strains in normal physiological loading conditions. The theoretical approach leads to an *extra-cellular* mechanism for amplifying stress, whereas, experimental investigations leading to a rate-dependent response, provided a cellular basis for understanding the osteogenic adaptation of bone to mechanical loading. Further understanding of how bone cells respond to stress at the cellular level might provide a deeper insight on how maintained bone health copes with low amounts of high amplitude loading. A phenomenological interpretation underlines the importance of both the rate-dependence, and the requirement of an initial stress-kick, for the stress response of bone cells. The phenomenon is that bone is able to sustain itself despite the sporadic occurrence of meager strains, whereas, bone cells are known *in vitro* to require stresses imparting higher strains. However, it might be possible that sporadic bouts of responses in terms of signaling molecule release, could account for sustained bone health. A normal person is in a condition of unloading during sleep. However, this does not necessarily support a predicament of bone loss. Thus, the theoretical attempt to explain strain amplification via extra-cellular matrix drag, while being important for understanding fluid shear stress stimulation, might not fully support an understanding of sustained bone metabolism despite normal conditions of low strains.

Implications of threshold activation: enhanced response to stochastic stress

As bone exhibits the property of an adaptive response to mechanical stress, various ways of imparting stress to bone has been shown to achieve enhanced bone formation. For instance, there is reason to believe that muscular activity might be related for stimulating strain on bone despite low magnitudes. Strong evidence for the relation between muscle and bone was shown for 778 healthy Argentinians by correlating “whole body bone mineral content”, as indicator

for bone strength, and “lean body mass”, as indicator for muscle strength (17). This undermines a possible excessive requirement for exercise to induce high enough strain magnitudes for stimulating bone cells. Another example is the use of low-magnitude high frequency loading, which has been shown to stimulate osteogenic response from various species (9). One other example is the use of low intensity pulsed ultrasound, which has been shown to have osteogenic benefits (18-20). Techniques of imparting stress by vibrating plates or ultrasound seem to exhibit effective stimulation of cells, however the underlying physical picture of the transfer of forces to the cellular effectors despite the soft tissue barrier, is not straightforward. The possible medical benefits of these techniques might overshadow the importance of understanding the underlying mechanisms of how they might work. However, it is only by a deeper understanding that further benefits could be achieved. The processes by which bone cells are stimulated by vibrating plates, ultrasound, or even musculatory vibration might not be directly the result of a force transfer to the cells themselves. As mentioned, intervening soft-tissue might attenuate the assault of vibratory stress from an already meager source.

We have shown the property that the bone cell response to stress is enhanced by noise. The nitric oxide released by bone cells reached a maximum at the application of an optimum noise-level by fluid shear stress. No distinct peak response was conclusive for the prostaglandin E₂ response. Our study used noise by fluid shear stress stimulation to find differences in the response of MLO-Y4 and MC3T3-E1 cells as models for osteocytes and osteoblasts, respectively. The results indicated differences in threshold-activation for NO and PGE₂ production for both cell types. A peak response is indicative of a small difference between the input signal and the threshold. Hence these results suggest that at low stress conditions with noise, MLO-Y4 cells could have a peak PGE₂ response, while MC3T3-E1 cells, a peak NO response. At conditions of high stress with noise, MLO-Y4 cells could have a peak NO response, while MC3T3-E1 cells, a PGE₂ response. It is possible that *in vivo*, osteoclasts are driven to be active close to osteocytic regions at low stress

conditions with noise. On the other hand, osteoclasts are driven to be active near osteoblastic regions at high stress conditions with noise. Clearly, low stress might promote bone loss; however, high stress seems to promote the activity of osteoclasts near osteoblasts. This supports the notion that high stresses ultimately leading to bone microdamage and osteocyte apoptosis, initiate bone remodelling (21). Whereas microdamage promotes low fluid fluid flow and osteocyte apoptosis, explaining the recruitment of osteoclasts (21, 22), very high stress by itself stimulates osteoclasts via PGE₂ upregulation. Furthermore, the possible role of noisy or stochastic stress in the mechanical adaptation of bone provides a partial explanation for the role of obscure effects of indirect stress applications to stimulate bone formation. The threshold-activation property of bone cells indicate a capacity for enhanced response at stress conditions obscured even by minute stress sources, as from muscular vibration, ultrasound, or vibratory motion, typified by low-magnitude high frequency loading.

Stress, cellular deformation, mechanosensing, and mechano-activity

Recent studies on the osteogenic activity of bone cells investigated the effects of stress using varying techniques (fluid flow, substrate strain, hydrostatic pressure, vibration stress). In these studies, the magnitude (and rate) of stress was shown to correlate with the cellular response, in terms of signaling molecules. This correlation was suggested to be deformation-dependent. Relating the effects of fluid flow and substrate straining have shown that the former induces higher release of signaling molecules (23, 24). A numerical study confirmed that the cellular deformation caused by stress induced by fluid flow is fundamentally different from that induced by substrate straining (25). Fluid shear stress has a larger overturning effect on the bone cells, while the effect of substrate strain is focused on cell-substrate attachments. These recent results confirm the importance of investigating how cells deform in response to stress for understanding the corresponding physiological response of cells.

The collaboration between experimental investigation and theoretical analysis of the response of bone cells to stress has proven effective for advanced understanding of underlying processes in bone mechanotransduction. The role of osteocytes, as the mechanosensors in bone *par excellance*, has been elucidated in the past years with more detail. Computational models for cells have previously treated the cytoplasm and cytoskeleton as a continuum (26). Recognizing the importance of the cytoskeleton has led to more recent approaches that treat the cytoskeleton more closely to its physical reality, as consistent of interconnected fibers.

Using a two-particle *in vitro* assay for measuring the viscoelasticity of cells, with the recently derived two-particle microrheology, we probed the mechano-activity and mechanosensitivity of various bone cell types and fibroblasts. Mechano-activity is characterized by the induction of force traction on attachment sites by cells, and mechanosensitivity is the ability of cells to sense forces. We found that osteocytic cell types (primary osteocytes from chicken and MLO-Y4 cells) induce a relatively higher traction force on attached particles than osteoblastic cells (primary osteoblasts from chicken and MC3T3-E1 cells). Fibroblastic cells (CCL-224) are even more mechano-active compared to MLO-Y4 cells, which explains the propensity of fibroblasts for motility *in vitro*. In our two-particle *in vitro* assay, MLO-Y4 cells release nitric oxide simultaneous with increasing force application. Another typical response to increasing force application is the induction of force traction on the attached beads by cells, simultaneous with morphological adaptation from a spherical to a polar shape defining ends at the attachment points. It is clear that force traction, morphology change, and possibly the release of signaling molecules are all related in similar pathways, in response to environmental stress conditions.

Towards quantitative description of bone cell mechanosensitivity

We have outlined above two discernible properties of bone cell response to fluid shear stress, which are, rate-dependence and threshold-activation. The

rate-dependent response was interestingly demonstrated by bone cells in a broad range of frequencies induced by vibration stress, showing a distinctive correlation to the acceleration rate (chapter 6). This rate-dependent response showed an anti-correlated release of NO and PGE₂. As mentioned in the preceding sections, these signaling molecules modulate the activity of osteoclasts. Hence, loading frequency can fine-tune the localized recruitment and inhibition of osteoclasts. The loading rate is believed to be the important parameter for stimulating bone formation (27, 28). However, the underlying cellular mechanisms are now slowly being revealed. By recognizing the mathematical precision of bone mechanical adaptation, as Wolff did, the science of understanding the mechanobiology of bone has been subject also to numerical simulations (29, 30). The final local effects on bone, under conditions of loading are further understood by having a quantifiable interplay between cell types, due to the resulting release of signaling molecules. Complex systems are generally exhibiting power-law phenomena that might prove useful in characterizing behaviors of biological systems (for a review on complex biological systems and scale invariance phenomena see (31)). A power-law description is typical for complex systems, which are generally exhibiting scale invariance. Power-laws and scale invariance have been used in studying phase transitions in materials and in describing systems that spontaneously self-arrange (31).

We can derive an empirical power-law for bone cells. Based on our results, we propose an empirical quantifiable property of bone cells, that is, the correlation of the accumulated amount of signaling molecule to the cell's experienced frequency of stress. Thus,

$$[M] \propto s\left(\frac{\sigma - \theta}{\sigma}\right)\omega^\beta \quad [1]$$

where s is the normalized sigmoid function to enforce threshold-activation, with a threshold θ , and the experienced stress σ . $[M]$ is the accumulated amount of the signaling molecule M and the frequency $f = \omega/(2\pi)$, and β determines the power-law relation between stress and response. Equation [1] incorporates in a

power law, the property of bone cells that the released signaling molecules, is related to the frequency of stress, above a threshold. In Chapter 3, we showed that $\beta = 1$ for fluid shear stress stimulation, and in chapter 5, we showed that $\beta = \pm 3$ for translational vibration stress acting on attached bone cells. Thus, β is a property associated with the type of stress. Whereas $\beta = 1$ for contact stress (*e.g.*, fluid shear stress, for low frequencies, < 10 Hz), $\beta = \pm 3$ for stress induced by body forces (*e.g.*, motion of the nucleus through cytoplasm, for high frequencies, > 10 Hz). The absolute value of β is then useful for finding possible new mechanisms by which bone cells sense loading at different frequency ranges. In Chapter 6 we have also shown that the release of NO and PGE₂ anti-correlated. We showed that for NO, $\beta > 0$ and for PGE₂, $\beta < 0$, since NO released positively correlated with ω^3 , while PGE₂ released negatively correlated with ω^3 . Thus, β is also a property of the specific signaling molecule. The sign of β for the associated signaling molecule indicates upregulation ($\beta > 0$) or downregulation ($\beta < 0$) in relation to the loading frequency.

The threshold activation, enforced by the sigmoid function we introduced in [1] was partially demonstrated in Chapter 4, where we showed that without an initial stress-kick, no rate dependent response occurred. Threshold-activation was also demonstrated by the possibility of stochastic resonance in the way bone cells respond to fluid shear stress. Note however, that the accumulated signaling molecule released [M] is the sum of all molecules released by a population of cells. Also, the threshold for NO and PGE₂ were demonstrated to be unequal. Thus, the threshold θ , is also a property of the cell population under question in relation to a specific signaling molecule. The threshold is reached when a critical number of cells have produced enough amounts of signaling molecules [M]. Further proof of this assumption can be demonstrated by showing that single cells do not have the same stress thresholds for releasing a measurable amount of signaling molecules. From our results in Chapter 7, we have only shown the possibility that the release of signaling molecules might be related to a change in the mechanical properties of the cell. Physiological

conditions are probably influenced by the activity of collaborating aggregates of cells. Hence, experimental results suggesting power-laws on cell cultures *in vitro* might not necessarily translate to single cell properties but considering that a biological system is complex, the property of scale invariance, might suggest that single cells posses similar power-laws.

The validity of equation [1] is anticipated to be limited to a range of frequencies possibly below 100 Hz, for an actual mechanical loading regime on the cell. In chapter 6 we used frequencies 5, 30, 60 and 100 Hz and found a linear correlation between the total NO and PGE₂ released by bone cells, with ω^3 . In chapter 7 we have shown that bone cells are basically elastic until ~ 10 Hz, having a viscoelastic transition between 10-100 Hz, beyond which, a viscoelastic stiffening occurs. Transmembrane proteins and ultimately, the cell cytoskeleton might be related to mechanosensing by cells (32). Since the mechanical properties of cells depend on the cytoskeleton, changes in cell compliance might be a direct indication of cell mechanosensitive properties. Thus, a linear relation between the physiological responses of bone cells to ω^β , is possibly related to changes in the viscoelasticity of cells.

Implications for the extreme condition of unloading: microgravity

We have shown that bone cells are responsive to dynamic stress. This supports findings that the rate rather than the magnitude of loading is the important parameter for osteogenic properties of mechanical loading to bone (33). This insight has powerful implications on the local activity of osteocytes for directing the mechanical adaptation of bone. We have also shown that the released signaling molecules of bone cells are related to the frequency of stress in an empirical relation. Since the activation of bone cells is highly dependent on the frequency of experienced stress, bone cells might be capable of responding to very meager amounts of strain, after overcoming a stress threshold. Thus, under extreme conditions of unloading, it might be possible to counteract the onslaught of bone loss by sporadic bouts of high impact loading. There is a large amount of data on the catabolic effects to bone of prolonged

unloading (34-36), and suggested counteractive remedies or preventive measures for bone loss, which are both based on exercise or pharmacological applications (37-39). Regardless of the counteractive procedure for bone loss, the approach has to eventually target the bone cells. It has been suggested that imbalances in the activity of bone cells for directing bone resorption or formation contributes to bone loss (34). We have shown here relations between what we consider fundamental parameters of mechanotransduction in bone, which are the applied stress, the amount of signaling molecules released by osteocytes, and their possible roles for directing the local activity of osteoclasts and osteoblasts. Bone loss can be understood as resulting from a disturbance of the homeostasis of these parameters. However, since these parameters are closely related as we have shown, it might be possible to restore their homeostasis despite extreme conditions of unloading.

Studies by Tabony et al. (40-42) have shown that microtubule self-organization *in vitro* is gravity-dependent and that this self-organization affects the transport of intra-cellular particles. Since, a reorganization of microtubules might affect the cell viscoelastic properties, gravity or the loss of gravity might affect the way cells sense forces. To address the underlying cellular mechanisms for studies on bone loss in relation to microgravity, Cowin (43) addressed the question whether bone cells are able to read the changes in gravitational field or detect this indirectly via contact stresses. It would seem that the light weight of cells, undermines the role of gravity on cellular behavior. Thus, the question remains on how cells might detect microgravity directly. We probed the activity of bone cells by measuring the forces induced by cells on attached fibronectin-coated beads (chapter 7). We showed that the force fluctuation $\langle f^2 \rangle$ was proportional to ω^2 , which is a signature for continuums with slowly evolving internal processes (44). Although we probed the traction forces induced by cells on particles outside the cell, this force fluctuation is indicative of intra-cellular processes. The power-law for cellular force fluctuation is an indication for the diffusive properties of intra-cellular particles or organelles. Reaction-diffusion processes govern the relation

between microtubule re-organization, and possibly intra-cellular transport, which might be affected by gravity (41, 45). Thus, intra-cellular transport might be crucial for mechanosensing. Hence, cells might be able to detect changes in the gravitational field directly by the gain or loss of gravitational forces influencing the re-structuring of self-organizing polymers inside cells, thereby influencing intra-cellular transport. Thus, it is possible that the signature for force fluctuations inside cells might change under microgravity influencing bone cell mechanosensitivity as indicated by a changed release of signaling molecules.

REFERENCES

1. Frost HM 2003 Bone's mechanostat: a 2003 update. *Anat Rec A Discov Mol Cell Evol Biol* 275(2):1081-1101.
2. Cowin SC, Moss-Salentijn L, Moss ML 1991 Candidates for the mechanosensory system in bone. *J Biomech Eng* 113(2):191-197.
3. Burger EH, Klein-Nulend J 1999 Mechanotransduction in bone - Role of the lacuno-canalicular network. *FASEB J* 13(Supplement):S101-S112.
4. Wolff J 1892 *Gesetz der transformation der knochen*, Hirschwald, Berlin.
5. Piekarski K, Munro M 1977 Transport mechanism operating between blood supply and osteocytes in long bones. *Nature* 269(5623):80-82.
6. Cowin SC, Weinbaum S 1998 Strain amplification in the bone mechanosensory system. *Am J Med Sci* 316(3):184-188.

7. Turner CH, Owan I, Takano Y 1995 Mechanotransduction in bone: role of strain rate. *Am J Physiol Endocrinol Metab* 269(3):E438-E442.
8. Turner CH, Pavalko FM 1998 Mechanotransduction and functional response of the skeleton to physical stress: the mechanisms and mechanics of bone adaptation. *J Orthop Sci* 3(6):346-355.
9. Rubin CT, Sommerfeldt DW, Judex S, Qin YX 2001 Inhibition of osteopenia by low magnitude, high-frequency mechanical stimuli. *Drug Discov Tod* 6(16):848-858.
10. Fritton SP, McLeod J, Rubin CT 2000 Quantifying the strain history of bone: spatial uniformity and self-similarity of low-magnitude strains. *J Biomech* 33(3):317-325.
11. Tanaka M, Ejiri S, Nakajima M, Kohno S, Ozawa H 1999 Changes of cancellous bone mass in rat mandibular condyle following ovariectomy. *Bone* 25(3):339-347.
12. Lanyon LE, Rubin CT 1984 Static vs dynamic loads as an influence on bone remodelling. *J Biomech* 17(12):897-905.
13. Bacabac RG, Smit TH, Mullender MG, Van Loon JJWA, Klein-Nulend J 2005 Initial stress-kick is required for fluid shear stress-induced rate dependent activation of bone cells. *Ann Biomed Eng* 33(1):104-110.
14. Bacabac RG, Smit TH, Mullender MG, Dijcks SJ, Van Loon JJWA, Klein-Nulend J 2004 Nitric oxide production by bone cells is fluid shear stress rate dependent. *Biochem Biophys Res Commun* 315:823-829.

15. Han YF, Cowin SC, Schaffler MB, Weinbaum S 2004 Mechanotransduction and strain amplification in osteocyte cell processes. *Proc Natl Acad Sci USA* 101:16689-16694.
16. Weinbaum S, Cowin SC, Zeng Y 1994 A model for the excitation of osteocytes by mechanical loading-induced bone fluid shear stresses. *J Biomech* 27(3):339-360.
17. Zanchetta JR, Plotkin H, Filgueira MLA 1995 Bone Mass in Children - Normative Values for the 2-20-Year-Old Population. *Bone* 16(4):S393-S399.
18. Cook SD, Salkeld SL, Mse, Patron LP, Ryaby JP, Whitecloud TS 2001 Low-intensity pulsed ultrasound improves spinal fusion. *Spine J* 1(4):246-254.
19. Sakurakichi K, Tsuchiya H, Uehara K, Yamashiro T, Tomita K, Azuma Y 2004 Effects of timing of low-intensity pulsed ultrasound on distraction osteogenesis. *J Orthop Res* 22(2):395-403.
20. Schortinghuis J, Ruben JL, Raghoebar GM, Stegenga B, de Bont LG 2005 Does ultrasound stimulate osteoconduction? A placebo-controlled single-blind study using collagen membranes in the rat mandible. *Int J Oral Maxillofac Impl* 20(2):181-186.
21. Bentolila V, Boyce TM, Fyhrie DP, Drumb R, Skerry TM, Schaffler MB 1998 Intracortical remodeling in adult rat long bones after fatigue loading. *Bone* 23(3):275-281.
22. Burger EH, Klein-Nulend J, Smit TH 2003 Strain-derived canalicular fluid flow regulates osteoclast activity in a remodelling osteon - a proposal. *J Biomech* 36(10):1453-1459.

23. Owan I, Burr DB, Turner CH, Qiu J, Tu Y, Onyia JE, Duncan RL 1997 Mechanotransduction in bone: osteoblasts are more responsive to fluid forces than mechanical strain. *Am J Physiol* 273(3 Pt 1):C810-C815.
24. You J, Yellowley CE, Donahue HJ, Zhang Y, Chen Q, Jacobs CR 2000 Substrate deformation levels associated with routine physical activity are less stimulatory to bone cells relative to loading-induced oscillatory fluid flow. *J Biomech Eng* 122(4):387-393.
25. McGarry JG, Klein-Nulend J, Mullender MG, Prendergast PJ 2005 A comparison of strain and fluid shear stress in stimulating bone cell responses--a computational and experimental study. *FASEB J* 19(3):482-484.
26. Kamm, R. D., McVittie, A. K., and Bathe, M. On the role of continuum models in mechanobiology. 242, 1-9. 2000. ASME Internat Cong - Mech Biol.
27. Mosley JR, Lanyon LE 1998 Strain rate as a controlling influence on adaptive modeling in response to dynamic loading of the ulna in growing male rats. *Bone* 23(4):313-318.
28. Turner CH, Owan I, Takano Y 1995 Mechanotransduction in bone: role of strain rate. *Am J Physiol Endocrinol Metab* 269(3):E438-E442.
29. Weinans H, Homminga J, van Rietbergen B, Ruegsegger P, Huiskes R 1998 Mechanical effects of a single resorption lacuna in trabecular bone. *J Biomech* 31(1):152.
30. Frost HM 2003 Bone's mechanostat: a 2003 update. *Anat Rec A Discov Mol Cell Evol Biol* 275(2):1081-1101.

31. Gisiger T 2001 Scale invariance in biology: coincidence or footprint of a universal mechanism? *Biol Rev Camb Philos Soc* 76(2):161-209.
32. Wang N, Butler JP, Ingber DE 1993 Mechanotransduction across the cell surface and through the cytoskeleton. *Science* 260(5111):1124-1127.
33. Turner CH, Owan I, Takano Y 1995 Mechanotransduction in bone: role of strain rate. *Am J Physiol* 269(3 Pt 1):E438-E442.
34. Bikle DD, Halloran BP 1999 The response of bone to unloading. *J Bone Miner Metab* 17(4):233-244.
35. Loomer PM 2001 The impact of microgravity on bone metabolism in vitro and in vivo. *Crit Rev Oral Biol Med* 12(3):252-261.
36. Zerath E 1998 Effects of microgravity on bone and calcium homeostasis. *Adv Space Res* 21(8-9):1049-1058.
37. Greenleaf JE, Bulbulian R, Bernauer EM, Haskell WL, Moore T 1989 Exercise-training protocols for astronauts in microgravity. *J Appl Physiol* 67(6):2191-2204.
38. Norman TL, Bradley-Popovich G, Clovis N, Cutlip RG, Bryner RW 2000 Aerobic exercise as a countermeasure for microgravity-induced bone loss and muscle atrophy in a rat hindlimb suspension model. *Aviat Space Environ Med* 71(6):593-598.
39. Wimalawansa SM, Chapa MT, Wei JN, Westlund KN, Quast MJ, Wimalawansa SJ 1999 Reversal of weightlessness-induced musculoskeletal losses with androgens: quantification by MRI. *J Appl Physiol* 86(6):1841-1846.

40. Tabony J, Job D 1992 Gravitational symmetry breaking in microtubular dissipative structures. *Proc Natl Acad Sci USA* 89(15):6948-6952.
41. Glade N, Demongeot J, Tabony J 2004 Microtubule self-organisation by reaction-diffusion processes causes collective transport and organisation of cellular particles. *BMC Cell Biol* 5(1):23.
42. Papaseit C, Pochon N, Tabony J 2000 Microtubule self-organization is gravity-dependent. *Proc Natl Acad Sci USA* 97(15):8364-8368.
43. Cowin SC 1998 On Mechanosensation in Bone Under Microgravity. *Bone* 22(1):119S-125S.
44. Lau AW, Hoffman BD, Davies A, Crocker JC, Lubensky TC 2003 Microrheology, stress fluctuations, and active behavior of living cells. *Phys Rev Lett* 91(19):198101-1-198101-4.
45. Tabony J, Glade N, Papaseit C, Demongeot J 2002 Microtubule self-organisation and its gravity dependence. *Adv Space Biol Med* 8:19-58.

GENERAL SUMMARY

Bone is a biological system that demonstrates adaptive response to mechanical loading both at the tissue and cellular levels. It is currently thought that bone cells do not directly sense the loading of the bone matrix, but rather respond to the strain-induced flow of interstitial fluid. In response to flow, bone cells produce signaling molecules like nitric oxide (NO) or prostaglandin E₂ (PGE₂) that drive the adaptive response of bone to mechanical loading. Several studies have shown that the rate of the mechanical load or stress rather than its magnitude relates to bone formation. Thus, the rate of loading seems to be a decisive factor in bone formation and maintenance. However, the underlying physical picture for understanding how the rate of stress might relate to a meaningful physiological response remains poorly understood.

In this thesis we found that bone cells release increased amounts of NO in relation to the rate of fluid shear stress. This supports the notion that bone formation *in vivo* is stimulated by dynamic rather than static loads. This rate-dependent response was found to occur, provided that the cells initially experience a stress-kick (*i.e.*, a sudden increase of stress). Both these findings provide an explanation for sustained bone formation despite the sporadic occurrence of high amplitude strains in normal physiological loading conditions. High rates of stress and stress-kicks are expected in mechanical loading experienced during high-impact activities, as may occur in sports or exercise. Thus, although high-impact activities might be infrequent, the resulting stresses could stimulate bone cells to trigger the adaptive responses of bone.

We have shown the property that the bone cell response to stress is enhanced by the addition of noise. The nitric oxide released by bone cells reached a maximum at the application of an optimum noise-level by fluid shear stress. Our study used noise by fluid shear stress stimulation to find differences in the response of MLO-Y4 and MC3T3-E1 cells, used as models for osteocytes and osteoblasts, respectively. By using a theoretical model, relating

General summary

stress information to the molecular response of bone cells, under the influence of noise, this study suggested that there are differences in threshold-activation for NO and PGE₂ production for both osteocytes and osteoblasts. Thus, at conditions of high stress with noise, MLO-Y4 cells could have a peak NO response, while MC3T3-E1 cells, a PGE₂ response. Since NO is known to drive away osteoclasts, and PGE₂ might promote the recruitment of osteoclasts, it is possible that *in vivo*, osteoclasts are driven to be active close to osteocytic regions at low stress conditions with noise. On the other hand, osteoclasts are driven to be active near osteoblastic regions at high stress conditions with noise. Clearly, low stress might promote bone loss; however, high stress seems to promote the activity of osteoclasts near osteoblasts. Furthermore, the possible role of noisy stress in the mechanical adaptation of bone provides a partial explanation for the positive effects of indirect stress applications to stimulate bone formation. The threshold-activation property of bone cells indicates a capacity for enhanced response at stress conditions obscured even by minute stress sources, as from musculatory vibration, ultrasound, or vibratory motion, typified by low-magnitude high frequency loading.

Using a two-particle *in vitro* assay for characterizing the viscoelasticity of cells, we probed the mechano-activity and mechanosensitivity of various bone cell types and fibroblasts. Mechano-activity is characterized by the induction of force traction on attachment sites by cells, and mechanosensitivity is the ability of cells to sense forces. We found that osteocytic cell types (primary osteocytes from chicken and MLO-Y4 cells) induce a relatively higher traction force on attached particles than osteoblastic cells (primary osteoblasts from chicken and MC3T3-E1 cells). Fibroblastic cells (CCL-224) are even more mechano-active compared to MLO-Y4 cells, which explains the propensity of fibroblasts for motility *in vitro*. In our two-particle *in vitro* assay, MLO-Y4 cells release nitric oxide simultaneous with increasing force application. It is clear that force traction, morphology change, and possibly the release of signaling molecules are all related in similar pathways, in response to environmental stress conditions.

We have outlined above two discernible properties of bone cell response to fluid shear stress, which are, rate-dependence and threshold-activation. The rate-dependent response was interestingly demonstrated by bone cells in a broad range of frequencies induced by vibration stress. The final local effects on bone, under conditions of loading are further understood by having a quantifiable interplay between cell types, due to the resulting release of signaling molecules.

We have shown that bone cells are responsive to dynamic stress. This supports findings that the rate rather than the magnitude of loading is the important parameter for osteogenic properties of mechanical loading to bone. This insight has relevant implications on the local activity of osteocytes for directing the mechanical adaptation of bone. We have also shown that the released signaling molecules of bone cells are related to the frequency of stress in an empirical relation. Since the activation of bone cells is highly dependent on the frequency of experienced stress, bone cells might be capable of responding to very meager amounts of strain, after overcoming a stress threshold. Thus, under extreme conditions of unloading (*e.g.*, microgravity environment) it might be possible to counteract the onslaught of bone loss by sporadic bouts of high-impact loading. We have shown here relations between what we consider relevant parameters of mechanotransduction in bone, which are the applied stress, the amount of signaling molecules released by osteocytes, and their possible roles for directing the local activity of osteoclasts and osteoblasts. Bone loss can be understood as resulting from a disturbance of the homeostasis of these parameters. Since these parameters are closely related as we have shown, it might be possible to restore their homeostasis despite extreme conditions of unloading.

However, the question remains as to how cells might detect microgravity directly. We probed the activity of bone cells by measuring the forces induced by cells on attached fibronectin-coated beads. We showed that the force fluctuation of bone cells had a characteristic frequency spectrum signature. This force fluctuation is indicative of intra-cellular processes. The

General summary

characteristic signature was shown to be an indication for the diffusive properties of intra-cellular particles or organelles. Diffusive processes govern the relation between microtubule re-organization, and possibly intra-cellular transport, which might be affected by gravity. Thus, intra-cellular transport might be crucial for mechanosensing. Bone cells might be able to detect changes in the gravitational field directly by the gain or loss of gravitational forces influencing the re-structuring of self-organizing polymers inside cells, thereby influencing intra-cellular transport. Thus, it is possible that the signature for force fluctuations inside cells might change under microgravity influencing bone cell mechanosensitivity as indicated by a changed release of signaling molecules.

ALGEMENE SAMENVATTING

Bot is een biologisch systeem dat zich zowel op weefsel- als op cellulair niveau aanpast aan mechanische belasting. Het huidige denkbeeld is dat botcellen de belasting op de botmatrix niet direct waarnemen, maar dat ze reageren op de strain (vervorming)-geïnduceerde stroming van interstitiële vloeistof. Als gevolg van deze vloeistofstroom produceren botcellen signalmoleculen, zoals stikstofoxide (NO) en prostaglandine E₂ (PGE₂), die de adaptieve respons van bot op mechanische belasting bepalen. Verschillende studies hebben aangetoond dat de snelheid van de mechanische belasting of stress bepalend is voor de botvorming, maar niet zozeer de hoogte van de belasting of stress. Het lijkt er dus op dat de snelheid van de belasting een bepalende factor is voor de botvorming en onderhoud. De achterliggende fysica om de relatie tussen de stress-snelheid en de fysiologische respons te begrijpen is echter nog onduidelijk.

In dit proefschrift hebben we aangetoond dat er een relatie is tussen de verhoging van de stikstofoxideproductie door botcellen en de snelheid van de vloeistofschuifspanning. Dit ondersteunt het idee dat botvorming *in vivo* meer wordt gestimuleerd door dynamische- dan door statische belasting. Deze snelheids-afhankelijke reactie trad op als de cellen eerst een zogenaamde stress-kick (een abrupte stress-toename) hadden ervaren. Beide waarnemingen kunnen aanhoudende botvorming verklaren, ondanks de sporadisch voorkomende hoge amplitude strains (vervormingen) bij normale belasting. Hoge stress-snelheden en stress-kicks zijn te verwachten bij activiteiten met een hoge impact zoals tijdens het sporten of flinke lichaamsbeweging. Dus ondanks het feit dat hoge impact activiteiten niet frequent voorkomen, zou de uit deze activiteit voortkomende stress botcellen kunnen stimuleren tot het aanzetten van de adaptieve respons van bot.

Wij hebben aangetoond dat ruis de respons van botcellen op stress verhoogt. De productie van stikstofoxide door botcellen was maximaal wanneer een optimale ruis door vloeistofschuifspanning werd gegeven. In onze studie werd

Algemene samenvatting

ruit door stimulatie met vloeistofschuifspanning gebruikt om mogelijke verschillen te vinden in de respons van MLO-Y4 en MC3T3-E1 cellen, die model staan voor osteocyten en osteoblasten. Door een theoretisch model te gebruiken dat een verband legt tussen stress-informatie en moleculaire respons van botcellen onder invloed van ruis, hebben we aangetoond dat er verschillen zijn in drempelwaarde-activatie voor NO en PGE₂ productie voor zowel osteocyten als osteoblasten. In situaties met hoge stress en ruis hebben MLO-Y4 cellen een hoge NO respons en MC3T3-E1 cellen een hoge PGE₂ respons. Omdat het is bekend dat NO osteoclasten op afstand houdt en dat PGE₂ de aanmaak van osteoclasten kan bevorderen, is het mogelijk dat *in vivo* osteoclasten worden geactiveerd daar waar osteocyten gelegen zijn die onder lage stress condities met ruis verkeren. Aan de andere kant worden osteoclasten geactiveerd daar waar osteoblasten zich onder hoge stress condities met ruis bevinden. Het is duidelijk dat lage stress condities leiden tot botverlies, maar dat hoge stress condities de activiteit van osteoclasten in de buurt van osteoblasten bevorderen. Verder geeft de mogelijke rol van stress door ruis bij de mechanische adaptatie van bot maar een gedeeltelijke verklaring voor het positieve effect van indirecte stress-toepassingen om botvorming te stimuleren. De drempelwaarde-activatie van botcellen duidt op het vermogen om een verhoogde respons te geven onder stresscondities die vertroebeld worden door kortdurende stress-bronnen, zoals spiervibraties, ultrasound, of vibrerende beweging, allen gekenmerkt door een hoge frequentie, lage amplitude belasting.

Wij hebben door middel van een *in vitro* assay, waarbij met twee bolletjes de viscoelasticiteit van cellen werd gekarakteriseerd, de mechanische activiteit en de mechanische gevoeligheid bepaald van verschillende soorten botcellen en fibroblasten. Mechano-activiteit wordt gekenmerkt door de inductie van trekkrachten op de aanhechtingsplaatsen van cellen, en mechano-sensitiviteit is het vermogen van cellen om krachten waar te nemen. Wij vonden dat osteocyt-achtige cellen (primaire kippen-osteocyten en MLO-Y4 cellen) relatief een hogere trekkracht induceren op aan de cel gehechte bolletjes dan osteoblast-achtige cellen (primaire kippen-osteoblasten en MC3T3-E1 cellen). Fibroblast-

achtige cellen (CCL-224) waren zelfs meer mechano-actief in vergelijking tot MLO-Y4 cellen, hetgeen de beweeglijkheid van fibroblasten *in vitro* verklaard. MLO-Y4 cellen produceerden NO gelijktijdig met de uitoefening van een toenemende kracht op de aan de cel gehechtte bolletjes. Het is duidelijk dat trekkracht, vormverandering, en mogelijk de productie van signalmoleculen gerelateerd zijn aan dezelfde pathways in respons op omgevings stress-condities.

Hierboven hebben we twee te onderscheiden eigenschappen van de botcel-respons op vloeistofschuifspanning beschreven, namelijk snelheid-afhankelijkheid en drempelwaarde-activatie. Interessant genoeg werd de snelheden-afhankelijke respons door botcellen aangetoond bij een brede reeks frequenties die werden geïnduceerd door vibratie-stress. De uiteindelijke lokale effecten op belast bot zijn verder te begrijpen door een kwantificeerbaar samenspel tussen verschillende celtypes, als gevolg van de productie van signalmoleculen.

Wij hebben aangetoond dat botcellen reageren op dynamische stress. Dit ondersteunt waarnemingen dat de snelheid van de belasting, maar niet zozeer de hoogte ervan een belangrijke parameter is voor de osteogene eigenschappen van mechanische belasting op bot. Dit inzicht heeft relevante gevolgen voor de lokale activiteit van osteocyten om de mechanische adaptatie van bot te regisseren. Wij hebben eveneens aangetoond dat de afgifte van signalmoleculen door botcellen op een empirische manier is gerelateerd aan de stress-frequentie. Omdat de activatie van botcellen in hoge mate afhankelijk is van de stress-frequentie die ze waarnemen, zouden botcellen kunnen reageren op zeer kleine hoeveelheden strain (vervorming) na overschrijding van een drempelwaarde. Hierdoor zou het kunnen dat onder extreme situaties van “disuse” (gewichtsloosheid) het hoge botverlies voorkomen kan worden door sporadische hoge impact belasting. Wij hebben verbanden aangetoond tussen parameters die wij relevant achten voor de mechano-transductie in bot, dat wil zeggen de toegepaste stress, de hoeveelheid signalmoleculen geproduceerd door osteocyten, en de mogelijke rol van osteocyten als

Algemene samenvatting

regisseurs van de lokale activiteit van osteoclasten en osteoblasten. Botverlies kan worden uitgelegd als het resultaat van een verstoring van de homeostase van deze parameters. Omdat deze parameters aan elkaar gerelateerd zijn, zoals wij hebben aangetoond, zou het kunnen dat hun homeostase hersteld wordt ondanks de extreme omstandigheden van “disuse”.

De vraag hoe cellen gewichtsloosheid rechtstreeks kunnen waarnemen blijft echter bestaan. Wij hebben de activiteit van botcellen bepaald door de krachten te meten die de cellen induceren op aan de cel gehechte bolletjes, die zijn gecoat met fibronectine. We hebben aangetoond dat de krachtschommeling van botcellen een karakteristiek frequentiepatroon heeft. Deze krachtschommeling is kenmerkend voor intracellulaire processen. Het karakteristieke patroon was een aanwijzing voor de verspreide eigenschappen van intracellulaire deeltjes en celorganellen. Verspreide processen besturen de relatie tussen de reorganisatie van microtubuli, en mogelijk intracellulair transport, die door de zwaartekracht beïnvloed zouden kunnen worden. Intracellulair transport zou daarom cruciaal kunnen zijn voor mechano-sensing. Botcellen zouden veranderingen in het zwaartekrachtsveld rechtstreeks kunnen waarnemen doordat winst of verlies aan zwaartekracht de restructurering van zelf-organiserende polymeren binnen de cel beïnvloedt, en daardoor het intracellulaire transport. Het is daarom mogelijk dat het patroon van krachtenschommelingen binnen een cel verandert onder gewichtsloosheid, hetgeen de botcel mechano-gevoeligheid beïnvloedt zoals blijkt uit een veranderde productie van signalmoleculen.

A word of gratitude

A lot that cannot be said is at times best expressed in the words: “Thank you”. Here, I mention some of the countless number of persons who are instrumental, in more ways imaginable, for the fruits of my studies and making my stay in The Netherlands a delight.

To the following people, I share my deepest gratitude.

Prof. Jenneke Klein-Nulend, for her uncompromised support for her students, which I consider a priceless gift in my journey as a PhD researcher, and for that peculiar way of providing me the challenge to strive, which has proven most useful for reaching the finish line with energy left for an extra mile- something I would not exchange for gold, and for those invaluable lessons on how to express thoughts into scientifically legible writing and explicable presentations. Prof. Rob Heethaar, for his careful mentoring at the crucial moments and for being my link to Medical Physics, which attests to the possible applications of my studies. Dr. Theo Smit, for his guidance and expressing the joyous collaboration between Biology and Physics by coming up with piercing scientific questions and insightful summaries. Dr. Jack van Loon, also for his guidance and keeping the spirit(s) high despite our hectic preparations for FLOW, and for his natural appeal for finding scientific pursuits, terrestrial or extra-terrestrial (ground or microgravity, that is). Prof. Els Burger, for her inspired presence, intuitive discussions during anyone’s presentation, and for assuring me that there is Physics in the study of cells. Prof. Vincent Everts, for setting the example for me to be early at work, and for his generous interest in my research.

I also do not forget other professors and scientists whose influence and generous collaboration ever remain invaluable. Prof. Christoph Schmidt and Prof. Fred MacKintosh, for providing the venue for Physics and for reminding me that science is cool. The late Prof. Frans Nieuwstadt, for his enthusiasm and welcoming collaboration. Dr. Mathieu Pourquieu, for making numerical fluid dynamics fun on *non-microsoft* machines. Prof. Steve Cowin, who is always prompt in returning emails, for your inspired articles and lectures.

Colleagues whose expertise was key to the Molecular Biology of the PhD project and will be helpful for the upcoming research. Dr. Marco Helder and Dr. Behrouz Zandieh Doulabi, for designing the primers for our FLOW experiment. Dr. Ruud Bank, for the connection to tissue engineering, and your thoughts on cell mechanics, clinics, and physics.

For my paranympths, and constant source of support Cor Semeins and Jolanda de Blieck. Corski, for providing the practical steps to stress cells with fluid shear, and for not losing faith that I might someday learn Dutch; Jolanda, for calling me *Mellie*, for your contagious laughter and ever tireless hospitality, and for the long days spent on our bench work for FLOW. The unofficial paranympth and colleague Ette Tadjoedin, for her cooking that has become indispensable for my hungry off-days, and for her company that easily became familiar. Dirk-Jan Bervoets, for the orders *today* that arrives *yesterday*. Marion van Duin, for providing the venue to learn an afternoon Dutch sport, which probably spawned bowling, golf, and hockey. Don Lyaruu, for being my OCB supervisor for my three-month SEM work in the *doctorandus*. Ton Bronckers, for our conversations on imaging molecules and for your curious questions about the Philippines. Clara Korstjens, for showing me how to operate the *Leica microscope* without wreaking havoc for other users. Paulien Holzmann, for her hushed *Monalisa smile. The Wan and only*, for the glass and plastic containers, and the exotic snacks.

Wonderful acquaintances from the *merging of brains* between sections and fields. Margriet Mullender, for our abstracts and papers on fluid flow. Theo van den Bos, Teun de Vries. Roel Breuls, for helping me explain *viscoelasticity*. Ineke Jansen and Ton Shoenmaker, for *osteoclasts*. Elena, for *theoretical physics*.

I do not forget students of science like myself, whose acquaintance and backing I can never do without. Aviral Vatsa, for being the *beerless* company that is surprisingly (and) superb, and for sharing interests on bone cells. Djien Tan, for our kindred fondness for the insightful interactions in our *cell mechanics meetings*, and for selflessly volunteering to transcribe the minutes. Agnes *Aggie* Berendsen, for making inimitable acoustic reverberations (and having *conversationality*) that's refreshing during long days in front of a computer, for

her kind soul. Marlene Knippenberg, for her similar tastes in movies (books?), and her ready bag of chocolates tucked hidden in a secret table drawer. Sandra Tjabringa, for making the process of printing the PhD thesis a *piece ‘o cake*. Zufu Lu, for our parallel stature amid the familiarity of the colossal. Ana Santos, just in time, for being a gracious neighbor, for her honesty. Roel Hoogendoorn, *the goat guy*, for letting me help him calculate *something* using *mathematica*. Daisuke Mizuno, for joining me in confusing *all-nighter* experimentation and *eurekas* (*damn-I’m-good* moments) with billiards and beers (startlingly, *damn-I’m-good* moments too).

I do not forget old acquaintances that has undergone the rigors of study in our group and succeeded, whose company is dearly missed. Astrid Bakker, for sharing protocols, providing perceptive discussions on cells that never failed to keep my attention and for that day in Belgium, that miraculously left me untainted by my allergy to shrimps. Manon Joldersma, also for providing protocols, for teaching me how to open and close the CO₂ tank and for being the generous seer of the “stickies” (or post-its) at the villa-AIO, for liking *Tanuki* too. Saskia Dijcks, for being the student I can look in the eye (despite heels), and for her discipline. Chris Faber and Hein Stallmann, the duo whose company with beers, one time in Leiden, brought out appealing conversations. Ilara Zerbo, who unconsciously reminded the old lesson, that a smile brings wonders.

All the people involved in making it possible for us to participate in the Dutch Expedition for Life Science, Technology and Atmospheric Research (DELTA), mission to the International Space Station (ISS), made possible in part, by the Dutch Ministry of Economic Affairs and the Ministry of Education, Culture and Science. Dr. Marc Heppener of the European Space Agency (ESA) and his staff, for the scientific implementation in DELTA. Prof. André Kuipers, also of ESA, as the Dutch cosmonaut, who was flight engineer for the Soyuz flight to the ISS, that hosted our experiment FLOW (to test the sensitivity of bone cells to stress at microgravity). The Dutch Experiment Support Center (DESC), whose presence was beneficial to many aspects of the DELTA mission.

Dr. Rolf de Groot of SRON Netherlands Institute for Space Research, for funding the project “Bone cell mechanosensitivity and microgravity”, project nr. MG-055.

The technical team of the Centre for Concepts in Mechatronics (CCM), Edwin Langerak, Jan Rietema, and Antoon Koppen, whose tireless efforts, *night and day*, accompanied our experimental preparations throughout the DELTA mission.

The Russian team, whose expert management and hospitality provided the venue for our scientific preparations before the Soyuz flight in Kazachstan and for hosting us in Moscow.

The two other PhD students, Maarten Moes and Björn Sieberer, who were with me in Moscow and Kazachstan, who also prepared experiments for the Dutch Soyuz Mission, for the *vodka* and *beer* concocted with a twist of scientific discussions.

Moving towards where the sun rises, I express my gratitude to the people I met in Cebu, The Philippines, who have provided me the first difficult steps towards science (away from philosophy). Of the University of San Carlos’ (USC’s) Physics, Math and Chemistry Departments, Mario Tan, Tony Mayo, Rene Cabrera, Dioscy Villagonzalo, Marcedon Fernandez, Nelson Rosaroso, Susan Cahig, Cherile Yap, Helen de los Reyes, Joy Luna, Sir Romel, ma’am Joy and ma’am Gallos, who all taught the basis of it all. The Dutch Physics Development Project (PDP) team, who has made Physics teaching and doing research an example of excellence to the country. Gerrit Kuik (and Mae-Anne), for reconstructing the meaning of “no problem” and for your indispensable *computer software*, also, for finding people in Cebu, outside USC, with whom we shared our amusements on research. Onno Dijkstra, for the challenging assignments (that costs tons of yellow paper—the same goes for Gerrit). Ben Zuidberg, for his enthusiastic support of my stretch in Holland, and for being influential for granting funds for the *optical tweezers*. Kees Karremans, for your expertise on lasers and the evenings with the gang, losing our way in Cebu on my *beetle* or the borrowed *sakbayan*. Ed and Daday Van den Berg, for conjuring magic tricks to demonstrate science reminiscent of alchemists and wizards of old.

The Center for International Cooperation (CIS)- for providing a haven for assurance in foreign territory, especially in the early years of my studies. Rob Merkus, for overseeing *the Filipino connection* in Amsterdam, and for your help on purchasing the countless parts of the *tweezer setup*. Rien Kool, for being the *cool liaison* in the early years of the PDP. Dr. Gerard Thijs, for being the link between Cebu and Amsterdam, and for safeguarding my studies with zeal. The CIS staff, Dia, for helping me find apartments. Henny, for your invaluable help in keeping the equipment orders and setting the transfer of my future equipment for research to USC. Yeng, for conversing in *Tagalog*, and for that one fine afternoon of *salo-salo* with *adobo*.

The *Filipino gang*, who came to *Holland* with me to study (and to see for ourselves whether the *windmills* are actually functional). Dr. Roland Otadoy, who were in Holland when I arrived, for preparing the *coffee* religiously. Edcel Salumbides, with whom I found my own *proof* for the *Pythagorian theorem* in unseemly places. Arni Sicam, for learning Dutch. Renante Violanda, for almost setting up the *tweezers*. Marlo, for not losing my equipment orders. Raymund Sarmiento, for keeping up with interesting topics to talk about. All, for their selfless aid for my *annual-moving-to-another-apartment-in-Amsterdam* (which became tradition).

People I met in the early years of my studies in The Netherlands, who were avid practitioners of the culinary arts as I once were. Etsuko, for teaching me how to roll a *sushi*, fry an *okonomoyaki* (Osaka style) without breaking it, serve (well, drink) *sake*, for warning me of *wasabe*, and for having a very hospitable family who tolerated my cooking when I had my short laboratory visits in Japan. Teri, for *Wednesday poetry*, for the steaks *ala africana*, and showing me how to use spices and mushrooms in cooking, and for trusting my cooking. For their friends, who, like me, also enjoyed *wine and laughing*.

I do not forget too my old pals and prefects in the seminary days, who taught the value of a *study period* and its alternative, the *extended study period*. The community that taught the virtues of life found in *poverty*, to treasure the essence

of one's soul, in *chastity*, to desire the joy of human contact, and in *obedience*, to liberate one's true path.

Members of the *Societas Verbi Divini* (SVD) from Cebu, Fr. Herman van Engelen, my earliest mentor for Physics. Fr. Ted Murnane, whose support is a ready ally. Fr. Heinz Kulueke, for his leadership. Fr. Ding Fabiosa, for his spirituality. Br. Rick *Atienza* and Br. Tony Flores, Br. Mike Ancheta and Dong for easing my early Cebu days. Br. Eugene Orog and Br. Noel Tecson, for the discipline. SVD's here in Europe, Fr. Kees Maas, for welcoming my presence in the *Nederlands-Belgische Provincie*, and for his hospitality in Breda.

Least forgotten is home. Mom, dad and my sisters, for their warmth. My parents, for the *Ilonggo* and *Mindoreño* heritage that mixes well with being *Manileño*. Mom, for her unceasing devotion, for calling me *nonoy*, for being the only one in this universe who can cook my favorite spaghetti and *adobo*, and for your faith in all of us. My late dad, for the nickname *nonoy*, for teaching me what *sine* and *cosine* was (before I even heard of *trigonometry*), and for giving me a *slide rule* (when I was 12) that amazed my minuscule mind. My sisters: Ma. Karen (*Kae*), for being eldest in my absence; Ma. Ethel (*Et*), for being the other one who can dance; Ma. Michelle Anne (*I-an*), for the movies we like watching and the lazy afternoon's *pork & beans*; Ma. Diane *Fae* (*Jing*), for your emails, and for lending me your oversized t-shirts when I'm on vacation at home. My dear sisters, for calling me *kuya*-- no matter what.

Curriculum Vitae



Name: Bacabac, Rommel G.

Date and place of birth: 29 June 1969, Manila, Philippines

PhD Studies:

2001-2005 Project: "Bone cell mechanosensitivity and microgravity"

Hosting institution: Dept Oral Cell Biology

ACTA-Universiteit van Amsterdam & Vrije Universiteit

The Netherlands

Funding: SRON Netherlands Institute for Space Research

Project nr. MG-055

Promotors: prof.dr. Jenneke Klein-Nulend

prof.dr. Rob M. Heethaar

Co-promotors: dr.ir. Theo H. Smit

dr. Jack J.W.A. Van Loon

Postdoctoral Research:

2005-2006 Project: "Mechanosensitive cells in 3D environment
and microgravity"

Hosting institution: Dept Oral Cell Biology

ACTA-Universiteit van Amsterdam & Vrije Universiteit

The Netherlands

Head of project: Prof. Jenneke Klein-Nulend

Head of department: Prof. Vincent Everts

Collaborators:

Dept Physics and Medical Technology: dr.ir. Theo H. Smit

Dutch Experiment Support Center: dr. Jack J.W.A. Van Loon

Dept Physics of Complex Systems: Prof. Christoph F. Schmidt

Dept Theoretical Physics: Prof. Fred C. MacKintosh

Education:

Physics and Mathematics:

- 2001 Vrije Universiteit Amsterdam, The Netherlands
 MS Experimental Physics
- 1998 University of San Carlos (USC), Cebu City, Philippines
 BS Physics
- 1992-1993 University of San Carlos (USC), Cebu City, Philippines
(summer) Units for MS Mathematics
- 1992-1993 Ateneo de Davao University, Davao City, Philippines
 Advanced Mathematics courses

Philosophical disciplines:

- 1993-1994 Ateneo de Davao University, Davao City, Philippines
 Units for MA in Religious education
- 1991-1993 Regional Major Seminary, Davao City, Philippines
 Theological studies
- 1990 Christ the King Mission Seminary, Quezon City, Philippines
 AB Classical Philosophy (with distinction: Magna cum laude)

High School:

- 1982-1986 Christ the King Mission Seminary, Quezon City, Philippines
(with highest honors: Valedictorian)

Awards:

- 2003 5th International Bone Fluid Flow Workshop, Ohio, USA
 BFF Experimental Award of Excellence
- 2004 Meeting of the Netherlands Institute for Dental Sciences
 Poster award
- 2005 7th International Bone Fluid Flow Workshop, New York, USA
 Travel Award

Grant:

2002 Funded by the Physics Development Project
PDP grant # PHL-146

“Development of an optical tweezer setup”: Funds were received by RG Bacabac via the Center for International Cooperation (CIS) in the Netherlands, to assemble and build a double-laser optical tweezer setup in an inverted microscope system for research on the microrheology of mechanosensitive cells, and applications on soft matter physics. This project was carried out in close collaboration of the Dept Physics of Complex Systems, Vrije Universiteit and the Dept Oral Cell Biology, ACTA-Universiteit van Amsterdam and Vrije Universiteit.

Publications:

Bacabac RG, Smit TH, Cowin SC, Van Loon JJWA, Nieuwstadt FTM, Klein-Nulend J: Dynamic shear stress in parallel-plate flow chambers. *Journal of Biomechanics* 38: 159-167, 2005.

Bacabac RG, Smit TH, Mullender MG, Dijcks SJ, Van Loon JJWA, Klein-Nulend J: Nitric Oxide production by bone cells is fluid shear stress rate dependent. *Biochemical and Biophysical Research Communications* 315:823-829, 2004.

Bacabac RG, Smit TH, Mullender MG, Van Loon JJWA, Klein-Nulend J: An initial stress-kick is required for the fluid shear stress-induced activation of bone cells. *Annals of Biomedical Engineering* 33(1):104-110, 2005. (manuscript based on: 5th International Bone Fluid Flow Workshop 2003- “BFF Experimental Award of Excellence Abstract Presentation”, Cleveland, Ohio, USA).

Bacabac RG, Smit TH, Heethaar RM, van Loon JJWA, Pourquie MJMB, Nieuwstadt FTM, Klein-Nulend J: Characteristics of the parallel-plate

- flow chamber for mechanical stimulation of bone cells under microgravity. *Journal of Gravitational Physiology* 9:P181-P182, 2002.
- Bacabac RG, Van Loon JJWA, Smit TH, Klein-Nulend J: Stochastic resonance in rapid bone cell response to fluid shear stress. (submitted).
- Bacabac RG, Smit TH, Van Loon JJWA, Zandieh Doulabi B, Helder M, Klein-Nulend J: Bone cell responses to high-frequency vibration stress: does the nucleus oscillate within the cytoplasm? (submitted).
- Bacabac RG, Smit TH, Van Loon JJWA, Klein-Nulend J: Rapid nitric oxide production by bone cells in response to mechanical vibration. *Journal of Gravitational Physiology* (in press).
- Bacabac RG, Mizuno DS, Smit TH, Van Loon JJWA, Schmidt CF, MacKintosh FC, Klein-Nulend J: Microrheology of mechanosensitive cells (manuscript in preparation).
- Klein-Nulend J, Bacabac RG, Veldhuijzen JP, Van Loon JJWA: Microgravity and bone cell mechanosensitivity. *Advances in Space Research* 32(8):1551-1559, 2003.
- Klein-Nulend J, Bacabac RG, Van Loon JJWA, Veldhuijzen J: Botverlies door gewichtslosheid: Raakvlakken met osteoporose. *Osteoporose Journaal* (in press).
- Klein-Nulend J, Bacabac RG, Mullender MG: Mechanobiology of bone tissue. *Pathologie Biologie* (in press).
- Mullender M, Dijeks SJ, Bacabac RG, Semeins CM, Klein-Nulend J: The effect of mechanical loading on MC3T3-E1 cells is modulated by flow characteristics (submitted).
- Klein-Nulend J, Bacabac RG, van Loon JJWA: Botverlies door gewichtslosheid: raakvlakken met osteoporose. *Nederlands Tijdschrift voor Calcium- en Botstofwisseling* 8(29):62-65, 2005.
- Klein-Nulend J, Vatsa A, Bacabac RG, Tan DS, Smit TH: The role of osteocytes in bone mechanotransduction. *Current Opinion in Orthopaedics* 16:316-324, 2005.

Klein-Nulend J, Bacabac RG, Vatsa A, Tan SD, Smit ThH, Van Loon JJWA: Modulation of gene expression in bone cells during strain-adapted bone remodelling. *Journal of Gravitational Physiology* (in press).

International meetings:

- 2001 3rd NL-Gravity and Astrobiology Symposium, Amsterdam, The Netherlands (oral presentation).
- 2002 4th Bone Fluid Flow Meeting—Bone Fluid Flow, Adaptation, and Regeneration, Amsterdam, The Netherlands (poster presentation).
- 2002 8th European Symposium on Life Sciences, 23rd Annual International Gravitational Physiology Meeting, Stockholm, Sweden (oral presentation).
- 2002 Advanced School and Workshop on “Bone Mechanics – Mathematical and Mechanical Models for Analysis and Synthesis”, Lisbon, Portugal (oral presentation).
- 2003 49th Annual Meeting, Orthopaedic Research Society, New Orleans, Louisiana, USA (oral presentation).
- 2003 24th Annual International Gravitational Physiology Meeting, Santa Monica, California, USA (oral presentation).
- 2003 European Low Gravity Research Association (ELGRA) Biennial Meeting, Munich, Germany (oral presentation).
- 2003 Biology and Physics at Interfaces, From SingleMolecules to Cells, Jülich, Germany (poster presentation).
- 2003 5th International Bone Fluid Flow Workshop, Cleveland, Ohio, USA (oral presentation: “BFF Experimental Award of Excellence Abstract Presentation”).
- 2004 14th European Society of Biomechanics Conference, ‘s-Hertogenbosch, The Netherlands (oral presentation).

- 2004 50th Annual Meeting, Orthopaedic Research Society, San Francisco, California, USA (oral presentation).
- 2004 American Society of Gravitational and Space Biology Meeting, Brooklyn, NY, USA (poster presentation).
- 2005 51st Annual meeting of the Orthopaedic Research Society, Washington, D.C., MD, USA (oral presentation).
- 2005 International Society of Gravitational Physiology (ISGP) Joint Life Science Conference, Cologne, Germany (oral presentation).
- 2005 7th International Bone Fluid Flow Workshop *Translational Bone Fluid Flow*, New York City, NY, USA (oral presentation).
- 2005 45th American Society for Cell Biology Annual Meeting, San Francisco, CA, USA (poster presentation).

Professional societies:

Interuniversitaire Onderzoeksschool Tandheelkunde
The Dutch Society for Calcium and Bone Metabolism
American Society for Gravitational and Space Biology
European Low Gravity Research Association
Samahang Pisika ng Pilipinas



Project: **Microgravity and Bone Cell Mechanosensitivity**
(ESA European Space Agency Project # 98-HEDS-02)
(SRON Netherlands Institute for Space Research Project # MG-055)

Principal investigator: Prof. J. Klein-Nulend
Co-principal investigator: Dr. J.J.W.A. van Loon
Researcher: RG Bacabac

In this PhD project, we sent our experiment “FLOW” as one of the biological experiment entries to the Dutch Soyuz Mission “DELTA” (Dutch Expedition for Life Science, Technology and Atmospheric Research; Soyuz launched April 19, 2004).

The experiment FLOW investigated bone cell mechanosensitivity in weightlessness. The scientific aim of this experiment was to test the sensitivity of primary bone cell cultures (osteocytes, osteoblasts and periostial fibroblasts isolated from chicken calvaria) to mechanical loading by fluid shear stress under conditions of microgravity and simulated gravitation. FLOW was flown on-board the Soyuz on its mission to the International Space Station (ISS).

The DELTA mission carried scientific experiments conducted by the ESA astronaut André Kuipers on board the ISS.

The DELTA mission was made possible, in part, by the Ministry of Economic Affairs and the Ministry of Education, Culture and Science. Both ministries emphasized the important role played by The Netherlands and Europe in international space travel.

